



UNIVERSIDADE DA BEIRA INTERIOR

Engenharia

Preliminary Development of an Onboard Weight and Balance Estimator for Commercial Aircraft

(Versão Entregue Após Defesa)

Filipe André Vales Chaves

Dissertação para Obtenção do Grau de Mestre em

Engenharia Aeronáutica

(Ciclo de Estudos Integrado)

Orientador: Prof. Doutor Miguel Ângelo Rodrigues Silvestre

Coorientador: Prof. Doutor Pedro Vieira Gamboa

Covilhã, março de 2018

“It had long since come to my attention that people of accomplishment rarely sat back and let things happen to them. They went out and happened to things.”

(Leonardo da Vinci)

To my grandparents Arsénio Silva and Dioníso Vales.

Acknowledgements

As I finish this cycle I would like to thank more than a handful of people who somehow supported me throughout my studies.

First, I would like to thank my mentor and friend, Miguel Silvestre. Over the past few years he has either joined me or allowed me to join him in several different projects, and in each single one of them, I have learned one or two life lessons. Much of my critical thinking and rigorous approach to problems are thanks to him; a whole lot of my aeronautics knowledge as well.

Second, to my friend and co-supervisor, Pedro Gamboa. He helped me more than just a few times, including when I won the Cranfield Aerospace Experience 2015. Thank you.

Third, to my friends. The ones that I met at Covilhã but also the ones I already had back at home. They are, fortunately, too many to mention individually.

Fourth, to Azores Airlines and Grupo SATA, to Miguel Amaral, Otílio Machado, Paulo Ornelas, Nuno Campos, Pedro Lopes, Ângelo Oliveira and especially to Isabel Barata, for making this project possible.

Finally, and most importantly, I would like to thank my family for always standing by my side through hard times. And this includes this funny little critter called Alexandra. I still don't quite understand how I found her, but I am certainly grateful that I did. You make everything a lot more fun, thank you for your love and patience. "Cacaw" you too!

Abstract

A novel approach to onboard in-flight weight and balance estimation systems is presented.

Data from an Airbus A320 fleet from an airline were used to assess the feasibility of the approach. Simple flight mechanics in combination with statistics allowed for the identification of weight and centre of gravity position using cruise angle of attack, Mach number and elevator deflection values.

The good agreement between the theoretical model and the obtained values for the lift curve slope as a function of Mach as well as the standard error of the estimate for centre of gravity position and cruise flying weight indicate that the method is sound.

The major implication of this work is that the development of onboard and in-flight weight and balance systems can be significantly simpler than previous literature suggested. The impact of this work could be immediate for airlines since all the tools required to implement the system as described are readily available. This could have an effect in operating costs, safety and environment.

Keywords

Weight and Balance, Estimators, Onboard, In-flight, Airlines

Resumo

É apresentada uma nova abordagem aos sistemas embarcados de peso e centragem em voo.

Dados de uma frota A320 foram fornecidos por uma companhia aérea para testar a viabilidade da abordagem. Relações fundamentais da mecânica do voo, combinadas com análise estatística, permitiram identificar o peso e posição do centro de gravidade usando informação do ângulo de ataque, número de Mach e valor de deflexão do estabilizador horizontal.

A concordância entre um modelo teórico e os valores obtidos para o declive da curva de sustentação em função do número de Mach, bem como o erro padrão da estimativa do peso e da posição do centro de gravidade, atestam a viabilidade do método.

O presente trabalho mostra que o desenvolvimento de sistemas embarcados de peso e centragem pode ser mais simples do que anteriormente assumido na literatura. O impacto pode ser imediato para companhias aéreas interessadas uma vez que todas as ferramentas necessárias para a sua implementação estão prontamente disponíveis. Custos operacionais, segurança e ambiente são algumas das áreas que podem beneficiar deste trabalho.

Palavras-Chave

Peso e centragem, Estimadores, Embarcados, Em voo, Aviões de passageiros

Table of Contents

Acknowledgements	vii
Abstract.....	ix
Keywords	ix
Resumo	xi
Palavras-Chave	xi
Table of Contents.....	xiii
List of Figures	xv
List of Tables	xvii
Nomenclature	xix
List of Symbols	xxi
1 Introduction	1
1.1 Motivation.....	1
1.2 Azores Airlines.....	3
1.3 Objective.....	4
1.4 Contribution	4
1.5 Dissertation Outline	5
2 Literature Review	7
2.1 Aircraft Weight and Balance Fundamentals.....	7
2.1.1 Effect on Performance	9
2.1.1.1 Stall Speed.....	9
2.1.1.2 Takeoff Distance.....	9
2.1.1.3 Landing Distance	10
2.1.1.4 Cruise Trim Drag.....	11
2.2 Safety	13
2.2.1 Reduced Takeoff Performance	14
2.2.2 Tailstrike	14
2.2.3 Degraded Handling Qualities	14
2.2.4 Rejected Takeoff	14
2.2.5 Runway Overrun	14
2.2.6 Takeoff/Go-around Engine Thrust.....	14
2.2.7 Overweight Takeoff	14
2.2.8 Reduced Obstacle Clearance	14
2.3 Operational Limitations Related to Weight and Balance	15
2.3.1 Takeoff Limitations	15
2.3.2 Taxi and Takeoff Run Limitations	15

2.3.3	Stability and Control Limitations	16
2.3.4	Final Approach Limitations	17
2.3.5	Landing Limitations	18
2.4	Onboard Weight and Balance Systems Review	18
3	Methodology.....	23
3.1	Onboard Weight and Measurement and Correction.....	23
3.2	Estimating the Lift Coefficient Function	24
3.3	Flight Logged Dataset	25
3.4	Centre of Gravity Measurement and Correction	26
3.5	Regression Analysis	29
4	Results and Discussion.....	33
4.1	Lift Coefficient Determination	33
4.2	Cruise Flying Weight Estimation	37
4.3	Centre of Gravity Position Estimation.....	41
5	Conclusion	47
5.1	Summary	47
5.2	Future Work	48
	Bibliography.....	49
	Appendix A Linear Regression Assumptions Check	55
Appendix A 1	Linear Regression Assumptions Check for Weight Determination.....	57
Appendix A 2	Linear Regression Assumptions Check for Weight Determination with a Single Function	62
	Appendix B Multiple Linear Regression Assumptions Check	65
Appendix B 1	Multiple Linear Regression Assumptions Check for Centre of Gravity Determination	67
	Appendix C Publications.....	71
List of Publications	73

List of Figures

Figure 1.1 - Share of fuel costs on total operating costs of SATA.	1
Figure 1.2 - 2 Yearly distributions of fuel consumption research articles in peer reviewed journals and jet fuel prices [2].	2
Figure 1.3 - The new paint scheme of Azores Airlines. The A330-200 has a very distinctive whale painted on the side.	4
Figure 2.1 - Equilibrium of wing and tail lifts [24].	11
Figure 2.2 - Influence of CG position on trim drag [24].	12
Figure 2.3 - Natural aircraft response to pitch disturbance, for different amounts of pitch stability.	16
Figure 2.4 - Pitch-up behaviour for an airspeed increase with different S.M.	17
Figure 2.5- Load indicating gauge system by Eldon Westrum applied to an aircraft.	18
Figure 2.6 - Scale and boarding pass W&B system.	20
Figure 3.1 - Example of parameter variation. A stable frame report occurs whenever the parameter variation is within prescribed limits for a defined amount of time.	26
Figure 3.2 - Non-dimensional forces and moments.	27
Figure 4.1 - Data points and linear regression line for Mach 0.76.	33
Figure 4.2 - Data points and linear regression line for Mach 0.80.	34
Figure 4.3 - Obtained lift curves for the different Mach numbers (development dataset).	35
Figure 4.4 - Estimated Airbus A320 lift curve slope vs Mach number based on Kuchemann [66] and obtained from flight data. Non-dimensionalized by the Mach 0.78 lift slope value.	36
Figure 4.5 - Distribution of points with constant δHT ($\delta HT=5.4$) and 4.5 b) Distribution of points with constant lift coefficient ($CL=0.5$).	38
Figure 4.6 - Distribution of weight estimation error for the development dataset and for the evaluation dataset.	39
Figure 4.7 - Distribution of weight estimation error for the development dataset and for the evaluation dataset using a single function.	40
Figure 4.8 - a) Data points dispersion and prediction line with constant lift coefficient ($CL = 0.5$) and 10 b) Data points dispersion and prediction line with constant δHT ($\delta HT = 7$ deg). .	42
Figure 4.9 - Distribution of centre of gravity estimation error for the development dataset and for the evaluation dataset.	43
Figure A 1. 1 - Scatter plot for angle of attack vs lift coefficient for different Mach numbers.	57
Figure A 1. 2 - Scatter plot for angle of attack vs unstandardized residual for Mach 0.76.	58
Figure A 1. 3 - Scatter plot for angle of attack vs unstandardized residual for Mach 0.80.	58
Figure A 1. 4 - Normal Q-Q plot of unstandardized residual for Mach 0.76.	59
Figure A 1. 5 - Normal Q-Q plot of unstandardized residual for Mach 0.80.	60
Figure A 1. 6 - Histogram of unstandardized residual for Mach 0.76.	60

Figure A 1. 7 - Histogram of unstandardized residual for Mach 0.80. 61

Figure A 2. 1 - Scatter plot for angle of attack vs unstandardized residual for single linear regression model. 62

Figure A 2. 2 - Boxplot of unstandardized residual for single linear regression model. 63

Figure A 2. 3 - Normal Q-Q plot of unstandardized residual for single linear regression model. 64

Figure A 2. 4 - Histogram of unstandardized residual for single linear regression model. 64

Figure B 1. 1 - Scatter plot for regression standardized predicted value vs regression standardized residual. 68

Figure B 1. 2 - Boxplot of unstandardized residual for multiple linear regression model. 68

Figure B 1. 3 - Normal Q-Q plot of unstandardized residual for multiple linear regression model. 69

Figure B 1. 4 - Histogram of unstandardized residual for multiple linear regression model. .. 70

List of Tables

Table 4.1 - Summary of the results for the linear regressions.....	34
Table 4.2 - Summary of the results for the multiple linear regression.....	41
Table A 1. 1 - Summary of normality, independence of errors and collinearity assumptions tests.	59

Nomenclature

ACMS - Aircraft Condition Monitoring System

AIDS - Aircraft Integrated Data System

CFD - Computational Fluid Dynamics

DMU- Data Management Unit

FDIMU - Flight Data Interface Management Unit

FMS - Flight Management System

IATA - International Air Transport Association

ISA - International Standard Atmosphere

MAC - Mean Aerodynamic Chord

W&B - Weight and Balance

List of Symbols

A - Aspect Ratio

a - Lift Slope

a_0 - Incompressible Flow Lift Slope

c - Wing Chord

CAS - Calibrated Airspeed

CI - Confidence Interval

CG - Centre of Gravity

C_{Di} - Induced Drag Coefficient

$C_{D_{trim}}$ - Trim Drag Coefficient

C_L - Lift Coefficient

$C_{L_{MAX}}$ - Maximum Lift Coefficient

C_M - Pitching Moment Coefficient

$C_{M,0}$ - Pitching Moment about Reference Point O

$C_{M,0}^a$ - Aerodynamic Pitching Moment about Reference Point O

C_T - Thrust Coefficient

C_W - Weight Coefficient

C_X - Force Coefficient along x Axis

C_Z - Force Coefficient along Z Axis

D - Drag

df - Degrees of Freedom

e - Oswald Efficiency Factor

EAS - Equivalent Airspeed

F - F-test Statistic

g - Gravitational Acceleration [m/s^2]

HT- Horizontal Tail

k_c - Compressibility Coefficient

L - Lift

M - Mach Number

M_y - Pitching Moment

N_p - Neutral Point

p - P-Value

q - Relative Wind Dynamic Pressure
 QA - Aircraft Quality Number
 R^2 - Coefficient of Determination
 r - Correlation Coefficient
 S - Planform Wing Area
 S_{GR} - Takeoff Ground Roll Distance
 S_{RO} - Takeoff Rotation Distance
 $S.M.$ - Static Margin
 SS_M - Model Sum of Squares
 SS_T - Total Sum of Squares
 t - t-test Statistic
 T - Thrust
 $TOL(N)$ - Individual Variation of N Value
 $VAR(N)$ - Individual Variance of N Value
 V_{LO} -Lift-off Speed
 V_s -Stall Speed
 W - Weight
 W_{pax} - Estimated Passenger Weight
 \bar{W}_{pax} - Standardized Passenger Weights

Greek Symbols

α - Angle of Attack
 α_T - Thrust Line Angle
 B - Regression Coefficients
 δ_{Elev} - Elevator Deflection
 δ_{HT} - Equivalent Horizontal Tail Deflection
 ε - Residual Error Term
 γ - Flight Path Angle
 Λ -Wing Sweep
 σ - Standard Deviation
 θ - Equivalent Horizontal Tail Deflection
 ρ_0 - Mean Sea Level Air Density

1 Introduction

1.1 Motivation

The Air Transport industry is responsible for the transportation of goods and people by air all over the world. These flights are performed by certified air carriers and general aviation [1]. It contributes massively to the connection of people, cultures, regions and countries, promoting and supporting trade and tourism. As such, it is no wonder the Air Transport industry is a major player in both the economic and social development of nations [2].

However, the industry faces tremendous challenges [2] such as the growth of air traffic, current and future competition from other transportation industries, economic downturns, operational challenges, design challenges, the safety asymptote [3], carbon emissions and overall environmental footprint targets, fuel prices, and fuel consumption. Of these challenges, fuel consumption is perhaps the greatest due to the way it is connected to all the others; fuel consumption is directly related to emissions and environmental impact, profitability and competitiveness of the industry, and aircraft design decisions.

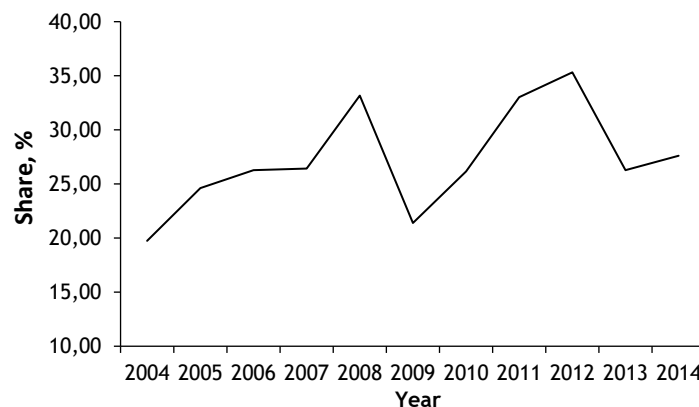


Figure 1.1 - Share of fuel costs on total operating costs of SATA [4].

The International Air Transport Association (IATA) reports that fuel represents as much as 30% of operating costs for the typical airline [5-7], thus having an enormous impact on profitability. SATA airline company is no different; Figure 1.1 shows the share of fuel costs on total operating costs of SATA [4]. This made airlines adopt measures that aim to reduce fuel consumption. SATA, for example, has developed fuel efficiency programs [4]. However, airlines are not alone; the academic community has taken interest in the topic as attested in Figure 1.2 [2].

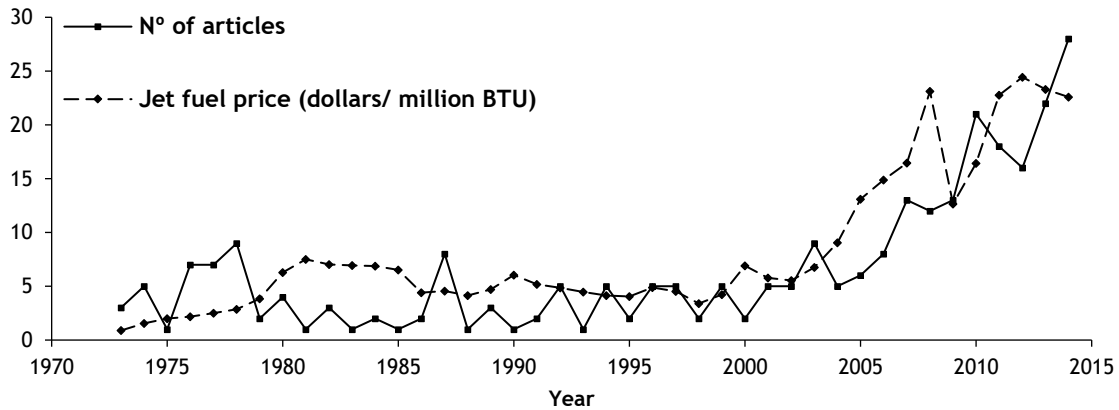


Figure 1.2 - 2 Yearly distributions of fuel consumption research articles in peer reviewed journals and jet fuel prices [2].

This is where weight and balance (W&B) comes into play. For any given aircraft, weight is the major parameter influencing performance and fuel consumption [8]. Centre of gravity (CG) also plays a role; Gabriel et al. [9] found that for the Airbus A330 the difference in fuel consumption from the least favorable to the most favorable CG position was 211 kg per flight. This small difference, over a typical life cycle of 40,000 flights, represents 8,440,000 kg (about 1%) of fuel saved. At the time of writing, with the jet fuel price at 0.97\$ per gallon, this is as much as 2,689,955\$ saved (about 1%) and a cut in total emissions of about 26,539,039 kg of CO₂ (about 1%) per aircraft over the course of its life cycle. Furthermore, incorrect W&B management may also result in several safety issues, e.g. tail strikes and runway overruns.

To reap benefit both in terms of operational safety and performance, it is necessary to accurately manage W&B. Current standard dispatch methodologies that use load and trim sheets are prone to lead to error due to human factors but also due to technical factors such as mismatches between standard passenger weights and actual weights. They provide an acceptable estimate at best. At worst, they can lead to gross potentially fatal inaccuracies [10]. Inaccurate W&B also leads to improper optimization of the aircraft for the cruise stage leading to unnecessary fuel burn and increased emissions; this is harmful to the environment and costs money to operators.

Onboard W&B systems are, from a conceptual point of view, the best solution to these problems [11], this is especially true if these are on-ground. Machines that are well designed and maintained significantly reduce the potential for human error; in the case of onboard W&B systems, these can act as scales and CG estimators that potentially lead to much more accurate measurements. In the short-term these can be an additional system that provides a cross-check to current methods. In the long-run, with matured technology, these can replace load and trim sheets altogether and speed up the whole dispatch process. In-flight onboard W&B systems can

provide further benefits if used in conjunction with on-ground systems. W&B affects, in a substantial way, the static and dynamic flight characteristics of an aircraft making this information desirable for automatic flight control, fault detection (failure to deploy stores, presence of fuel leak, etc.) and identification systems [12]. Current methods to update W&B information in-flight are based on fuel flow measurements; so, the development of new in-flight W&B systems can also provide an alternative/backup system to such methods. Additionally, in-flight W&B systems hold potential for in-flight icing identification [13].

However, both on-ground and in-flight systems suffer from specific problems. These range from high maintenance requirements and extensive use of sub-systems and sensors that may increase aircraft acquisition costs, to complex problem formulations that difficult real time W&B identification, among others. The consequence is that 85 years after the first formal mention of onboard W&B systems for aircraft [14], these are still not widely used for W&B procedures in everyday operations.

Given the importance of the W&B topic to the larger fuel consumption problem, considering the prominence of fuel consumption to the yet larger scenario of air carrier profitability and the air transport industry competitiveness and with the limitations of current W&B methods in mind, the *raison d'être* of the present work is to provide an alternative that may facilitate the adoption of onboard W&B systems, of the in-flight kind, into everyday operations.

1.2 Azores Airlines

Grupo SATA encompasses a collection of companies dedicated to air transportation. The company was founded in 1941 with the name “Sociedade Açoriana de Estudos Aéreos” by a notable group of people: José Bensaúde, Augusto d’Áthaide, Albano da Silva Oliveira, António de Medeiros de Almeida and Augusto Rebelo Arruda [15].

In 1998 SATA Internacional was established to operate the jet aircraft that were previously used by SATA Air Açores. The company operates to over 20 destinations outside of the Azores, including Lisbon, Porto, Toronto, Boston and several others in Europe. In 2015, the company was rebranded as Azores Airlines and saw changes to the logo and color scheme.

Currently, the Azores Airlines fleet comprises:

- 3 Airbus A310-300;
- 3 Airbus A320-200;
- 1 Airbus A330-200.

Soon, the A310 will be phased-out and the new A321neo and A321LR will be phased-in. The core values of the company are reliability, sympathy and innovation. The support given by

Azores Airlines to the present work is intimately aligned with the core value of innovation to improve operations and customer service.

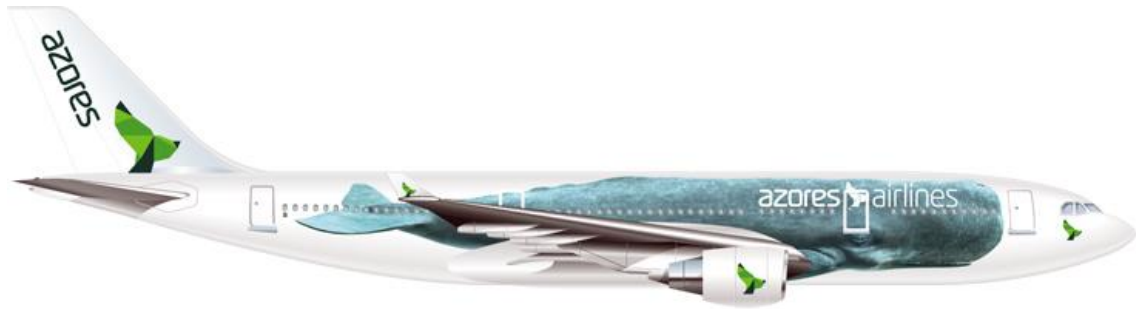


Figure 1.3 - The new paint scheme of Azores Airlines. The A330-200 has a very distinctive whale painted on the side.

1.3 Objective

The objective of the present work is to develop and assess an onboard in-flight W&B method for use in commercial aircraft. Due to the disadvantages of current systems, the following criterion was chosen to guide the development of the estimator:

- The development of the method must rely on data and information provided by standard systems that are already present in most commercial aircraft, i.e. no additional systems should be necessary as to prevent an increase in acquisition and maintenance costs or any additional weight to be carried on board. This should be facilitated by the requirement from the International Civil Aviation Organization (ICAO) that mandates air operators, with aircraft over 27 metric ton, to implement flight data monitoring (FDM) programs [16].

1.4 Contribution

The present work demonstrates that traditional statistics such as regression analysis in combination with fundamental flight mechanics equations is a suitable method to develop a CG position and current weight predictor in a commercial aircraft during the cruise stage. Furthermore, since the method relies on data that comes from sensors and systems that are already available on most if not all commercial aircraft, the presented work can be immediately adapted and developed by other research groups and more importantly airlines.

The estimator can be used in the following ways:

- As a backup to current W&B methods;
- To update W&B information during flight. This can help to optimize cruise speed and update landing weight information. Also, if the aircraft is equipped with trim tanks, the

estimator can be a further source of information for the forward/aft fuel transfers that optimize the CG position;

- As a source of information to automatic flight controls;
- As a tool to identify outliers, i.e. mismatches between load and trim sheet calculations and W&B estimation in-flight. This provides an additional layer to FDM programmes;
- As a potential identification system for in-flight icing [13].

1.5 Dissertation Outline

After this introductory chapter, the present work is divided in the following manner:

Chapter 2 introduces the fundamental theory of W&B and its effect on performance, safety and aircraft operations is presented. Closing the chapter is a literature review of previous onboard W&B research.

Chapter 3 presents the methodology. Information on how the data was collected is provided as well as some general characteristics of the data. Then, the formulation of the problem through fundamental flight mechanics equations is presented. The chapter ends with the presentations of the performed regression analysis.

Chapter 4 presents the results and discussion of the research.

Chapter 5 closes the present work with an overview of the research, discussion of limitations and suggestions for future work.

2 Literature Review

2.1 Aircraft Weight and Balance Fundamentals

The fundamental theory behind W&B is the law of lever; the law of lever simply states that any lever is balanced when the moment about its fulcrum is zero. The moment is the multiplication of a force by the arm; the arm is the distance from the datum to any point of interest and in turn, the datum is a point from which all measurements are taken. Usually, the nose of the aircraft is used as the datum. The two fundamental principles to be observed are [17]:

- The total weight of the aircraft should never exceed the certified limits for each of the phases of the operation;
- The centre of gravity must be kept within the certified limits for the operational weight of the aircraft.

To establish the initial operational empty weight, the manufacturer will typically use ramp-type scales. After establishing the empty weight, the operator has the option to use individual operational empty weights or to use fleet operating empty weights on W&B calculations. With the operational empty weight established, the weight of fuel, catering, cargo, crew and passengers can simply be added to determine the all-up weight of the aircraft. To facilitate the calculation of moments and determining the location of the centre of gravity, moments are usually converted into an index, and the cabin is split into several individual sections, each with its own centroid. Load and trim sheets are typically used to perform the W&B calculations; using this methodology, each seat row is assigned a moment arm and the passenger's weight is assumed acting on the centre of the seat. Passenger weights have been standardized. Since cargo and fuel are typically weighted, or have their weight determined with high accuracy, carry-on luggage and passengers become a major source of inaccuracies on W&B calculations. The inaccuracy of an item location in a cabin causes a moment, Equation 2.1 [8,18]:

$$M_i = W_i(x_i \pm \Delta x_i) \quad 2.1$$

where Δx_i is the uncertainty in the moment arm x_i of item i having a weight W_i . The moment error is given by Equation 2.2:

$$E_i = \pm W_i \Delta x_i \quad 2.2$$

and increases with both the weight of the item and its uncertainty. The moment inaccuracy due to both weight and location is given by Equation 2.3:

$$M_i = (W_i \pm \Delta W_i)(x_i \pm \Delta x_i) \quad 2.3$$

and the error can be expanded into Equation 2.4:

$$E_i = W_i \Delta x_i + \Delta W_i x_i + \Delta W_i \Delta x_i \quad 2.4$$

With regard to passenger weights, there will be a distribution of weights that generates a passenger weight inaccuracy given by Equation 2.5 [8]:

$$W_{pax} = \overline{W}_{pax} + \Delta W_{pax} \quad 2.5$$

Assuming a normal distribution around the average value \overline{W}_{pax} and a standard deviation σ , we assume that $\Delta W_{pax} = 3\sigma$. So, if $i=1, \dots, n$ denotes the cabin index, and \overline{W}_{pax} denotes the total passenger weight in cabin i , we have the passenger weights given by Equation 2.6:

$$W_{pax} = n_i \overline{W}_{pax} + \Delta W_{pax} \quad 2.6$$

The inaccuracy is the same for all cabins so that:

$$\Delta W_{pax} = \left(\sum_i^n \Delta W_{pax_i}^2 \right)^{\frac{1}{2}} = \sqrt{n(3\sigma)^2} = 3\sigma\sqrt{n} \quad 2.7$$

Looking at Equations 2.6 and 2.7, it becomes evident that if the assumed Gaussian distribution is incorrect, either due to the mean or due to the standard deviation, or even both being wrong, significant inaccuracies may arise. Studies have shown that the increased incidence of excessive weight of the population, unaccounted for by updates to standard weights, has potentially caused significant monetary losses due to excessive fuel consumption [19,20].

To account for potential inaccuracies, operators will typically introduce curtailments to the certified loading envelope. These curtailments must account for the seating of passengers in the cabin, fuel density variations, fuel movement and fuel usage in-flight, passenger and crew members movement in-flight, effects of potable water and lavatory fluids movements in-flight and potential baggage or cargo shifts.

2.1.1 Effect on Performance

The effect of weight and CG location on aircraft performance cannot be overstated. In this section, a summary of the most relevant effects is presented. References [8,18,21-23] may be consulted for further insight.

For stability reasons, the CG is always kept ahead of the aircraft neutral point (Np), or aircraft aerodynamic center [18]. The neutral point is the CG position that gives neutral stability. For reference, CG_{Fwd} designates a CG position that is further ahead than CG_{Rear} . Nevertheless, both are ahead of the Cp in all flight conditions.

The greater the arm between CG and Np the greater the zero-elevator nominal cruise pitch down moment will be and thus the greater the required cruise trim negative lift on the horizontal stabilizer (HS) required for the equilibrium, to compensate with pitch up moment. A greater negative lift on the HS will thus result in an overall lift degradation and increase in drag [18]. Since the arm for CG_{Fwd} is greater than CG_{Rear} , these side effects are more notorious with an advanced CG position. On the other hand, there is usually a tight limit on the rearward CG envelope to preserve the longitudinal stability of the aircraft.

2.1.1.1 Stall Speed

Equation 2.8 shows that for a given altitude and weight, all else being equal, stall speed is greater when the lift on the horizontal tail increases. As explained before, negative lift on the horizontal tail (L_{HS}) is greater for a forward CG position, thus stall speed increases when the CG approaches the front end of the envelope. In terms of weight, all else being equal, the greater the weight the greater the stall speed.

$$V_S = \sqrt{\frac{2n(W + L_{HS})}{\rho S C_{L_{MAX}}}} \quad 2.8$$

2.1.1.2 Takeoff Distance

Takeoff can be divided into 4 phases: acceleration, rotation, transition and climb to obstacle height. The ground roll distance, Equation 2.9, shows that for the same weight, all else being equal, the greater the negative lift on the horizontal tail, the greater the ground roll will be due to a larger friction drag between the tires and the runway. Also, more negative L_{HS} will result in more trim drag in the initial climb to obstacle height, which contributes to further increasing the takeoff distance. Finally, since lift-off velocity (V_{LO}) is typically given by $V_{LO} \geq 1.2 V_S$ [18] and, as seen in the previous Section, stall speed is greater for CG_{Rear} , this also contributes to greater takeoff roll. In conclusion, better performance is achieved with CG_{Rear} . For the same takeoff weight, ground roll distance is smaller for CG_{Rear} . For an equal ground roll distance, takeoff weight can be larger with CG_{Rear} . Equation 2.9 also shows that greater weight leads to greater takeoff distance.

$$S_{GR} = \frac{WV_{LO}^2}{2g[T - D - \mu(W + L_{HS} - L)]} \quad 2.9$$

For the rotation phase, the distance travelled can be approximated by Equation 2.10. CG_{Fwd} will result in a greater pitch down moment, making rotation harder and thus resulting in a greater Δ_t ; this, in combination with a greater V_{LO} for the same weight, lets us conclude that better performance in rotation is achieved for CG_{Rear} .

$$S_{RO} = V_{LO}\Delta t \quad 2.10$$

Climb performance is also affected. Considering $\alpha \approx \gamma$ and the thrust line to coincide with the aircraft longitudinal axis, the set of equations that describe climb are:

$$F_x = T - D - W \sin \gamma = 0 \quad 2.11$$

$$F_y = L - L_{HS} - W \cos \gamma = 0 \quad 2.12$$

$$M_{CG} = L_{\Delta x} - L_{HS}\Delta X \quad 2.13$$

On Equation 2.13 Δx is the distance from the CG to the wing lift vector and ΔX is the distance from the CG to the HS lift vector. From Equation 2.11 we arrive at:

$$\sin \gamma = \frac{T - D}{W} \quad 2.14$$

From Equation 2.14, the climb angle will be smaller when excess thrust is reduced. For the same T and W this happens when drag is higher. Furthermore, for the same climb angle, the weight can be higher for higher excess thrust. In conclusion, a smaller arm between CG and Cp will lead to better climb performance due to lower drag, this happens for CG_{Rear} .

2.1.1.3 Landing Distance

Equation 2.15 provides an approximation for the deceleration distance after the touchdown. V_{TD} is the speed during the transition phase, this is $V_{TD} \geq 1.3V_S$. We can conclude that a reduced speed during transition, for the same weight, will lead to a smaller landing distance. On the other hand, for the same landing distance with V_{TD} being lower, landing weight can be higher. As a result, better performance on landing is achieved for CG_{Rear} .

$$S_{DECEL} = \frac{W V_{TD}^2}{2g [T - D - \mu(W + L_{HS} - L)]} \quad 2.15$$

2.1.1.4 Cruise Trim Drag

During cruise, the HS must create a moment to compensate for the pitch down moment of the wing, causing trim drag. The increment in induced drag coefficient contributed by the wing because of trim is given by Equation 2.16 [24]:

$$\Delta C_{Di} = -2C_{Di} \frac{C_{LHT}}{C_L} \frac{S_{HT}}{S} \quad 2.16$$

The induced drag of the tail, in terms of wing area, is given by Equation 2.17:

$$C_{DiHT} = \frac{S_T}{S} \frac{C_L^2}{\pi A e} \left(\frac{C_{LHT}}{C_L} \right)^2 \frac{A e}{A_{HT} e_{HT}} \quad 2.17$$

The total increment in induced drag coefficient is given by Equation 2.18:

$$\Delta C_{D_{trim}} = \frac{S_{HT}}{S} \frac{C_{LHT}}{C_L} \left(\frac{C_{LHT} A e}{C_L A_{HT} e_{HT}} - 2 \right) C_{Di} \quad 2.18$$

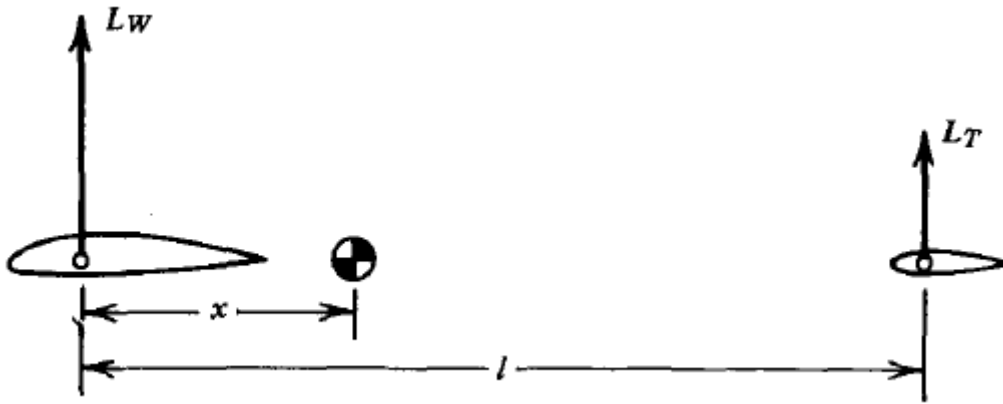


Figure 2.1 - Equilibrium of wing and tail lifts [24].

Considering Figure 2.1 , were X is the distance of the CG aft of the wing aerodynamic center and l is the distance from the aerodynamic center of the wing to the aerodynamic center of the tail, we have:

$$\frac{X}{l} = \frac{S_{HT} C_{LHT}}{S C_L} \quad 2.19$$

Substituting Equation 2.19 into Equation 2.18 we have:

$$\frac{\Delta C_{D_{Trim}}}{C_{D_i}} = \frac{X}{l} \left[\frac{X}{l} \left(\frac{b}{b_{HT}} \right)^2 \frac{e}{e_{HT}} - 2 \right] \quad 2.20$$

Equation 2.20 presents the trim drag as a fraction of the original induced drag, as influenced by X/l. Figure 2.2 shows the influence of the centre of gravity on trim drag [24].

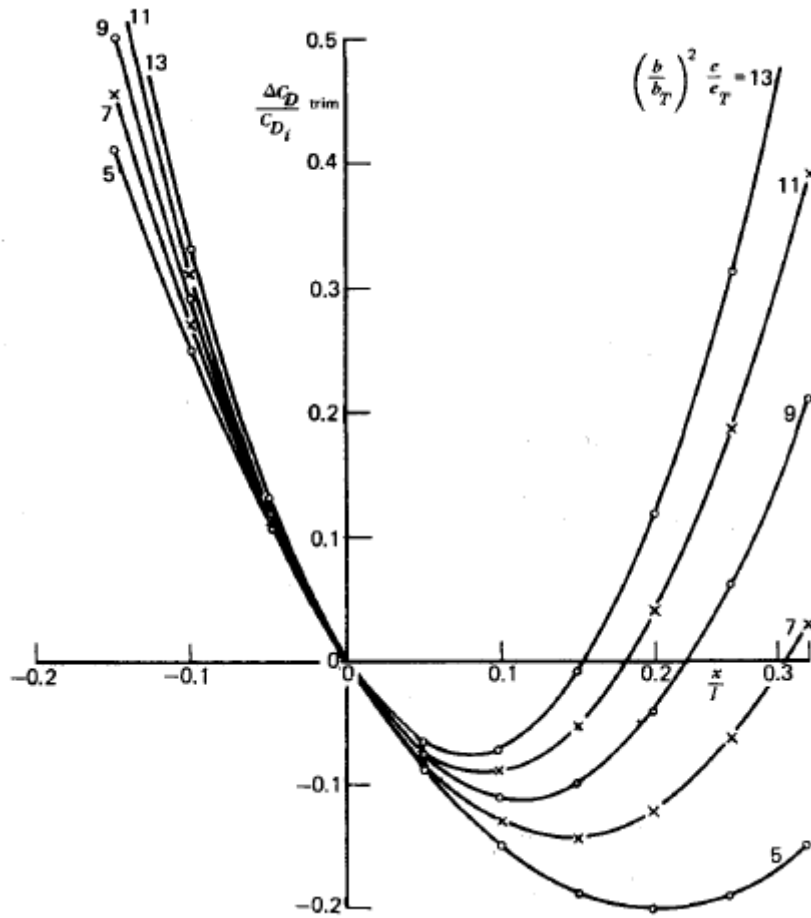


Figure 2.2 - Influence of CG position on trim drag [24].

Trim drag will be higher for a forward CG position, CG_{Fwd} . Since during level cruise $T=D$ and fuel consumption is dependent on thrust, fuel consumption will be higher for a forward CG. Also, drag is higher for higher weights during cruise, so fuel consumption is greater for higher gross weights.

2.2 Safety

An incorrect W&B calculation is far more than just a nuisance, damage to property and the aircraft itself and even loss of life may ensue. Typically, problems arise due to human error. The seminal work by James Reason [25] can be checked if the reader is interested in knowing more about human factors, but a detailed description of these is beyond the scope of this work.

Overall, the risk of having a weight and balance accident is 8.5 times higher for cargo flights when compared to passenger flights [11]. However, occurrences with passenger flights are not uncommon. References [11,26-31] provide further details.

The typical errors and inaccuracy's that lead to W&B problems are as follows:

- The zero-fuel weight (ZFW) is inadvertently used as takeoff weight (TOW);
- Transposition or transcription errors, such as introducing 123.000kg instead of 213.000kg;
- V speeds are incorrectly transcribed or transposed when manually introduced into the aircraft system;
- Aircraft data from a previous flight is used to calculate the V speeds;
- Crew fails to update takeoff parameters after a change in weather conditions or assigned runway;
- Selection of incorrect values from a load sheet or takeoff data card;
- Use of incorrect performance charts for the aircraft type;
- Involuntarily selecting the wrong row/column in the performance charts;
- Using the incorrect value when referencing the performance charts;
- Using incorrect unit of measurement;
- Weight and balance calculations not being made;
- Failure to secure cargo;
- Unlisted containers, pallets and/or bags being loaded;
- Containers, pallets and/or bags not being loaded;
- Incorrect number of passengers;
- Loading of the aircraft after delivery of the load sheet (unrecorded loading);
- Load sheet errors such as incorrect ZFW, incorrect recording of cargo and freight, etc;
- Passengers not respecting assigned seats;
- Passenger's carry-on luggage not being weighted;
- Differences between passenger's actual weight and standard weights used.

The problems arising from these errors will be described next.

2.2.1 Reduced Takeoff Performance

During takeoff, the aircraft may take longer to accelerate, appearing “sluggish” or “heavy”. This will inevitably lead to a longer takeoff run and potentially a runway overrun.

2.2.2 Tailstrike

In cases where the weight at takeoff is higher than what was inserted or calculated, rotation may be initiated at an airspeed lower than required and thus lift-off may not be achieved. Faced with this situation, the pilot may attempt to raise the aircraft’s nose even further which can result in the tail contacting the runway pavement surface.

2.2.3 Degraded Handling Qualities

After leaving the runway, the margin between the aircraft’s airspeed and the stall speed may be reduced until the aircraft accelerates up to normal climb speed. If the V_2 speed is also erroneous, this may not happen until after the aircraft passes through the acceleration height.

2.2.4 Rejected Takeoff

If the aircraft does not accelerate or lift-off as anticipated, the crew may reject the takeoff.

2.2.5 Runway Overrun

If the aircraft does not lift-off or if it fails to stop after a rejected takeoff, the rollout may extend beyond the end of the runway, resulting in an overrun.

2.2.6 Takeoff/Go-around Engine Thrust

If the aircraft does not accelerate or lift-off as anticipated, the crew may be forced to select takeoff/go-around (TO/GA) thrust setting, the maximum thrust the engines can deliver. This will result in higher fuel consumption, increased wear on the engine and higher noise levels.

2.2.7 Overweight Takeoff

This can occur if an erroneous takeoff weight is used to determine a suitable runway for takeoff.

2.2.8 Reduced Obstacle Clearance

If the takeoff is initiated at low speed, the aircraft will not achieve the required climb gradient and the clearance to obstacles in the takeoff path will be reduced.

2.3 Operational Limitations Related to Weight and Balance

The weight of the aircraft and the location of the CG will naturally result in some operational limitations that must be reflected on the design of the CG envelope; these limitations can be related to the aircraft structure, handling qualities or compromises between aircraft loading and performance [18]. The regulatory framework of CS 25 [32] establishes all the criteria that must be considered. In the following, a short review of these limitations is provided.

2.3.1 Takeoff Limitations

The most obvious limitation during takeoff is the maximum takeoff weight (MTOW). This is a fixed value that corresponds to the maximum weight at which an aircraft has shown to meet all applicable airworthiness requirements. A pilot is not allowed to attempt takeoff if the aircraft is heavier than MTOW. MTOW is defined based both on structural, as well as performance limitations/requirements, however the same model of aircraft can have different MTOW's; airlines can certify an aircraft for a lower MTOW, saving money in landing fees as well as ATC (Air Traffic Control) fees (which are based on MTOW). The inverse is also true; an aircraft may be certified for a higher MTOW if subjected to the necessary modifications (e.g., reinforced landing gear, reinforced wing spar, etc.).

Another limitation is the maximum allowable takeoff weight; unlike MTOW, which is a fixed value, maximum allowable takeoff weight varies according to the flap/slat setting, aerodrome altitude, temperature, runway length, wind conditions, runway surface conditions and obstacles on the takeoff flight path. It is used in situations where it is not possible to takeoff at MTOW due to operational limitations; thus, it can never be higher than MTOW.

CG position will also impose some structural limitations; an aft CG position will increase the load on the main landing gear (MLG), thus the strength of the MLG at high takeoff weights limits how aft the CG position can be. The opposite is true for forward CG position; the more forward the CG position, the higher the load on the nose landing gear, thus the strength of the nose landing gear limits how forward the CG position can be at high takeoff weights. Another limitation is the strength of the wing which influences the CG position limits at takeoff.

2.3.2 Taxi and Takeoff Run Limitations

While operating the aircraft on the ground, nose landing gear steering is the only way to control the aircraft during taxi and at the beginning of the takeoff when the airspeed is not sufficient to make rudder inputs effective. To be able to steer the aircraft with the nose gear, enough adherence is needed. Adherence is dependent on both the friction coefficient of the tires and the normal reaction of the nose gear (which, in turn, is dependent on the weight carried by the nose landing gear). Thus, the position of the CG will dictate how much weight is applied on the nose gear, and thus its effectiveness; the further aft the CG, the lesser the adherence. Furthermore, while applying takeoff thrust, nose gear adherence may be reduced on aircraft with engines positioned under the wing (below the CG). CG position will limit performance

during rotation; if the CG is too far forward, rotation may become hard or even impossible. Too far aft, and the pitch rate may become dangerously high; this can easily result in a tailstrike. In practice, the aircraft is trimmed during takeoff so that, regardless of CG position, the “feel” that the pilot gets is always the same.

The aircraft is also subject to a weight limit while on ramp or taxiing, called maximum ramp weight (MRW). This weight is greater than MTOW since it includes the weight of the fuel that will be burned during runup and taxi for takeoff.

2.3.3 Stability and Control Limitations

The CG position and horizontal tail size and position are the dominant factors controlling pitch stability of the aircraft. Moving the CG forward increases stability, making the aircraft resistant to angle of attack and speed changes and vice-versa. The static margin (S.M.) specifies the degree of pitch stability of an aircraft:

$$S.M. = \frac{X_{NP} - X_{CG}}{C} \tag{2.21}$$

with the neutral point estimated by:

$$\frac{X_{NP}}{C} \approx \frac{1}{4} + \frac{1 + \frac{2}{A}}{1 + \frac{2}{A_{HT}}} \left(1 - \frac{4}{A - 2} \right) V_{HT} \tag{2.22}$$

where A is the wing aspect ratio, A_H is the horizontal tail aspect ratio and V_H is the horizontal tail volume coefficient. Figure 2.3 [33] shows the natural aircraft response to different levels of pitch stability.

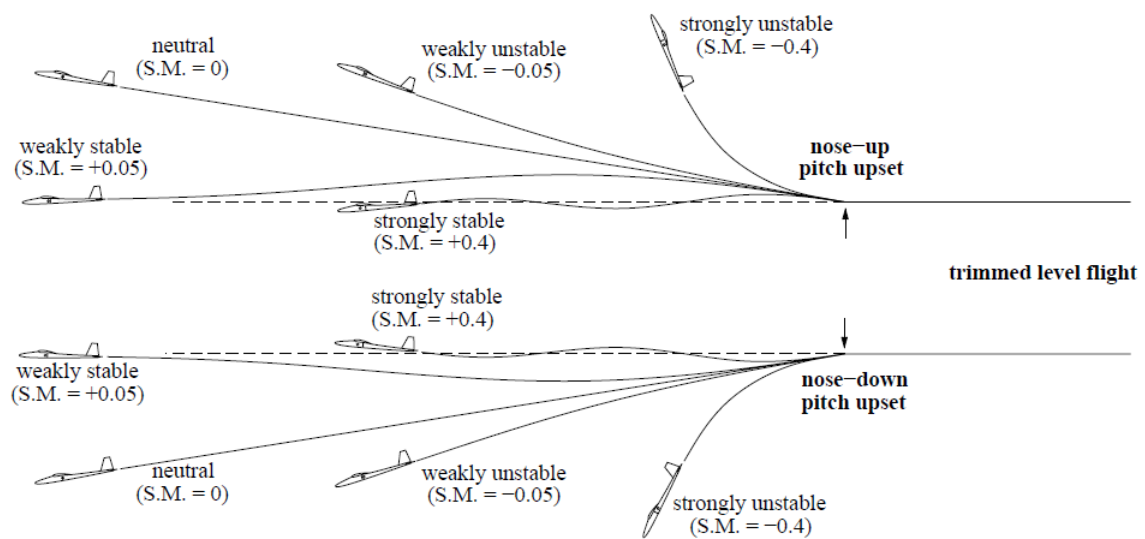


Figure 2.3 - Natural aircraft response to pitch disturbance, for different amounts of pitch stability [33].

To ensure the longitudinal stability of the aircraft, CG position will have to be ahead of the aerodynamic center or neutral point; if there is an upset, such as a gust or increase in angle of attack, a restoring pitch down moment will be created, bringing the aircraft's nose down to the initial position. The Np can thus be considered a practical aft CG limit [33].

However, stability and control work in opposition to each other; if CG position is too much forward, the aircraft will be very stable but impossible to maneuver because the elevator will reach maximum deflection before a sufficient pitching moment can be created. This effect is exacerbated at low airspeeds when control surfaces are even less effective. Large static margin will also cause large pitch trim changes with speed. Figure 2.4 shows the behavior of an aircraft to an airspeed increase due to power increase [33].

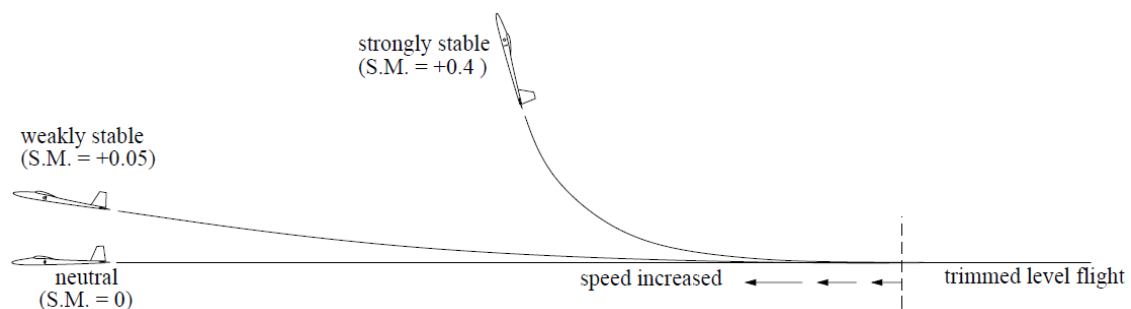


Figure 2.4 - Pitch-up behaviour for an airspeed increase with different $S.M$ [33].

Furthermore, during a turn, to compensate the increase of load factor and maintain a coordinated turn, elevator deflection will be needed. CS 25 regulations require that a maximum acceptable load factor of 2.5G can be reached, without structural damage. This means that the maximum forward CG position limit will also have to allow for this requirement to be met.

2.3.4 Final Approach Limitations

During approach, flaps and slats are used to increase the maximum lift coefficient; allowing lower approach speeds. The use of these high-lift devices will cause a large pitch down moment that has to be compensated by the horizontal stabilizer. The combination of the pitch down moment, caused by the high lift devices, with the pitch down moment caused by a forward CG position, can lead to a high horizontal stabilizer setting which may result in a horizontal stabilizer stall. Furthermore, if during the approach the speed is excessively reduced, the pilot will compensate by pushing forward on the controls, lowering the nose to regain speed and prevent a stall; if this maneuver is performed when there is an excessively forward CG position, the horizontal stabilizer can stall due to the attitude change.

If the aircraft must perform a go around, the thrust increase will cause a significant pitch up moment that has to be compensated by the elevator. This will limit the aft CG position.

2.3.5 Landing Limitations

The limitations during landing are like those of the takeoff phase, with the maximum landing weight (MLW) being the major limitation.

2.4 Onboard Weight and Balance Systems Review

The idea of using onboard W&B systems is not a new idea; the very first mention to an onboard W&B system goes back to 1932 when Eldon Westrum filled a patent for a so-called “Load Indicating Gauge for Vehicles” [14]. The system was composed by a set of levers, pivotally connected to a stationary part of the aircraft, and these in turn were connected to a set of bellows. These bellows were in turn connected with fluid conducting pipes that were connected to the load gauge. The system configuration is shown on Figure 2.5.

In 1945, Ernest Schlieben [34] presented a patent for a “System and Apparatus for Determining the Distribution of the Load in an Aircraft”. The mechanism was based on the principle that variations in pressure on the shock strut of a landing gear were proportional to the weight of the aircraft. In turn, piston displacement on the strut would also be proportional to the load. As such, attached to the piston on the gear strut was a set of resistors. Depending on the piston displacement, the resistance would also vary making a reading of load on a gauge possible. Reading of CG position would also be possible through individual resistors on each of the struts.

The year of 1948 saw two patents [35,36] for strain gauge based onboard W&B systems; these were filled in 1944, almost 6 years after the invention of strain gauges by Edward Simmons and Arthur Ruge in 1938. Further strain gauge-based systems have been created over the years [37-40].

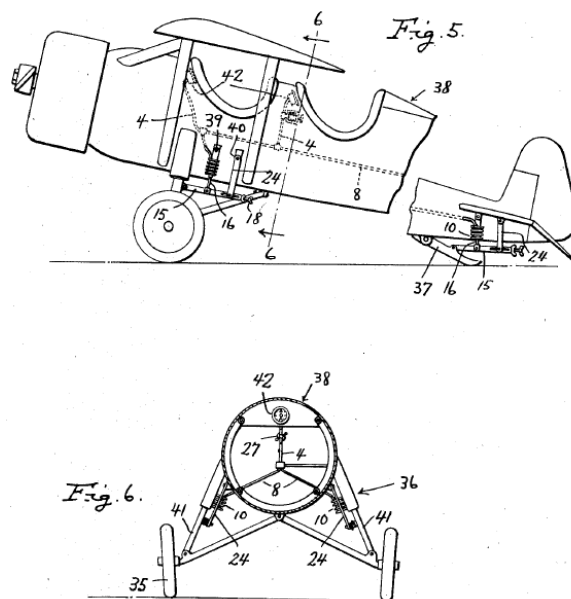


Figure 2.5- Load indicating gauge system by Eldon Westrum applied to an aircraft [14].

Fairchild Controls [41-43] created a system based on high accuracy pressure transducers for measuring oleo strut pressure. Other transducer-based systems followed around the same time [44-46]; these measured shear deflections and related this measurement to load on the landing gear.

Boeing published a patent in 1991 [47] describing a system for real time estimation of CG in-flight; the system used angle of attack, flap setting, and stabilizer position to derive the CG position. In 1996 [48] a second patent by Boeing improved upon this method by using additional factors such as expected load factor, dynamic pressure and reference wing area.

Airbus [49] presented an onboard W&B system based on Barkhausen Noise in 1999. The principle of operation is that the stress on the landing gear, caused by the weight of the aircraft, will induce a stress on the material itself that composes the landing gear. The stress causes both reversible and irreversible changes in the magnetization of materials. Magnetic changes in ferro-magnetic materials can be detected through Barkhausen Noise sensors installed on the landing gear and related to the weight of the aircraft.

Trinity Airweighs [50] developed another system based on the pressure of the landing gear oleo strut. To overcome the issue of static friction forces that plagued earlier systems, the Trinity system injects or withdraws a certain amount of hydraulic fluid or nitrogen gas to each of the landing gear struts. A similar method was proposed by General Electrodynamics [51].

In 2004 [12] an onboard in-flight W&B system was developed based on artificial neural networks; the authors used simulated flight test data to show that it was possible to recover weight and CG information based on angle of attack and elevator deflection through a nonparametric artificial network pretrained on flight test data.

ARINC, currently Rockwell Collins, developed a system where digital scales were used in conjunction with boarding pass scanners to feed passenger and carry-on luggage weight information to a processor [52], Figure 2.6. This processor would then combine this information with information about fuel quantity, cargo and other items to populate a load sheet. Some issues with this method are the fact that passengers may not sit down on their assigned seats and that carry-on luggage may also not be placed on the passenger's assigned row. Passenger privacy issues may also arise since individual passenger weight would be collected.

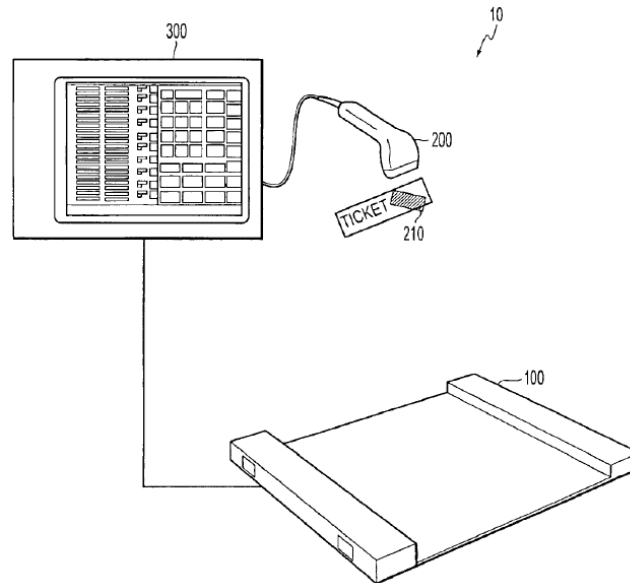


Figure 2.6 - Scale and boarding pass W&B system [52].

In 2008 another patent was published for an on-ground W&B system based on the landing gear [53]. The system was comprised by a memory that stored breakout friction data of the shock struts (determined during a calibration loading and unloading test), including breakout forces and pressures and actual loading on the struts as measured by a calibrated scale. The system also comprised a set of pressure sensors on each of the landing gear struts and an attitude sensor to sense the attitude relative to the horizontal during loading and unloading. To compute the vertical load on each of the struts, the system would consider the stored calibration breakout friction data and the shock strut pressures, landing gear loads and attitude of the aircraft. Boeing appears as an assignee of the same system in 2011 [54].

Further efforts on onboard in-flight W&B estimation were made in 2009; Abraham and Costello [55] developed a system for helicopters using Kalman filters, constructed with state vectors consisting of W&B states and rigid vehicle states. The method was later tested experimentally by Taylor and Rogers using radio-controlled helicopters [56].

Al-Malki et al. [57,58] improved upon the Abraham and Costello method by using an Inertial Measurement Unit that does not need the aircraft dynamic model.

Honeywell [59,60] developed an on-ground W&B system that only estimated the CG position; the system had a sensor on the nose landing gear and combined the information from this sensor with weight information from a load and trim sheet to determine the location of the CG. The reasoning for this configuration was that load and trim sheet methods already provide a sufficiently accurate estimate of the aircraft's weight, plus aircraft performance is reasonably tolerant to minor weight uncertainty if the CG is within its envelope limits. The flaws of such

design are evident; the assumption that aircraft performance is tolerant to minor weight uncertainty couldn't be farther from the truth. Even minor uncertainties arising from changes in the biometric and anthropometric characteristics of passengers can have tremendous effects on aircraft performance and safety [19,20]. If less than minor uncertainties arise, such as due to unrecorded loading, the effects can be severely aggravated; the pilots will incorrectly calculate the V speeds, leading to a lack of performance during takeoff, which may lead to a runway overrun, even if CG position is within limits.

Further developments in in-flight CG position estimation, using Kalman filters, accelerometers and the ADMIRE aircraft model, were made by Stanley [61,62]. Similarly, to Idan et al. [12], the technique was developed and applied to a simulated aircraft, rather than a real one.

Eurocopter, now Airbus Helicopters, conducted a review on the feasibility of an onboard W&B system for rotary wing aircraft with wheeled landing gear [63].

Komendat [64] developed a method for estimating the CG position of an aircraft using solely traditional aircraft sensor, including attitude, air data, inertial and GPS models. The method however required the body to be truly rigid, a constant CG position across the period of information collection and the presence of dynamic conditions.

Costello made another contribution to onboard in-flight helicopter W&B estimation in 2015 [65], this time using an extended state observer for online estimation of helicopter mass and centre of gravity. Motion capture cameras were used in combination with flight test maneuvers designed to excite the steady-state and dynamic responses of the vehicle. The lateral and longitudinal CG locations could be estimated accurately, but the vertical CG position was harder to determine due to limited observability during maneuvers.

Thaiss and Caplan used a combination of artificial neural networks and Kalman filters to develop estimation models based on flight test data [66].

Currently, the use of fiber Bragg grating technology, which is sensitive to strain, for onboard and in-ground W&B has been explored [67].

The present work combines, for the first time, the use of conventional regression analysis with flight data of regular commercial flights to develop an onboard in-flight W&B estimator [13].

3 Methodology

3.1 Onboard Weight Measurement and Correction

The current passenger and cargo dispatching methodology is based on standardized weights for passengers and hand luggage to calculate aircraft weight data that is introduced into the Flight Management System. From this, a potential source of error for passenger's weight and respective carry-on luggage arises. However, since during cruise lift is equal to weight, it is possible to determine and correct weight information through the lift coefficient and atmospheric air properties in an existing permanent cruise flight setting, Equation 3.1. The weight can be calculated from:

$$W = q_{\infty} S C_L \quad 3.1$$

where C_L is the lift coefficient; S the wing planform area; q_{∞} is the relative wind dynamic pressure:

$$q_{\infty} = \frac{1}{2} \rho_0 EAS^2 \quad 3.2$$

where EAS is the Equivalent Air Speed; ρ_0 is the International Standard Atmosphere (ISA) mean sea level air density, 1.225 kg/m³. One problem with Equation 3.2 is that the cruise airspeed is available from the current onboard data acquisition system only in the form of Calibrated Air Speed (CAS). Per reference [68] the EAS can be calculated from CAS using:

$$EAS = k_c CAS \quad 3.3$$

In Equation 3.3, k_c is the compressibility coefficient whose value is 1 if CAS < 200 knots and is otherwise calculated by:

$$k_c = \frac{1}{100} \left(102.5 - \frac{Z \cdot CAS}{12} 10^{-5} \right) \quad 3.4$$

where Z is the altitude in feet and CAS is in knots.

The lift coefficient is a function of angle of attack (α) and Mach number (M). This function is known by the manufacturer and thus determination of weight should be possible from the use of the simple flight mechanics relation of Equation 3.1. To test the validity of such simple approach to onboard aircraft weight measurement, the logged flight data of an airline Airbus's A320-200 fleet was used. However, the C_L function is not known to us. The following section shall describe the method used to attain the relationship between α , M and the lift coefficient to estimate the weight of the aircraft. The primary uncertainty for the measured altitude is ± 0.5 feet and ± 0.5 m/s for CAS based on a datasheet provided by the airline. The uncertainty in the measured weight data is 2%.

3.2 Estimating the Lift Coefficient Function

The weight estimate comes from the values introduced by the crew. Since these values are based on standard values derived from statistical averages, an assumption is made that over the course of several flights the data points will become statistically distributed around a position which over time should approach the actual weight of the aircraft.

Thus, the lift coefficient should too become distributed around the actual lift coefficient. Its value can thus be estimated using Equation 3.5 from the weight estimate introduced by the crew and the logged flight data. Combining Equations 3.1 through 3.3:

$$C_L = \frac{2W}{\rho_0 k_c^2 CAS^2 S} \quad 3.5$$

where k_c is estimated from Equation 3.4.

To derive the C_L function, the α and Mach number of each CAS data point must be registered. This produces a dispersion of data points on a C_L vs α plot for each Mach number that expresses the true function of C_L which can be found using linear regression. To create a uniform function for all Mach numbers, non-linear and linear regressions were used to create a single function that estimates lift coefficient based on Mach number and angle of attack. Since the Mach number influences the lift versus α curve slope, then, the slope for each M is used as a measure of whether there is sound basis to the method by checking its obtained values against those estimated with a theoretical model [69]. Accordingly, the compressible branch of the lift curve slope can be calculated from:

$$\frac{\partial C_L}{\partial \alpha_{Compressible}} = \frac{a_0 \cos \Lambda}{\sqrt{1 - M_\infty^2 \cos^2 \Lambda + \left(\frac{a_0 \cos \Lambda}{\pi A}\right)^2} + \left(\frac{a_0 \cos \Lambda}{\pi A}\right)} \quad 3.6$$

While the incompressible branch is calculated by:

$$\frac{\partial C_L}{\partial \alpha_{Incompressible}} = \frac{a_0 \cos \Lambda}{\sqrt{1 + \left(\frac{a_0 \cos \Lambda}{\pi A}\right)^2 + \left(\frac{a_0 \cos \Lambda}{\pi A}\right)^2}} \quad 3.7$$

where a_0 is the lift-curve slope given by thin airfoil theory (2π), Λ is the wing sweep and A is the aspect ratio.

3.3 Flight Logged Dataset

The data for this study was gathered from the A320's "Cruise Performance Reports <02>". This data was provided by an airline sponsoring the project. One of the functions of the Data Management Unit/ Flight Data Interface Management Unit (DMU/FDIMU) is the generation of aircraft and engine reports as result of triggering settings. These reports are part of the Airbus Standard Report which is a set of pre-programmed Aircraft Integrated Data System/Aircraft Condition Monitoring System (AIDS/ACMS) reports that are operative at delivery of the DMU/FDIMU [70]. The process by which these reports are produced and their contents have been defined and validated by Airbus and they depend on the aircraft and engine types [70].

A dataset was used to develop the current W&B estimator and was labeled the development dataset; this set had $n = 4225$ data points, however some of these were corrupted (missing data on some of the cells of the file received) and had to be filtered into non-usable data points and usable data points. Out of the initial $n = 4225$ points there were $n = 4184$ usable data points. The quality of the data points must be taken in consideration. For this, Airbus defined the Aircraft Quality Number (QA) which is defined as:

$$QA = \sum \bar{W}(N) \frac{VAR(N)}{TOL(N)^2} \quad 3.8$$

where N is the parameter number (it can be the $N1$, fuel flow...), $\bar{W}(N)$ is a weighting factor defined by Airbus (between 0 and 1), $VAR(N)$ is the individual variance and $TOL(N)$ is the individual variation value. The lower the QA, the lower the variation of the parameters and the better the stable frame report. A stable frame report happens whenever the variation of the target parameter is within an upper and lower bound (defined by Airbus or the airline), see Figure 3.1 .

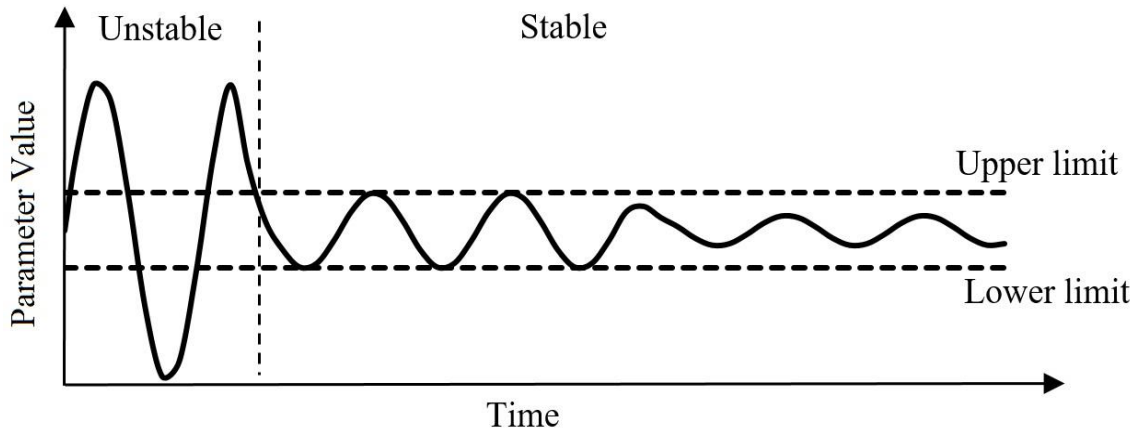


Figure 3.1 - Example of parameter variation. A stable frame report occurs whenever the parameter variation is within prescribed limits for a defined amount of time.

QA varies between 0 and 999. Common values seen in routine monitoring are around 40 [70]. For the development dataset, the average QA was 16.723, 95% CI [16.382, 17.064], which indicates better than average quality of the reports.

A second separate dataset was provided by the airline for validation of the method and was labeled evaluation dataset. The evaluation dataset had $n = 2392$ data points of which $n = 1795$ were usable; the average QA of the evaluation dataset was 21.348, 95% CI [20.782, 21.913], i.e. lower quality than that of the development dataset.

3.4 Centre of Gravity Measurement and Correction

In steady symmetric flight, there is equilibrium between lift L , drag D , thrust T and weight W and the pitching moment M_y on the airplane is zero. Per [12], transforming these forces and moments into standard dimensionless quantities (coefficients), where the product of dynamic pressure q_∞ and wing area S are used as a unit of force and the wing mean aerodynamic chord (c) is used as a unit of length, we get the dimensionless total pitching moment C_M and weight C_W defined by:

$$C_M = \frac{M_y}{q_\infty S} \quad 3.9$$

$$C_W = \frac{W}{q_\infty S} \quad 3.10$$

The dimensionless lift, drag and propulsive forces are obtained in a similar fashion.

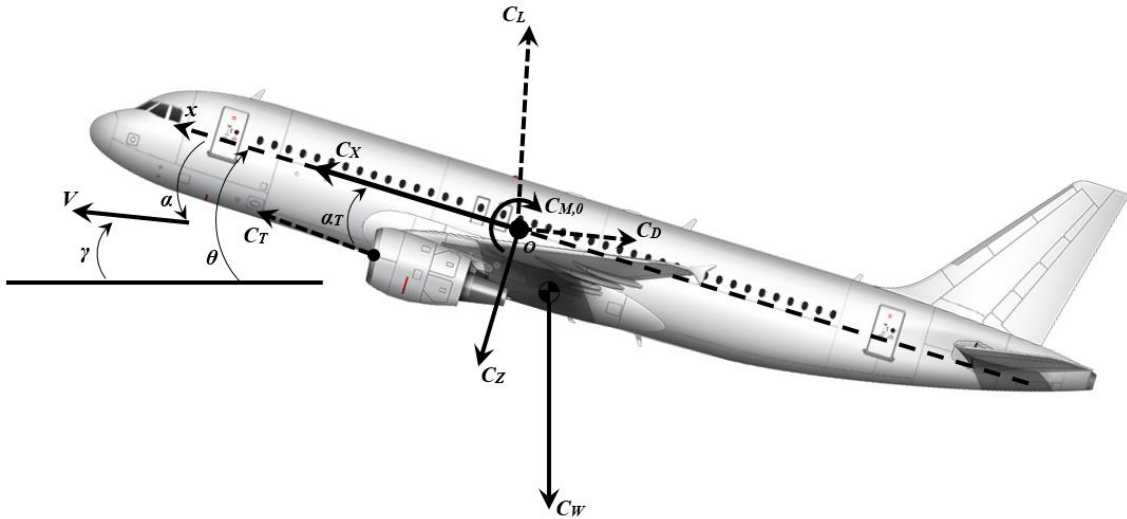


Figure 3.2 - Non-dimensional forces and moments. Image courtesy of <https://www.norebbo.com/>.

Equilibrium condition involves two equations of force balance and one of pitching-moment balance. From Figure 3.2 these are:

$$C_x - C_w \sin \theta = 0 \quad 3.11$$

$$C_z + C_w \cos \theta = 0 \quad 3.12$$

where:

$$C_x = C_L \sin \alpha - C_D \cos \alpha + C_T \cos \alpha_T \quad 3.13$$

$$C_z = -(C_L \cos \alpha + C_D \sin \alpha + C_T \sin \alpha_T) \quad 3.14$$

The conditions for vanishing pitching moment are:

$$C_{M,0} + C_z X_{CG} - C_x Z_{CG} = 0 \quad 3.15$$

where X_{CG} is the centre of gravity position and:

$$C_{M,0} = C_{M,0}^a + C_T X_T \sin \alpha_T + C_T Z_T \cos \alpha_T \quad 3.16$$

$C_{M,0}^a$ is the aerodynamic pitching moment which depends on the elevator deflection. The thrust line angle (α_T) is defined in the aircraft design stage as a function of X_T and Z_T such that the aircraft thrust setting has minimal influence in $C_{M,0}$. So, it is reasonable to assume that $C_{M,0} = C_{M,0}^a$ which is a function of the elevator deflection alone.

Using Equations 3.11 and 3.12 in Equation 3.15:

$$C_{M,0} + C_Z(X_{CG} + Z_{CG} \tan \theta) = 0 \quad 3.17$$

which can be solved for the CG position X_{CG} .

$$X_{CG} = - \left(\frac{C_{M,0}}{C_Z} + Z_{CG} \tan \theta \right) \quad 3.18$$

The pitching moment, lift and drag coefficients are functions of M , α and elevator deflection δ_e only. From Equation 3.18 it is possible to determine the location of the aircraft CG, which has been done previously in [12] using neural networks but only for numerically simulated flight-test data.

However, such implementation might prove rather complex or impractical to perform for routine airline operations. An alternative may be the use of statistical methods in a similar way as described in Section 3.2 for determining the C_L function but, in this case, making use of the available flight data with known estimates of X_{CG} as presented hereafter.

Some assumptions are made. First, it is assumed that Z_{CG} is nearly coincident with the origin of the reference frame and thus that the second term on the right-hand side of Equation 3.18 is negligible. The second and third terms of Equation 3.13 have the same order of magnitude and are opposite thus canceling each other out. As such, it is assumed that only lift coefficient and elevator deflection influence the prediction of X_{CG} position. Information on elevator deflection and stabilizer trim position can come directly from sensing systems on the aircraft, while lift coefficient can also be measured as described in Section 3.1.

To validate this method of determining X_{CG} it was applied to the A320 dataset. In the A320 we have differential elevator and moving stabilizer trim data directly from the aircraft sensors and data collection system. So, different combinations of elevators deflection and stabilizer trim position may result in the same influence on the pitching moment, i.e. due to the same local lift coefficient being produced by the horizontal tail.

Since there is no information available about the airfoils used on the horizontal tail of the A320, it is not possible to use CFD or other similar methods to reliably obtain the lift coefficients produced for every elevator deflection and stabilizer trim position. As such an equivalent horizontal tail deflection, named δ_{HT} , was defined. This δ_{HT} is based on the ratio of chords between the horizontal stabilizer and the elevator of the A320. δ_{HT} is given by:

$$\delta_{HT} = 0.2 \left(\frac{\delta_{Elev1} + \delta_{Elev2}}{2} \right) + 0.8(Stab) \quad 3.19$$

where *Stab* is the stabilizer deflection. The equivalent horizontal tail deflection was used to convert the elevator 1, elevator 2 and stabilizer deflection flight data points into a single δ_{HT} . Multiple linear regression was then used to relate the airplane's δ_{HT} and aircraft C_L with X_{CG} . The regression line produced can then be used in the W&B estimator as a tool to update the information that was originally introduced by the crew. The primary uncertainty in elevator 1 and 2 deflection is $\pm 0.5^\circ$ and $\pm 0.05^\circ$ for the stabilizer deflection based on a datasheet provided by the airline. The uncertainty in the measured X_{CG} data is 1%.

3.5 Regression Analysis

Regression analysis is one of the most widely used techniques to establish a relationship between a set of predictors (sometimes called independent variables) and an outcome (sometimes called dependent variable). In this subsection the basics of linear regression will be covered, for greater insight there are several excellent textbooks that can be referred to [71-74].

The linear univariate regression model between an outcome variable (*Y*) and one or more predictors *X* is given by [72]:

$$Y_i = \beta_0 + \beta_1 X_{i1} + \dots + \beta_n X_{in} + \varepsilon_i \quad 3.20$$

where β_n are the regression coefficients and ε_i is the residual term, which represents the difference between the predicted value and the value obtained. The regression coefficients are usually obtained by the method of least squares, described in detail in [71].

In multiple regression the selection of predictors, and the way in which they are entered in the model, can have a great impact; the predictors should typically be selected based on past research and theoretical importance of the variables [72]. Common methods for entering predictors are the hierarchical method, forced entry and stepwise methods. In hierarchical regression, the predictors are selected based on past work and the researcher selects the order

in which these are entered in the model. In forced entry, all variables are entered in the model simultaneously and selection of predictors is also based on theory. Stepwise methods include the forward and the backward method. In the forward stepwise method, the computer selects the predictor that best predicts the outcome variable, then it looks for the second variable and so forth until none of the predictors available can make a statistically significant contribution, based on a user defined level. Backward methods do the same but in reverse; the model starts out with all available predictors and, at each step, the predictor that makes the least contribution is dropped. Stepwise methods are thus guided purely by mathematical criteria, removing the bias that a researcher could have. However, stepwise methods are also criticized since statistically significant regression equations, that have been developed through this method, may not have any significance from an explanatory point of view; case in point, if you attempt to create a regression to explain global warming and use the number of pirates as a predictor, you may just find that the two are correlated, i.e. you could say that global warming is caused by a decrease in the global pirate population. This is obviously silly. Thus, stepwise methods are best used when there is an emphasis on pure predictability rather than explanatory (theoretical) power, or when the model building is exploratory [72].

Another important consideration is the sample size. The sample size required depends on the effect size (how well the predictors predict the outcome) and on statistical power to detect these effects. If the expected effect size is large, a sample size of 80 is sufficient all the way up to 20 predictors. If the expected effect size is medium, a sample size of 200 is sufficient all the way up to 20 predictors. To detect small effects sizes, at least 600 cases are needed for 2 predictors [75].

To assess how well the model fits the data (goodness of fit), the following statistics are used: coefficient of determination (R^2), F-test and t-test. The coefficient of determination is given by:

$$R^2 = \frac{SS_M}{SS_T} \quad 3.21$$

where the numerator term is the model sum of squares and the denominator the total sum of squares. The coefficient of determination is the percentage of response variable variation that is explained by the linear model.

The F-test provides a formal hypothesis test for the statistical significance of the relationship between the model and the response variable. Good models have large F-values (larger than 1); the exact magnitude is assessed using critical values for the corresponding degrees of freedom. The F-test value is given by:

$$F = \frac{R^2(n-k-1)}{k(1-R^2)} \quad 3.22$$

where R^2 is the coefficient of determination, n the sample size and n the number of predictor variables.

The t-test statistic tests if an individual variable significantly predicts the outcome (regression coefficients significantly different from 0). The t-test statistic is given by:

$$t = \frac{r}{\sqrt{\frac{1-r^2}{n-2}}} \quad 3.23$$

where r is the correlation coefficient and n the sample size.

Both the F-test and t-test constitute hypothesis tests. The F-test is used to check if any of the predictor variables influence the outcome variable, i.e., if the adjusted model is significant [71]; this is a hypothesis test where the null hypothesis is that one or all the regression coefficients are zero, and the alternative hypothesis is that there is at least one regressor different from zero. The t-test, as stated before, is used to test individual predictors, i.e., a hypothesis test where the null hypothesis is that the individual regression coefficient is zero, and the alternative hypothesis is that the regression coefficient is significantly different from zero. The F-test has a F-Snedecor distribution with p and $(n-p-1)$ degrees of freedom, where p is the number of predictors and n the sample size. The t-test has a t-Student distribution with $(n-p-1)$ degrees of freedom. The null hypothesis is rejected, in both cases, if $p\text{-value} < \alpha$. The value α is the significance level; this is the probability of rejecting the null hypothesis when the null hypothesis is true, i.e., a type I error. Traditionally, α is set at 0.05. The p-value is the probability of obtaining a result as extreme or more extreme than the result obtained when the null hypothesis is true; it allows to infer if a result is statistically significant or if it may result from pure luck alone.

Finally, to make sure that the model is generalizable, a set of assumptions must be met. These are:

- Linearity: The mean values of the outcome variable for each increment of the predictors should lie along a straight line [72]. It is assumed that the relationship between predictors and outcome is a linear one.
- Independence of errors: The residual terms should be independent, i.e. uncorrelated with each other.
- Homoscedasticity: The variance of the residuals should be constant; at each value of the predictor variable, the outcome variables should have the same variance.

- Multicollinearity: Predictors should not be highly correlated with each other.
- Normality of errors: Errors should be normally distributed.

If assumptions are violated, there are a few options available, such as robust regression or transformation of the raw variables [72].

The previous paragraphs provide an idea of the very basics of linear regression methods; further details are provided throughout the rest of this work as well as on the cited bibliography.

4 Results and Discussion

4.1 Lift Coefficient Determination

A simple linear regression was calculated to predict lift coefficient based on angle of attack. This was done for different Mach numbers as discussed in Section 3.1. Regarding the Mach numbers that had adequate amount of data for analysis were Mach 0.76, $n = 28$ data points, Mach 0.77, $n = 42$ data points, Mach 0.78, $n = 260$ data points, Mach 0.79, $n = 97$ data points and Mach 0.80, $n = 53$ data points. Based on the methodology described in [71], model assumptions were analyzed for linearity, normality, homogeneity and statistical independence of the errors, see Appendix A. Table 4.1 below summarizes the results for the regressions. Figure 4.1 and Figure 4.2 provide a visual representation of the same results.

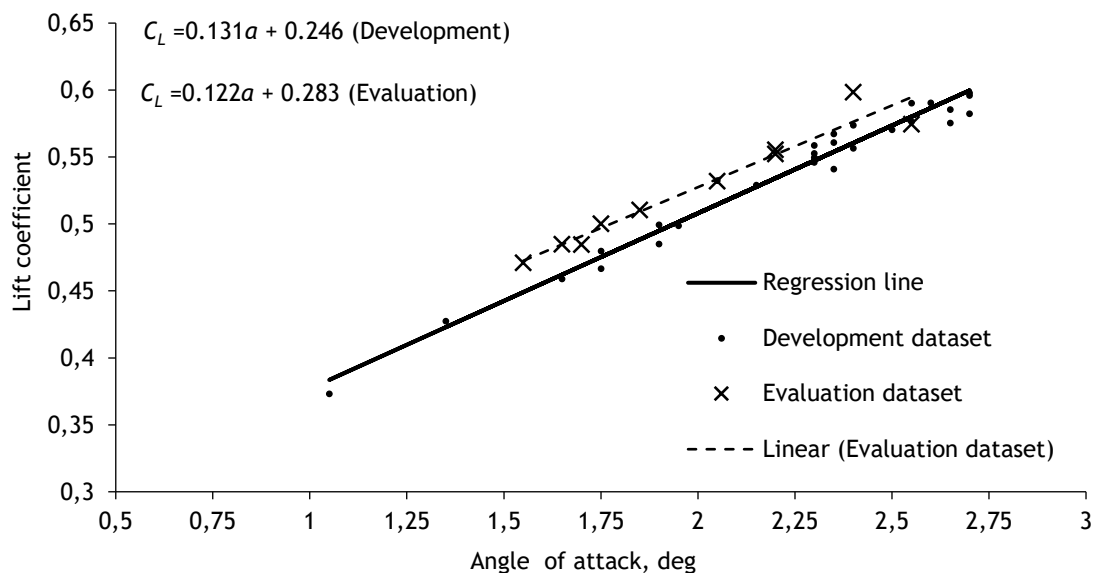


Figure 4.1 - Data points and linear regression line for Mach 0.76.

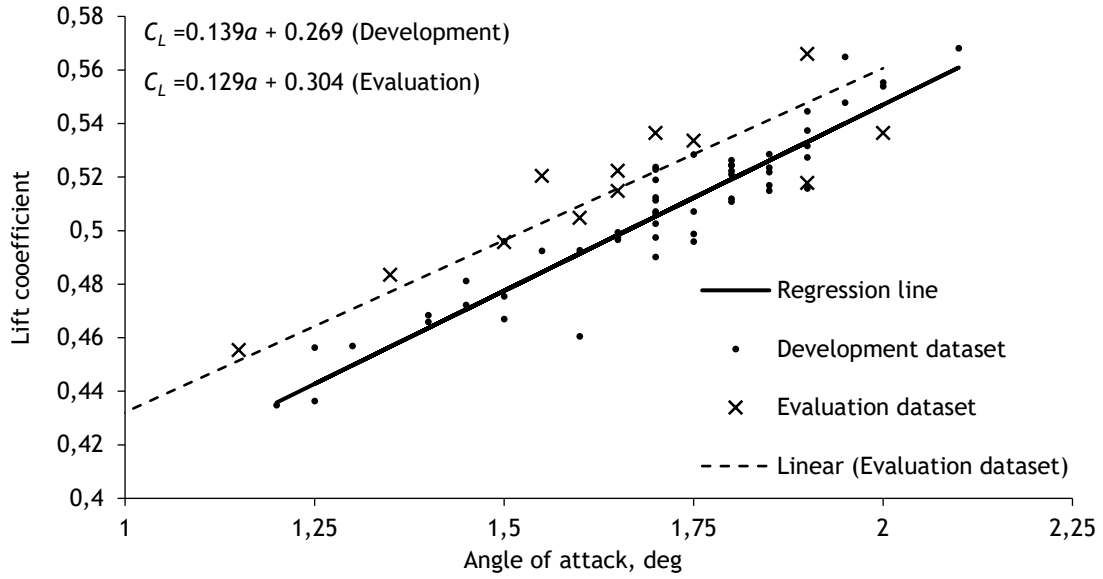


Figure 4.2 - Data points and linear regression line for Mach 0.80.

Table 4.1 - Summary of the results for the linear regressions.

Mach Number	F	R^2	B	B	t	95% CI for B	
	df		Intercept			Lower	Upper
0.76	1274***	0.98	0.131	0.990	35.36***	0.113	0.149
	1, 25		0.246				
0.77	760***	0.95	0.139	0.975	27.26***	0.121	0.157
	1, 39		0.241				
0.78	2402***	0.90	0.142	0.950	48.99***	0.120	0.158
	1, 257		0.245				
0.79	1323***	0.93	0.144	0.966	36.23***	0.126	0.162
	1, 94		0.247				
0.80	529***	0.91	0.139	0.955	22.73***	0.119	0.159
	1, 50		0.269				

Note. F , F-test statistic; df , degrees of freedom; R^2 , coefficient of determination; B , unstandardized slope; B , standardized slope; t , t-test statistic; CI, confidence interval. * $p < 0.05$, ** $p < 0.01$ and *** $p < 0.001$.

All regressions are highly significant as demonstrated by the p-value of the F-test statistic and with a high coefficient of determination which indicates that the model fits the data well (also an indication that a high number of the variance on the lift coefficient is explained by the angle of attack, which is per theory). Looking at the unstandardized slope and the associated 95% CI we see that it does not include zero, an indication that angle of attack influences the lift coefficient, as predicted in theory. The unstandardized slope in the context of this work is simply the lift curve slope. On the other hand, the standardized slope, sometimes called standardized beta, provides information on how many standard deviations a dependent variable will change per standard deviation increase in the predictor variable. In the context of univariate regression, it also works similarly to the correlation coefficient and thus the closer to 1 or -1 the stronger the relationship between independent and dependent variable. The unstandardized and standardized slopes are highly significant (as shown by the t-test statistic) with the standardized slope approaching the value of 1. The previous results show that linear regression models adapt well to our data and are valid for the purposes of this work. Some of the data points revealed a large deviation from the regression line. These points could be revealing of instances where current W&B methodologies have led to large discrepancies between the calculated and the actual weight. For the evaluation dataset, these large deviations can also be caused by discrepancies between the calculated and the actual weight, but the lower quality of the dataset also contributes to this effect (due to larger fluctuations when capturing the stable frame report). Figure 4.3 shows the compilation of the linear regressions obtained for all cruise Mach numbers.

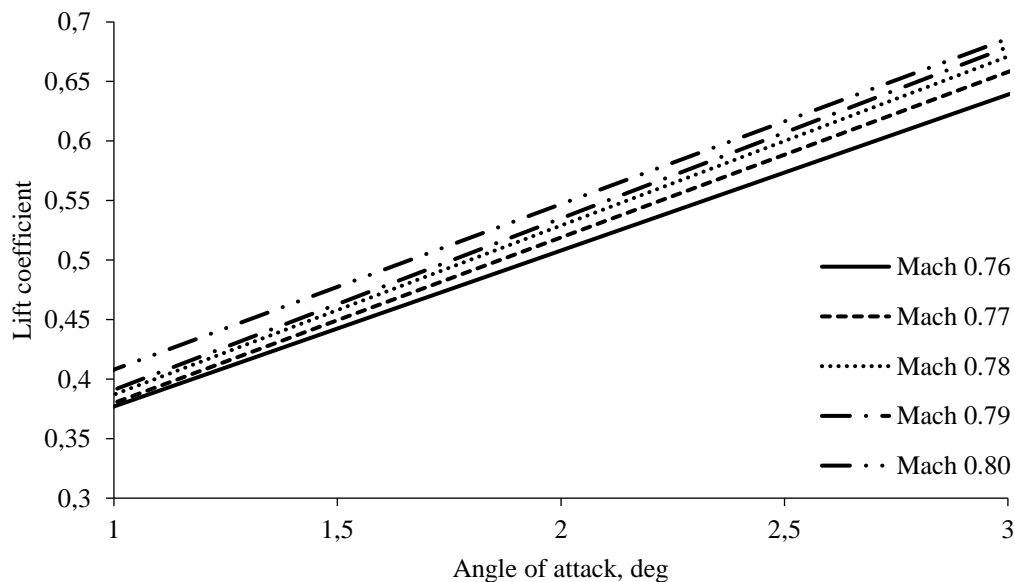


Figure 4.3 - Obtained lift curves for the different Mach numbers (development dataset).

After obtaining the lift curve slopes for different Mach numbers, these were compared with the values of the Kuchemann theoretical model, see Figure 4.4 .

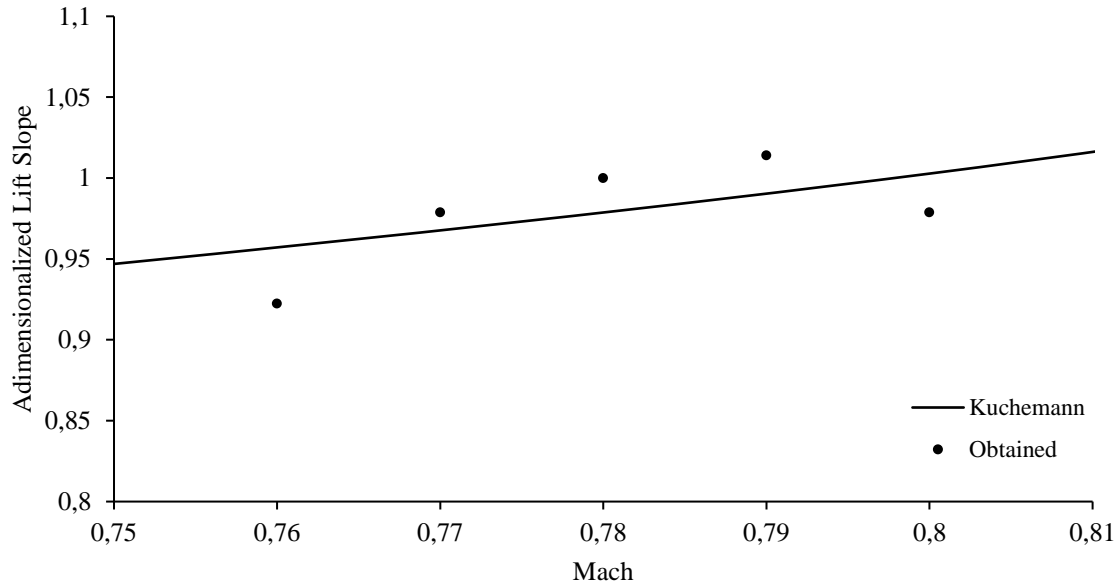


Figure 4.4 - Estimated Airbus A320 lift curve slope vs Mach number based on Kuchemann [66] and obtained from flight data. Non-dimensionalized by the Mach 0.78 lift slope value.

There is a good agreement between the theoretical model and the values that were experimentally obtained. This provides further evidence that the model is sound.

The previous results were used to create a single function that estimates lift coefficient based on Mach number and angle of attack. The equation developed was:

$$C_L = (-16.490M^2 + 25.903M - 10.050)\alpha + 0.287 \quad 4.1$$

The non-linear term of Equation 4.1 was determined using a non-linear quadratic regression.

This constitutes a significant regression equation, with $F(1, 478) = 2854$, $p < 0.001$, with an $R^2 = 0.85$. The 95% CI was [-30.28, -8.29] for the first parameter of the non-linear term, [13.14, 47.45] for the second parameter and [-18.44, -5.07] for the constant. The standard error of the estimate was 0.001165. Linear regression models are restricted equations where each term must be either a constant or the product of a parameter and a predictor variable and the equation is a sum of each of these terms. Because of this, it is possible to develop a hypothesis test where the parameters are either zero, having no effect, or different from zero, thus having

an effect in the response value. The p-value tests this null hypothesis in linear regression. Non-linear models can have several different equations with few restrictions on how parameters are used, bringing flexibility to the curve fitting; however, the null hypothesis value for each parameter depends on the expectation function, the place of the parameter in the expectation function and field of study. For this reason, and since expectation functions can vary so much, it is impossible to have a hypothesis test that works for all non-linear models. This also invalidates the use of p-values and R^2 to determine the significance and goodness of fit of non-linear models and as such, p-values and R^2 are not presented for the non-linear regression [76]. Instead, the standard error of the regression and the confidence intervals around each parameter were provided to assess the model fit. The fitting was considered acceptable.

4.2 Cruise Flying Weight Estimation

After obtaining the regression lines for the lift coefficient, it is finally possible to estimate and update the weight information based on lift coefficient, density, speed and wing surface area, as described in Section 3.1.

Figure 4.5 a) shows the results for the cruise flying weight versus the lift coefficient in a scatter plot. The data scatter is explained by the fact that the points in the graph are from different flights. The scatter also appears to be random meaning that the flying weight and the lift coefficient are independent variables.

Figure 4.5 b) shows the results for the cruise flying weight versus the equivalent horizontal tail deflection in a scatter plot. Here, the scatter seems not totally random and the motive can be that a horizontal tail deflection can, in fact, have an influence in the lift coefficient for a given angle of attack. Nevertheless, the data was not sufficient to obtain a reliable correlation function.

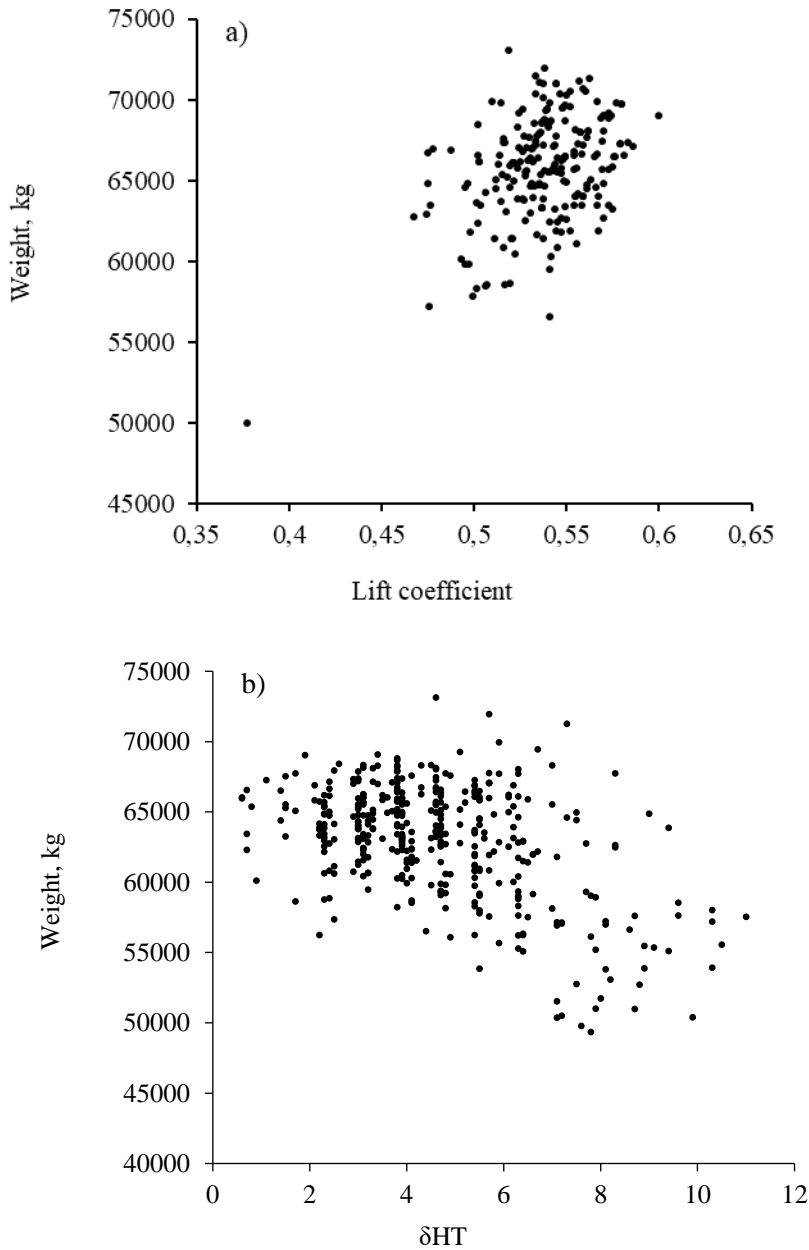


Figure 4.5 - Distribution of points with constant δHT ($\delta HT=5.4$) and 4.5 b) Distribution of points with constant lift coefficient ($CL=0.5$).

The cruise flying weight estimator was tested using the evaluation dataset to check how well the curves developed fit a different dataset.

The average mass standard error of the estimate for the regressions was 1236 kg. This value corresponds to about 1.9% of the development dataset mean cruise flying weight. Comparing the values introduced by the crew into the flight management computer with the expected or statistically predicted values it was verified that for the development dataset, in 99% of the tested points the error was no greater than 3408 kg, see Figure 4.6 .

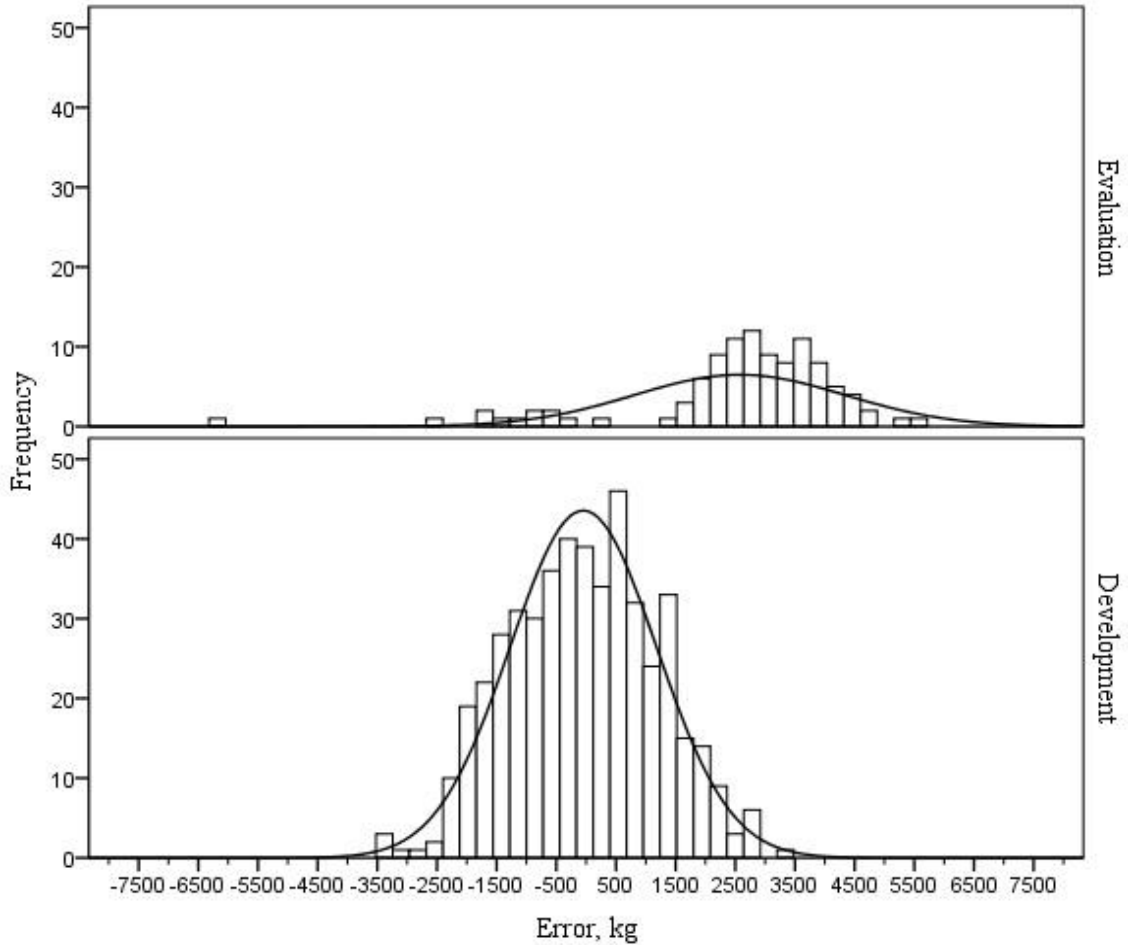


Figure 4.6 - Distribution of weight estimation error for the development dataset and for the evaluation dataset.

When applying the developed equation to the evaluation dataset, in 99% of the tested points the error was no greater than 6193 kg, see Figure 4.6 . The average error for the evaluation data set was 2574 kg, 95% CI [2227, 2921].

For the single function, Equation 4.1, the mass standard error of the estimate was 1501 kg. After obtaining the linear regression it is possible to compare the values introduced by the crew into the flight management computer with the expected or statistically predicted values. It was verified that for the development dataset, in 99% of the tested points the error was no greater than 5200 kg, see Figure 4.7 .

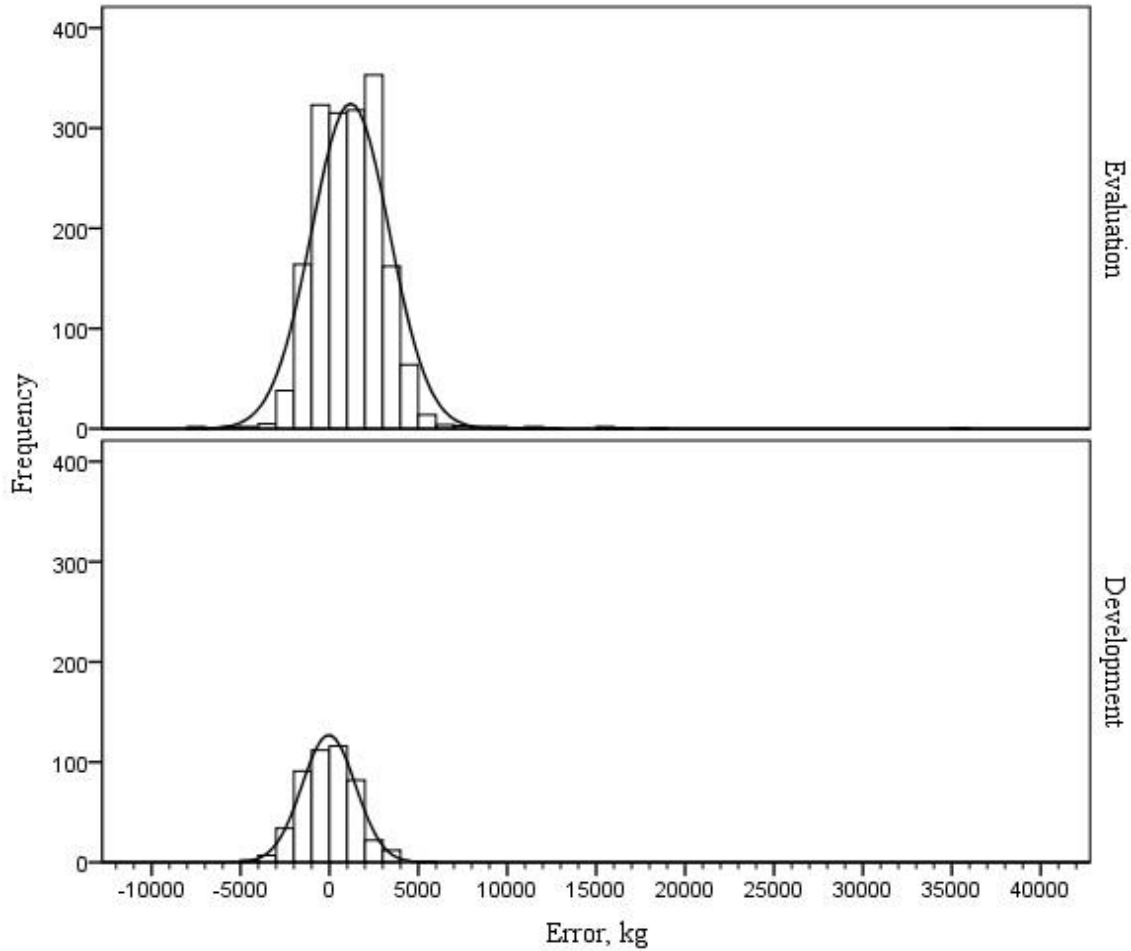


Figure 4.7 - Distribution of weight estimation error for the development dataset and for the evaluation dataset using a single function.

When applying the developed equation to the evaluation dataset, in 97% of the tested points the error was no greater than 5000 kg, see Figure 4.7 . The average error for the evaluation data set was 1182 kg, 95% CI [1080, 1284]. This reveals that the estimator had a good adaptation and predictive power for the evaluation dataset even though the dataset included data points with Mach values between 0.70 through 0.75. There were however some extreme outliers such as one data point with a difference over 35000 kg. These data points are associated with low Mach numbers, well outside the range for which the estimator was developed and could be a result of that.

4.3 Centre of Gravity Position Estimation

As described in Section 3.2, multiple linear regression was used to obtain from the airplane’s cruise trim horizontal tail equivalent deflection position and the lift coefficient obtained in Section 4.1. Model assumptions were analyzed namely linearity, normality, homogeneity and statistical independence of the errors, see Appendix B. Table 4.2 below summarizes the results for the multiple linear regression.

Table 4.2 - Summary of the results for the multiple linear regression.

F	R^2	Variable	B	B	t	95% CI for B	
df						Lower	Upper
9885***	0.83	CG	-0.591	-0.908	-139.093***	-0.598	-0.583
2, 3984		CL	14.749	0.232	35.586***	13.937	15.560

Note. F , F-test statistic; df , degrees of freedom; R^2 , coefficient of determination; B , unstandardized slope; B , standardized slope; t , t-test statistic; CI, confidence interval. * $p < 0.05$, ** $p < 0.01$ and *** $p < 0.001$.

Equation 4.2 presents the obtained regression solved for X_{CG} . The standard error was 1.35% of the MAC. Figure 4.8 shows the corresponding data dispersion, which is a consequence of the load and trim sheet methods currently in use (which use standard passenger weights and moment arms and indices to calculate the X_{CG} position), causing a statistical distribution of points around a position which over time should approach the actual X_{CG} position.

$$X_{CG} = 24.956 C_L - 1.692 \delta_{HT} + 25.928 \tag{4.2}$$

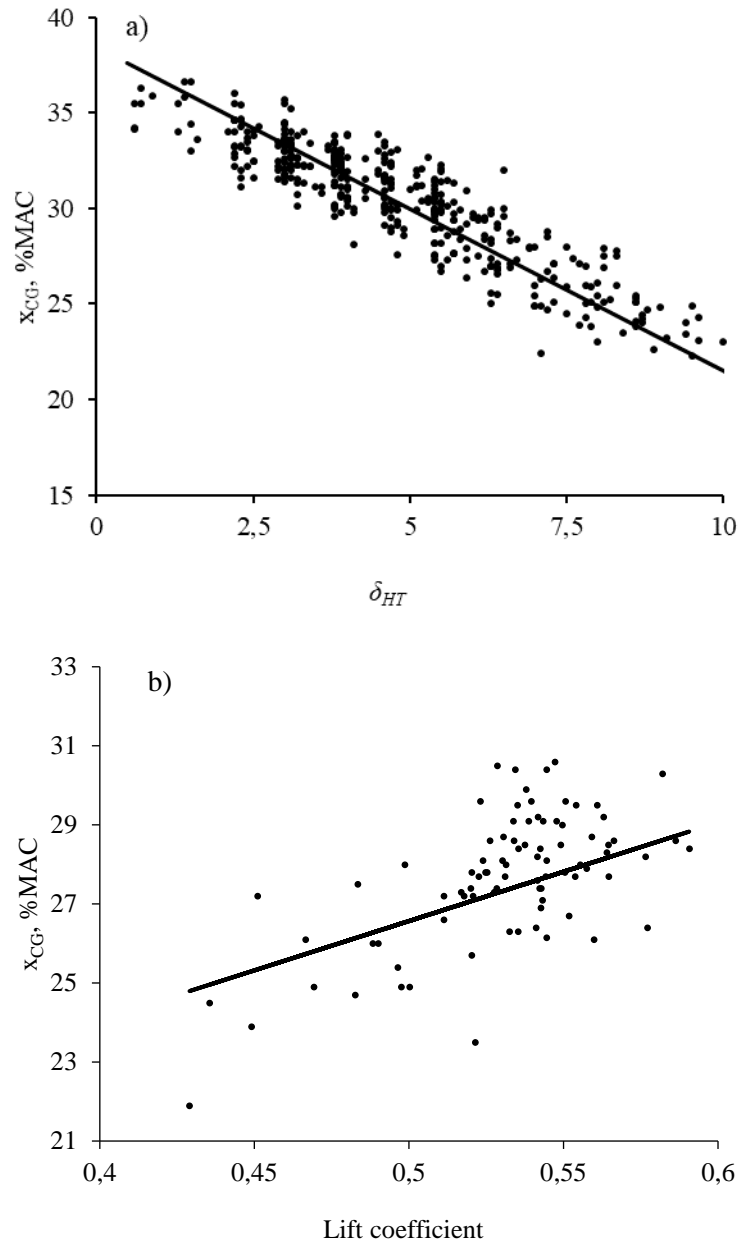


Figure 4.8 - a) Data points dispersion and prediction line with constant lift coefficient ($CL = 0.5$) and b) Data points dispersion and prediction line with constant δ_{HT} ($\delta_{HT} = 7$ deg).

After obtaining the linear regression line it is possible to compare the values introduced by the crew into the flight management computer with the expected or statistically predicted values. It was verified that for the development dataset, in 99% of the tested points the error was no greater than 3.15% of the MAC, see Figure 4.9 . When applying the developed equation to the evaluation dataset, in 99% of the tested points the error was no greater than 9.62% of the MAC. The average error was 1.24 % of the MAC, 95% CI [1.155, 1.328]. Please refer to Figure 4.9 .

The results suggest that the current weight and balance procedures do produce discrepancies between the CG position introduced by the crew and the true CG position although, for the most part of the data points, such discrepancies do not appear to be large enough to seriously jeopardize the safety of the flight.

The methods previously presented are subject to improvement over time. As flights are performed and more data points are produced better estimates can be attained, especially if the data points are of good quality. What this means to airlines is that conditions that can lead to better quality of the data points should be pursued. This can be achieved through proper maintenance of sensors and associated systems. Another method to achieve better quality of the data points is by making the criteria that lead to the recording of a stable frame report stricter [77].

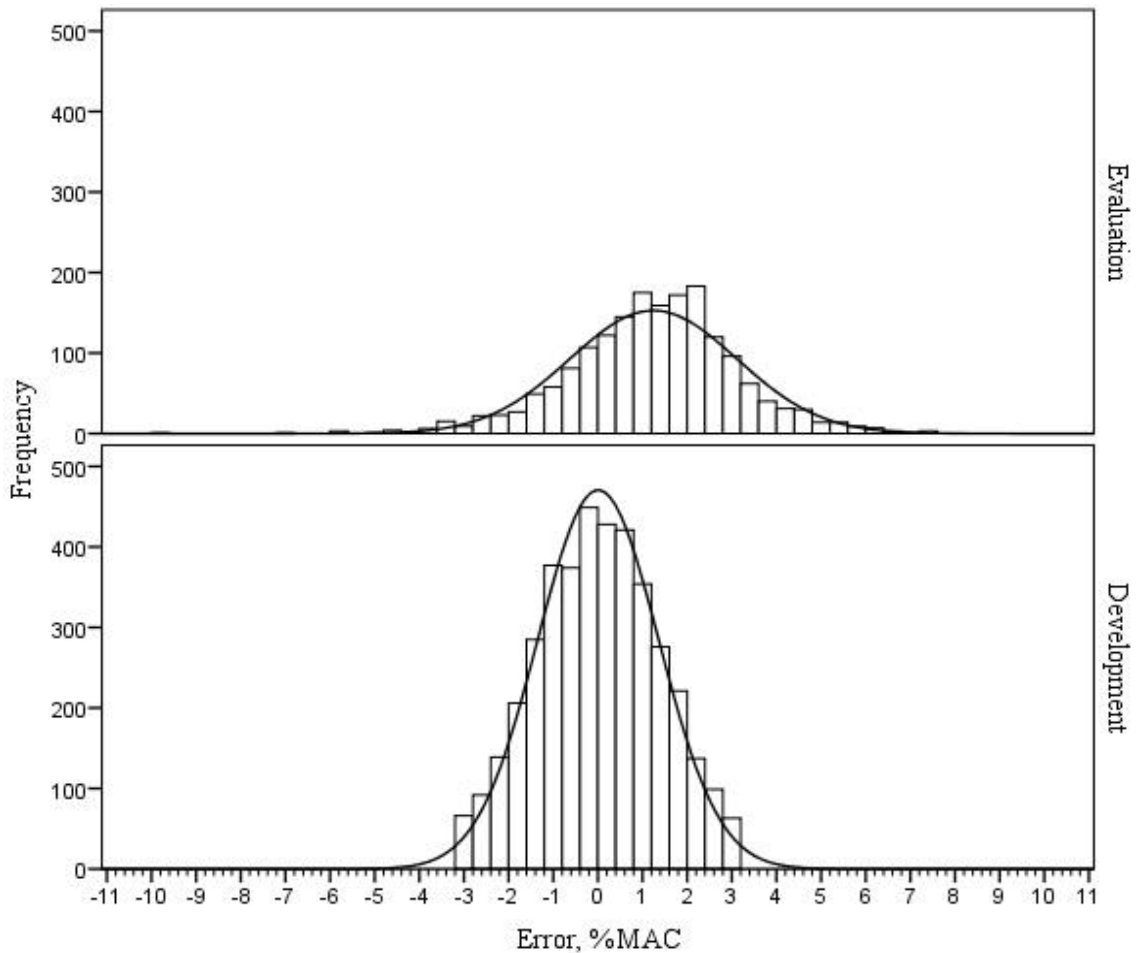


Figure 4.9 - Distribution of centre of gravity estimation error for the development dataset and for the evaluation dataset.

The system, as it was presented herein, is dependent on how accurate the development dataset is for the W&B data. This means that the estimator is also sensitive to the accuracy of the current standard passenger weights making it dependent on authorities, such as the FAA, since these are the entities responsible for the publishing and definition of these weights [78]. The deviations in weight in the evaluation dataset confirm that the system is susceptible to the quality of the data (the evaluation dataset had a higher QA, i.e., lower quality), but this problem should be easy to solve if accurate development datasets are used to improve the estimator, either by properly maintaining the aircraft systems, or by making the allowed parameter variation stricter [77]. These two faults can be resolved through a partnership with the manufacturer. Conceptually, using a combination of modern CFD, wind tunnel testing and flight testing, there is no reason why a modern airliner cannot be fully characterized in such a way, namely in the lift slope versus Mach number and CG position versus cruise elevator trim setting, as to allow the creation of a modern onboard in-flight weight and balance system that functions on the readings of angle of attack, Mach number, elevator deflection and thrust line effects. To this end and to better measure the accuracy of the proposed estimator, flight testing with well-defined centre of gravity positions and weights can be conducted, preferably by the manufacturer. After such assessment is made, and based on the flight test results, it should be determined if the methodology meets the criteria for onboard weight and balance systems [79].

Also, the results expose instances where there were large deviations between the weight predicted and the weight introduced by the crew, one can wonder if these were flights where the use of standard weights was inadequate and lead to significant error. Interestingly, the FAA is currently working on a draft for an update of the AC120-27E. The draft, named AC120-27F, will further increase standard weights revealing that the FAA acknowledges the need to consistently revise standard weights, another disadvantage of current methodologies [80].

To provide an idea of how the estimator may be used and the influence it can have in fuel consumption, we will offer a concise example. Suppose an A320 is cruising at 35000 feet; at this altitude, all else being equal, every additional ton represents an average increase in fuel consumption of 17.6 kg per engine per hour (values based on flight crew operating manual and considering cruise at optimum airspeed). The weight at the beginning of the cruise, because of the use of standard weights, is estimated at 64000 kg. At this weight, optimum speed would be around Mach 0.781. For the purposes of illustrating the use of the estimator, presume the pilot receives an indication from the system that points to actual weight being 60000 kg. At this stage, the pilot should first look for evidence that supports the indication: Was the aircraft accelerating faster than expected during the takeoff run? Was the aircraft “light” during rotation? Does current fuel flow match the expected values for the present conditions? If the evidence supports the indication the pilot may then adjust the cruising speed accordingly. At 60000 kg and cruising at 35000 feet, optimum speed is Mach 0.771. Optimizing the Mach number

would result in a reduction of fuel consumption of 19 kg per engine per hour, a seemingly small saving that can accumulate to several tons over the course of many flights. As for the influence of the centre of gravity, Airbus claims that due to complex aerodynamic interactions, centre of gravity position does not affect fuel consumption on the A320 [18]. Our data suggests there is a very small decrease in fuel consumption when the centre of gravity is near the rear limit, however fuel consumption modelling and discussion is beyond the scope of this work. The estimator can also be implemented in flight data monitoring programs for the detection of abnormal weight or centre of gravity deviations from expected values.

5 Conclusion

5.1 Summary

Weight and centre of gravity position information has been surveyed from data provided by a sponsoring airline with the objective of laying the foundation for further development of a new onboard W&B estimator tool.

The results, namely the good agreement between the lift slopes calculated and those of the theoretical model, suggest that there is a sound basis to the approach that was used. This may have significant implications since, so far, all efforts to develop onboard W&B systems relied on the addition of complex sensors, usually to the landing gear in the case of on-ground systems, or accelerometers combined with comparatively more complex theoretical formulations for in-flight estimator systems. Such approaches result in higher maintenance requirements to ensure calibration is maintained, higher maintenance costs as well as an increase in acquisition costs for the airlines since the aircraft comes equipped with more sensors. The use of sensors which are already available on the aircraft in combination with a simple theoretical formulation solves all these problems and provides an attractive alternative for airlines and manufacturers alike since development and implementation costs of the system, as presented, should be low. Through a simple software update this W&B estimator could be implemented. W&B information could be displayed to the pilot in-flight on one of the screens of the aircraft; a simple look-up table can also suffice.

However, the method does have its flaws. There is a trade-off between simplicity of the formulation and precision. This results in the simplest estimator to date but also the least precise. Since the system is not on-ground, it cannot be used as a faster dispatching tool and neither can it identify a serious W&B problem before flight which may lead to accident. On aircraft without trim tanks the pilot does not have the means to make use of the information to rebalance the aircraft, but it does have the chance to update weight information for the cruise phase and for the landing.

5.2 Future Work

A replication of this study but with data from other airlines, particularly airlines with large fleets and many flights per year, would quickly allow for the validation of the method presented herein and for its further development. The simplicity of the methodology means this could be done rather quickly. The methodology presented can also be used to develop events for Flight Data Monitoring (FDM) purposes.

The presence of onboard and in-flight W&B systems may provide different means for the detection of ice accumulation during flight. This could be done by detecting abnormal changes in weight during flight or detection of abnormal changes on the aerodynamic characteristics of the aircraft due to the formation of ice on the aerodynamic surfaces. In flight ice detection, has been addressed by researchers by more complex means [81,82].

Bibliography

- [1] J.G. Wensveen, *Air Transportation: A Management Perspective*, 7th Ed., Ashgate Publishing, 2011.
- [2] V. Singh, S.K. Sharma, Erratum to: Fuel consumption optimization in air transport: a review, classification, critique, simple meta-analysis, and future research implications (*Eur Transp Res Rev*, 10.1007/s12544-015-0160-x), *Eur. Transp. Res. Rev.* 8 (2016) 1. doi:10.1007/s12544-016-0193-9.
- [3] S. Dekker, C. Pitzer, Examining the asymptote in safety progress: A literature Review, *Int. J. Occup. Saf. Ergon.* 22 (2016) 57-65. doi:10.1080/10803548.2015.1112104.
- [4] SATA, *Relatório e Contas 2015 - Relatório Integrado Consolidado*, 2015.
- [5] IATA, *IATA Economic Briefing: Airline Fuel and Labour Cost Share*, 2010.
- [6] IATA, *US DOT 41 Airline Operational Cost Analysis Report*, 2011.
- [7] IATA, *Economic Performance of the Airline Industry*, 2015.
- [8] A. Filippone, *Advanced Aircraft Flight Performance*, Cambridge University Press, New York, 2012.
- [9] T. Gabriel, J.M. Silva, P. Gamboa, J. Silva, J. Viegas, N. Leal, An Optimized Approach to Reduced Fuel Costs in the Operational Procedures of an Airline, in: *8th World Congr. Struct. Multidiscip. Optim.*, Lisbon, 2009.
- [10] NTSB, *Loss of Pitch Control During Takeoff, Air Midwest Flight 5481, Raytheon (Beechcraft) 1900D, N233YV, Charlotte, North Carolina, January 8, 2003.*, Washington, DC, 2004.
- [11] G.W.H. van Es, *Analysis of aircraft weight and balance related safety occurrences*, 2007.
- [12] M. Idan, G. Iosilevskii, S. Nazarov, In-Flight Weight and Balance Identification Using Neural Networks, *J. Aircr.* 41 (2004) 137-143. doi:10.2514/1.592.
- [13] F.A.V. Chaves, M.A.R. Silvestre, P.V. Gamboa, Preliminary development of an onboard weight and balance estimator for commercial aircraft, *Aerosp. Sci. Technol.* 72 (2018) 316-326. doi:10.1016/j.ast.2017.11.018.
- [14] E. Westrum, *Load Indication Gauge for Vehicles*, U.S.Patent: 1,864,876A, 1932.
- [15] M. Sequeira Dias, *Diário de Navegação. 50 anos de operação da SATA*, SATA, Ponta Delgada, 1997.
- [16] ICAO, *Annex 6: Operation of Aircraft*, in: *Conv. Int. Civ. Aviat.*, 2010.
- [17] FAA, *Aircraft Weight and Balance Handbook*, U.S. Department of Transportation, 2016.
- [18] Airbus, *Getting to Grips with Weight and Balance*, Flight Operations Support & Line

Assistance, 2004.

- [19] D. Melis, J. Silva, M. Silvestre, R. Clothier, Characterisation of the Anthropometric Features of Airline Passengers and their Impact on Fuel Usage in the Australian Domestic Aviation Sector, in: 17th Aust. Aerosp. Congr., 2017.
- [20] D. Melis, J. Silva, R. Yeun, Impact of Biometric and Anthropometric Characteristics of Passengers on Aircraft Safety and Performance, *Transp. Rev.* (2017). doi:10.1080/01441647.2017.1396264.
- [21] Airbus, Optimum CG Position, in: 16th Perform. Oper. Conf., 2009.
- [22] J. Roskam, C.-T. Lan, *Airplane Aerodynamics and Performance*, Roskam Aviation and Engineering Corporation, 2000.
- [23] J.D. Anderson, *Aircraft Performance and Design*, McGraw Hill Co., 1999.
- [24] B.W. McCormick, *Aerodynamics, Aeronautics, and Flight Mechanics*, John Wiley & Sons, 1979.
- [25] J. Reason, *Human Error*, Cambridge University Press, 1991.
- [26] ATSB, *Aircraft loading occurrences*, 2011.
- [27] ATSB, *Take-off performance calculation and entry errors: A global perspective*, 2011.
- [28] NASA, *Callback Number 291*, (2003).
- [29] B. Berman, R.K. Dismukes, K. K. Jobe, *Performance Data Errors in Air Carrier Operations: Causes and Countermeasures*, Ames Research Center Moffett Field, California, 2012.
- [30] EASA, *SIB No.: 2016-02 Use of Erroneous Parameters at Take-off*, (2016).
- [31] Laboratory of Applied Anthropology, *Use of erroneous parameters at takeoff*, 2008. https://www.bea.aero/uploads/tx_scalaetudessecurite/use.of.erroneous.parameters.at.takeoff_03.pdf.
- [32] EASA, *Certification Specifications for Large Aeroplanes CS-25*, European Aviation Safety Agency, 2007.
- [33] Massachusetts Institute of Technology, *Lab 8 Notes - Basic Aircraft Design Rules*, (2006). <https://ocw.mit.edu/courses/aeronautics-and-astronautics/16-01-unified-engineering-i-ii-iii-iv-fall-2005-spring-2006/systems-labs-06/spl8.pdf> (accessed February 10, 2018).
- [34] E. Schlieben, A. Ogden, I. Berler, *System and Apparatus for Determining the Distribution of the Load in Aircraft*, U.S.Patent: 2,373,504, 1945.
- [35] M. Wardle, D. Akron, *Center of Gravity Location Indicator*, U.S.Patent: 2,453,607, 1948.
- [36] P. Magruder, W. Bender, *Strain Gauge Center of Gravity and Gross Weight Meter*, U.S.Patent: 2,443,045, 1948.
- [37] T. Blackmon, F. Porter, *Weight and Balance Indicator*, U.S.Patent: 2,615,330, 1952.

- [38] E. Kolisch, Equipment for Determining the Center of Gravity of Aircraft, U.S.Patent: 2,686,426, 1954.
- [39] J. Quinn, Weight and Center of Gravity Computing Apparatus, U.S.Patent: 2,735,291, 1956.
- [40] H. Kurkjian, Weight and Balance Determination, U.S.Patent: 3,194,058, 1965.
- [41] B. Hawkins, STAN - A New Concept in Aircraft Weight and Balance, in: 24th Annu. Conf. Soc. Allied Weight Eng., 1965.
- [42] B. Hawkins, STAN - Its Progress and Future, in: 25th Annu. Conf. Soc. Allied Weight Eng., 1966.
- [43] Unknown, STAN - Integral Weight and Balance System, in: 26th Annu. Conf. Soc. Allied Weight Eng., 1967.
- [44] G. Rice, STOW - A Proven Full-Capability Integral Weight and Balance System, in: 26th Annu. Conf. Soc. Allied Weight Eng., 1967.
- [45] B. Shapiro, Integral Aircraft Weight Systems, in: 26th Annu. Conf. Soc. Allied Weight Eng., 1967.
- [46] L. Ferrante, F. Waung, Lockheed L-1011 On-Board Weight and Balance System, in: 29th Annu. Conf. Soc. Allied Weight Eng., 1970.
- [47] M. Orgun, S. Flannigan, Method and Apparatus for Real Time Estimation of Aircraft Center of Gravity, U.S.Patent: 5,034,896, 1991.
- [48] T. Hsiu, B. Wu, Method and Apparatus for the Linear Real Time Estimation of an Aircraft Center of Gravity, U.S.Patent: 5,571,953, 1996.
- [49] U. Kehlenbeck, Airbus A340 Weight and Balance System, in: 58th Annu. Conf. Allied Weight Eng., 1999.
- [50] K. Nance, Trinity Airweighs Weight and Balance System, in: 59th Annu. Conf. Allied Weight Eng., 2000.
- [51] R. Bose, System and Method for On-Board Determination of Aircraft Weight and Load-Related Characteristics, U.S.Patent: 6,032,090, 2000.
- [52] R. Stefani, Aircraft Weight and Balance System, U.S.Patent: 6,923,375, 2005.
- [53] M. Long, G. Gouette, Onboard Aircraft Weight and Balance System, U.S.Patent: 2008/0119967, 2008.
- [54] M. Long, G. Gouette, Onboard Aircraft Weight and Balance System, U.S.Patent: 2011/0087424, 2011.
- [55] M. Abraham, M. Costello, In-Flight Estimation of Helicopter Gross Weight and Mass Center Location, *J. Aircr.* 46 (2009) 1042-1049. doi:10.2514/1.41018.
- [56] B. Taylor, J. Rogers, Experimental Investigation of Real-Time Helicopter Weight

- Estimation, *J. Aircr.* 51 (2014). doi:10.2514/1.C032449.
- [57] M. Al-Malki, M. Elshafei, Method and Apparatus for Tracking Center of Gravity of Air Vehicle, U.S.Patent: 2009/0143926, 2009.
- [58] Y. Al-Rawashdeh, M. Elshafei, M. Al-Malki, In-Flight Estimation of Center of Gravity Position Using All-Accelerometers, *Sensors*. 14 (2014) 17567-17585. doi:10.3390/s140917567.
- [59] L. Vetsch, Low Cost Aircraft Center of Gravity Monitoring Systems and Methods, U.S.Patent: 2010/0121560, 2010.
- [60] L. Vetsch, Low Cost Aircraft Center of Gravity Monitoring Systems and Methods, U.S.Patent: 8,060,296, 2011.
- [61] A. Stanley, R. Goodall, Estimation of the Centre of Gravity of a Manoeuvring Aircraft using Kalman filters and the ADMIRE Aircraft Model, in: 5th IFAC Symp. Mechatron. Syst., 2010.
- [62] A. Stanley, State estimation of in-flight aircraft centre of gravity, Loughborough University, 2011.
- [63] P. Schneider, K. Thrane, J. Wenzl, S. Matthiesen, Investigation into the Feasibility of an Onboard Weight and Balance System for Rotary Wing Aircraft with Wheeled Landing Gear, in: 71th Annu. Conf. Allied Weight Eng., 2012.
- [64] A.J. Komendat, Center-of-Gravity Estimation of an Aircraft Solely Using Traditional Aircraft Measurement Sensors, Rochester Institute of Technology, 2012.
- [65] M. Costello, Z. Sam, Extended State Observer for Helicopter Mass and Center-of-Gravity Estimation, *J. Aircr.* 52 (2015). doi:10.2514/1.C033112.
- [66] C. Thaïss, F. Caplan, Gross Weight and Center-of-Gravity Estimation Systems for the V-22, in: 71st AHS Annu. Forum, 2015.
- [67] A. Iele, M. Leone, R. Solimeno, C. Grasso, G. Persiano, A. Cutolo, M. Consales, A. Cusano, A Feasibility Analysis for the Development of Novel Aircraft Weight and Balance Monitoring Systems Based on Fiber Bragg Grating Sensors Technology, in: 8th Eur. Work. Struct. Heal. Monit., 2016.
- [68] J.M. Lescure, *Navigation aérienne*, E.N.A.C, 1981.
- [69] D. Kuchemann, A Simple Method for Calculating the Span and Chordwise Loading on Straight and Swept Wings of any Given Aspect Ratio at Subsonic Speeds, Aeronautical Research Council Reports and Memoranda, 1952.
- [70] Airbus, Getting to Grips with Aircraft Performance Monitoring, Airbus Flight Operations Support & Line Assistance, 2002.
- [71] M. João, *Análise Estatística com o SPSS Statistics*, ReportNumber, Lda, 2011.

- [72] A. Field, *Discovering Statistics Using SPSS.*, 2009.
- [73] A. Gelman, J. Hill, *Data Analysis Using Regression and Multilevel/Hierarchical Models*, Cambridge University Press, New York, 2006.
- [74] J. Hair, W. Black, B. Babin, R. Anderson, *Multivariate Data Analysis*, 7th ed., Pearson, 2009.
- [75] J. Miles, M. Shevlin, *Applying regression and correlation: a guide for students and researchers*, SAGE Publications, 2001.
- [76] A.-N. Spiess, N. Neumeyer, An evaluation of R2 as an inadequate measure for nonlinear models in pharmacological and biochemical research: a Monte Carlo approach, *BMC Pharmacol.* 10 (2010) 6. doi:10.1186/1471-2210-10-6.
- [77] C.J.L. Palmeiro, *Estudo e desenvolvimento de um algoritmo de detecção de pontos de estabilidade*, Instituto Superior Técnico, 2009.
- [78] FAA, *Advisory Circular AC 120-27E: Aircraft Weight and Balance Control*, (2005).
- [79] FAA, *Advisory Circular AC 20-161: Aircraft Onboard Weight and Balance Systems*, (2008).
- [80] FAA, *Advisory Circular AC 120-27F: Aircraft Weight and Balance Control*, (n.d.).
- [81] Y. Dong, J. Ai, Research on inflight parameter identification and icing location detection of the aircraft, *Aerosp. Sci. Technol.* 29 (2013) 305-312. doi:10.1016/j.ast.2013.03.012.
- [82] J.W. Melody, T. Başar, W.R. Perkins, P.G. Voulgaris, Parameter identification for inflight detection and characterization of aircraft icing, *Control Eng. Pract.* 8 (2000) 985-1001. doi:10.1016/S0967-0661(00)00046-0.
- [83] IBM, *IBM SPSS Statistics 20 Command Syntax Reference*, International Business Machines, 2011.

Appendix A

Linear Regression Assumptions Check

Appendix A 1 Linear Regression Assumptions Check for Weight Determination

The scatterplot of the independent variable (angle of attack) and the dependent variable (lift coefficient) indicates that the assumption of linearity is reasonable, Figure A 1. 1 ; as angle of attack increases, lift coefficient increases as well in a linear fashion.

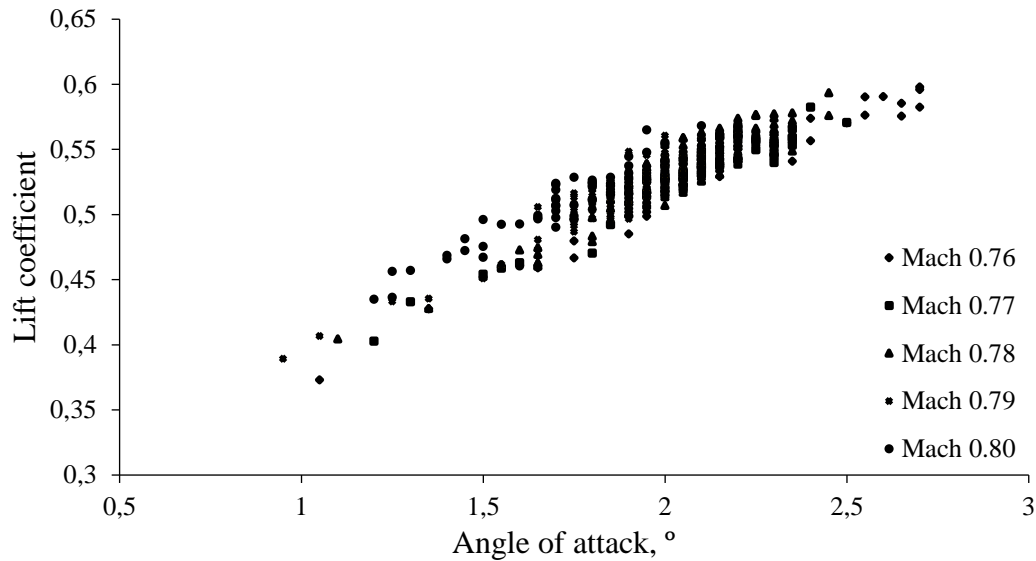


Figure A 1. 1 - Scatter plot for angle of attack vs lift coefficient for different Mach numbers.

A random display of points falling within an absolute value of 0.02 for Mach 0.76, 0.77, 0.79, 0.03 for Mach 0.78 and an absolute value of 0.04 for Mach 0.80, a scatterplot of unstandardized residuals against values of the independent variable provided further evidence of linearity [71], Figure A 1. 2 and Figure A 1. 3 show some of these tests.

Table A 1. 1 below summarizes the normality, independence of errors and collinearity tests [71]. Q-Q plot and the histogram of unstandardized residuals suggested normality was reasonable for all Mach numbers, Figure A 1. 4 through Figure A 1. 7 . A relatively random display of points, where the spread of residuals appears constant over the range of values of the independent variable (in the scatterplot of unstandardized residuals against values of the independent variable) provided evidence of homogeneity of variance. Analyses were performed with SPSS Statistics (v. 20; IBM SPSS, Chicago, IL). Outputs from the software are presented below. The considered probability for the occurrence of type I error (α) was 0.05 for all the analyses.

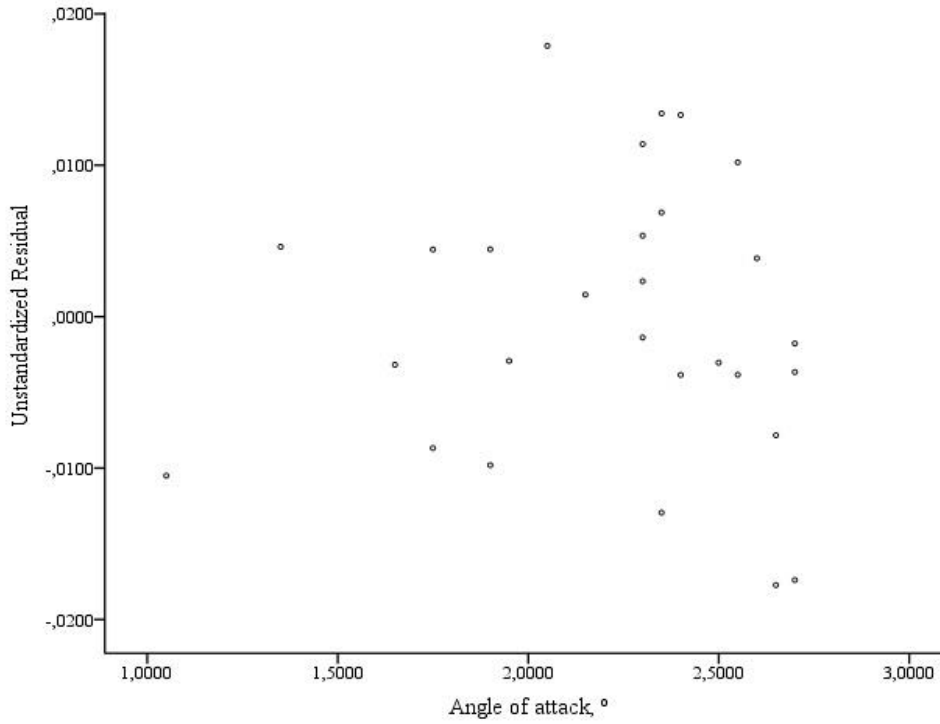


Figure A 1. 2 - Scatter plot for angle of attack vs unstandardized residual for Mach 0.76.

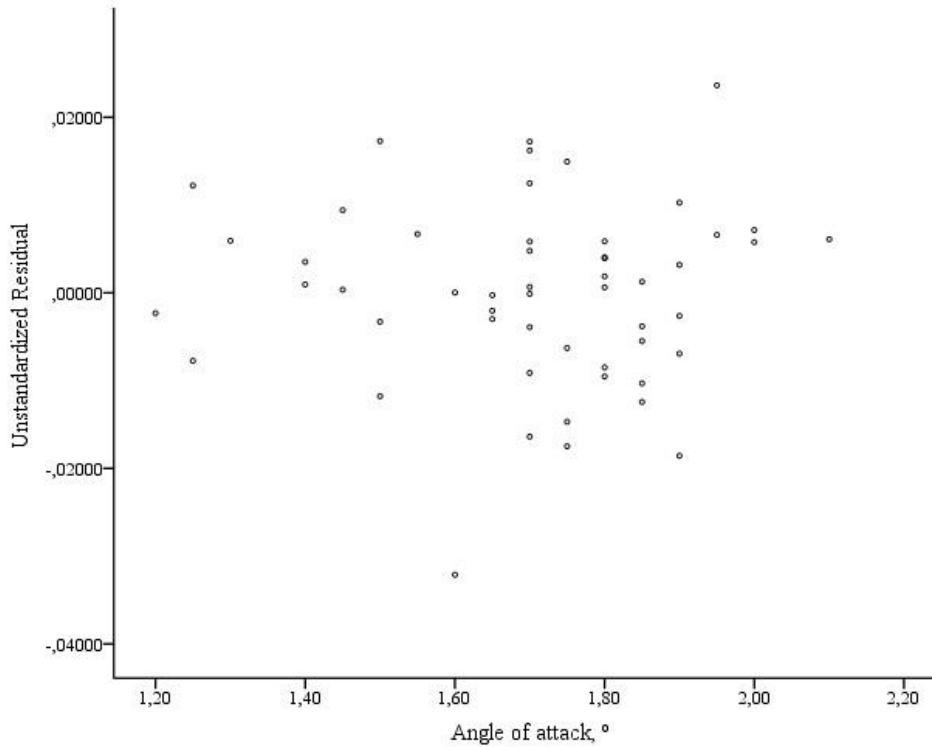


Figure A 1. 3 - Scatter plot for angle of attack vs unstandardized residual for Mach 0.80.

Table A 1. 1 - Summary of normality, independence of errors and collinearity assumptions tests.

Mach Number	Normality Test	Skewness	Kurtosis	Durbin-Watson	VIF
	df				
0.76	S-W (0.979)** 28	-0.005	-0.492	1.241	1
0.77	S-W (0.985)** 42	-0.021	-0.293	1.089	1
0.78	K-S (0.041)* 260	0.015	-0.596	0.963	1
0.79	K-S (0.075)* 97	0.397	-0.199	0.910	1
0.80	K-S (0.075)* 53	-0.389	0.860	1.153	1

Note. S-W, Shapiro-Wilk test; K-S, Kolmogorov-Smirnov test with Lilliefors significance correction; df, degrees of freedom; VIF, variance inflation factor. *p > 0.200 and ** p >> 0.200.

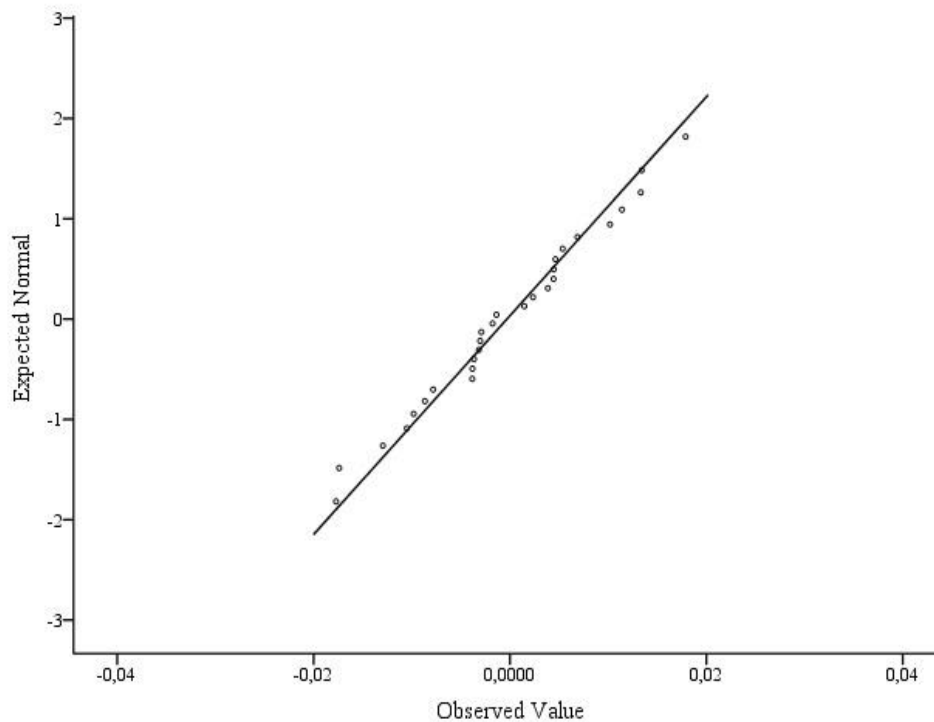


Figure A 1. 4 - Normal Q-Q plot of unstandardized residual for Mach 0.76.

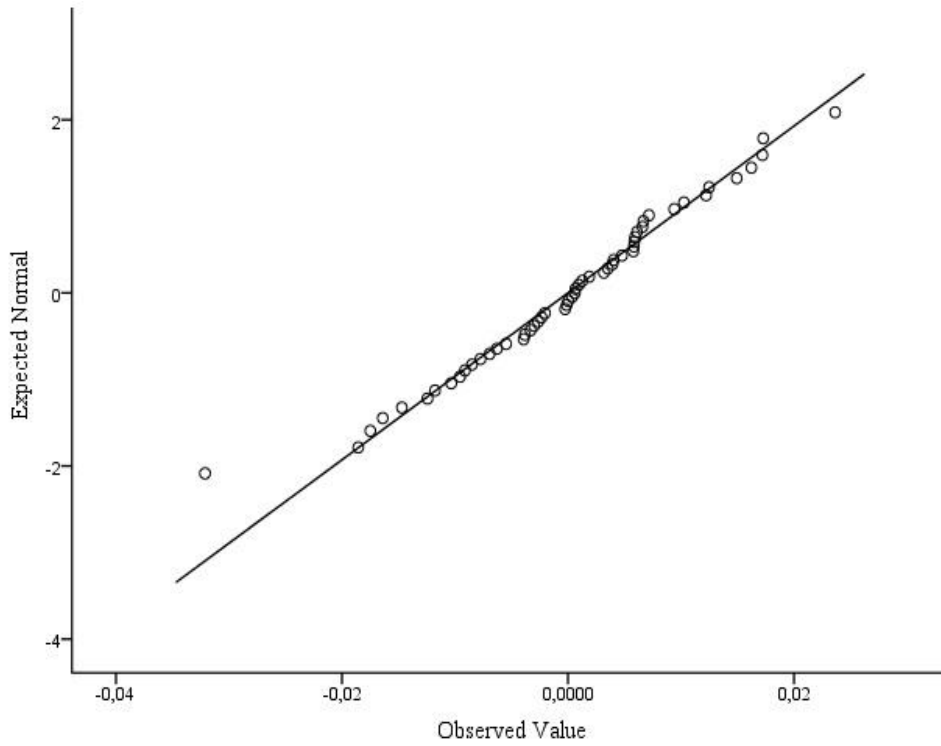


Figure A 1. 5 - Normal Q-Q plot of unstandardized residual for Mach 0.80.

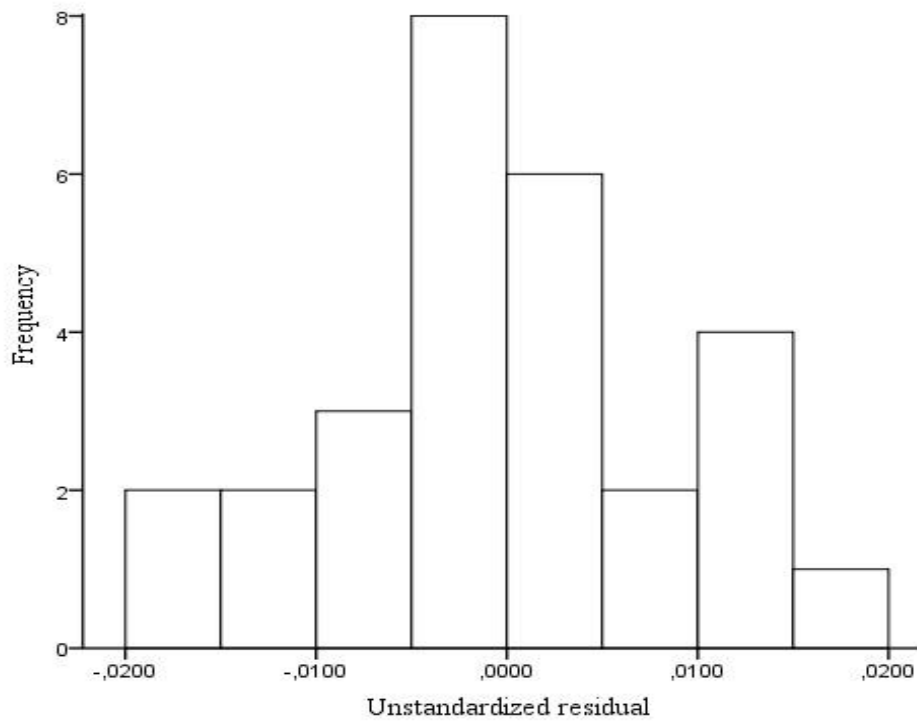


Figure A 1. 6 - Histogram of unstandardized residual for Mach 0.76.

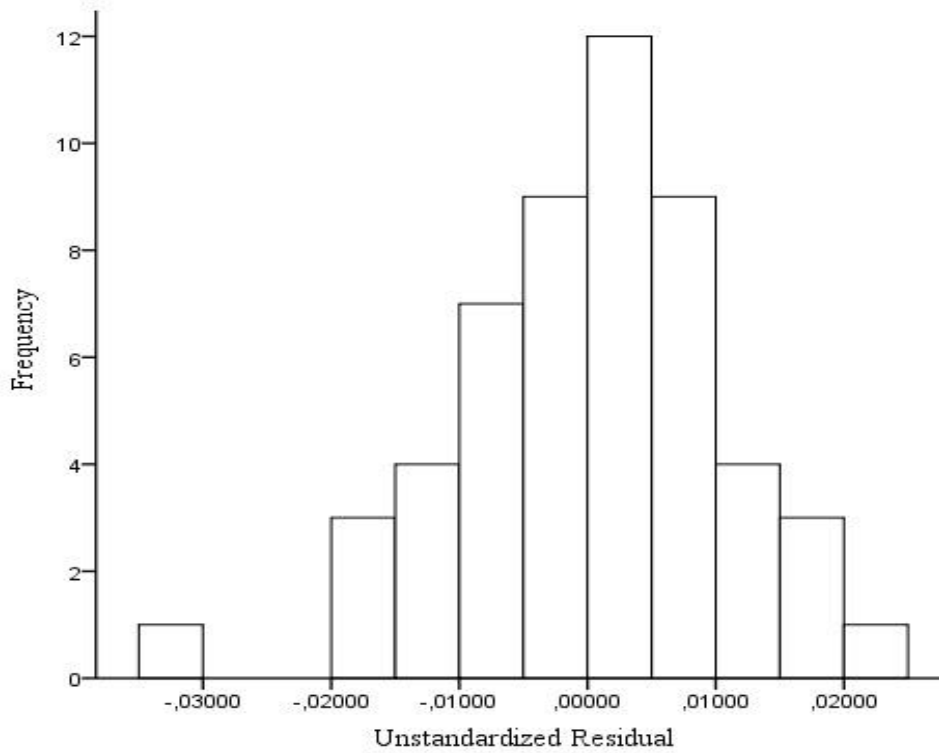


Figure A 1. 7 - Histogram of unstandardized residual for Mach 0.80.

All the datasets for weight measurement and correction revealed problems with independence of error as demonstrated by the Durbin-Watson statistic. Since the model is directly derived from theory and easily interpretable, it was decided to retain the model. To solve the autocorrelation problem, the Prais-Winsten estimation method was used based on the AREG command in SPSS [83].

After applying the method, the Durbin-Watson statistic values are as follows: $d = 2.203$ for Mach 0.76, $d = 2.089$ for Mach 0.77, $d = 2.354$ for Mach 0.78, $d = 2.384$ for Mach 0.79 and $d = 2.326$ for Mach 0.80.

Appendix A 2 Linear Regression Assumptions Check for Weight Determination with a Single Function

A relatively random scatterplot of unstandardized residuals against values of the independent variable provided evidence of linearity [71], Figure A 2. 1 .

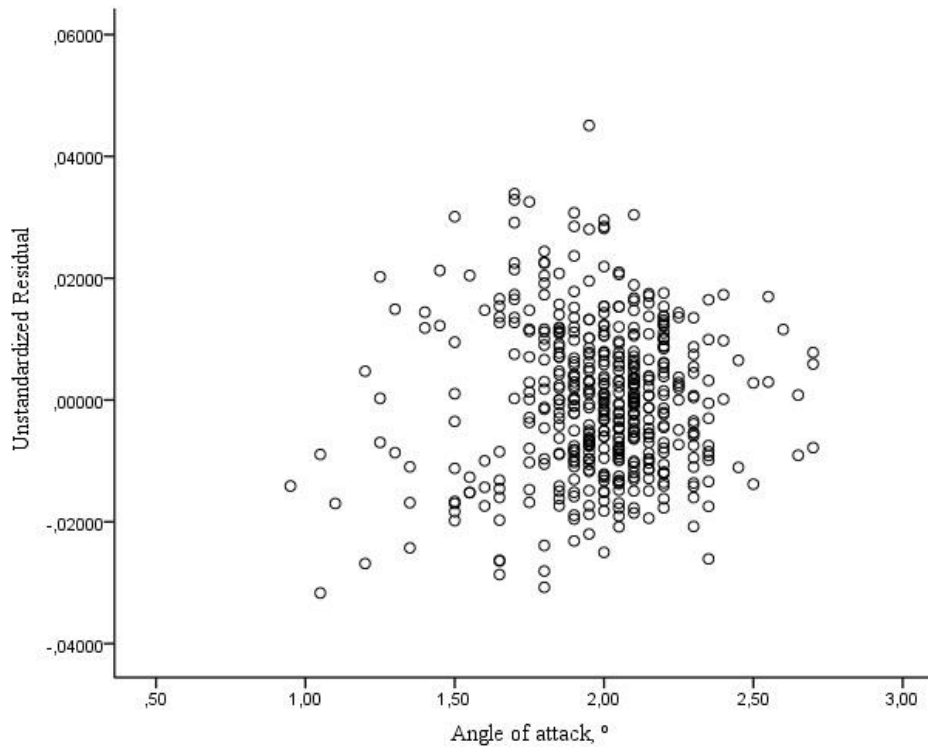


Figure A 2. 1 - Scatter plot for angle of attack vs unstandardized residual for single linear regression model.

Kolmogorov-Smirnov test, with Lilliefors significance correction, for normality ($K-S = .034$; $df = 480$; $p > .200$) and skewness (.256) and kurtosis (0.052) suggested that normality was a reasonable assumption.

The boxplot suggested a relatively normal distributional shape with a single outlier of the residuals, Figure A 2. 2 .

Q-Q plot and the histogram of unstandardized residuals suggested normality was reasonable, Figure A 2. 3 and Figure A 2. 4 . Independence of errors was assessed using the Durbin-Watson statistic $d = 1.488$, which was considered acceptable [71]. A relatively random display of points, where the spread of residuals appears constant over the range of values of the independent variable (in the scatterplot of unstandardized residuals against values of the independent variable) provided evidence of homogeneity of variance. Collinearity statistics revealed no collinearity, tolerance and VIF both equal to 1 which was considered acceptable. Analyses were

performed with SPSS Statistics software (v. 20; IBM SPSS, Chicago, IL). Outputs from the software are presented below. The considered probability for the occurrence of type I error (α) was 0.05 for all the analyses.

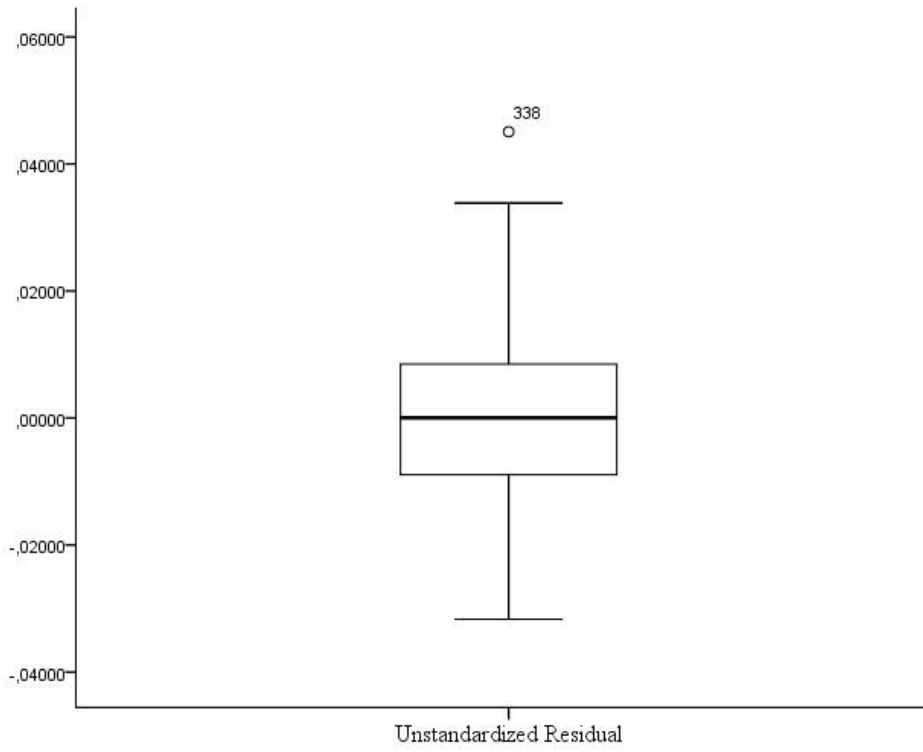


Figure A 2. 2 - Boxplot of unstandardized residual for single linear regression model.

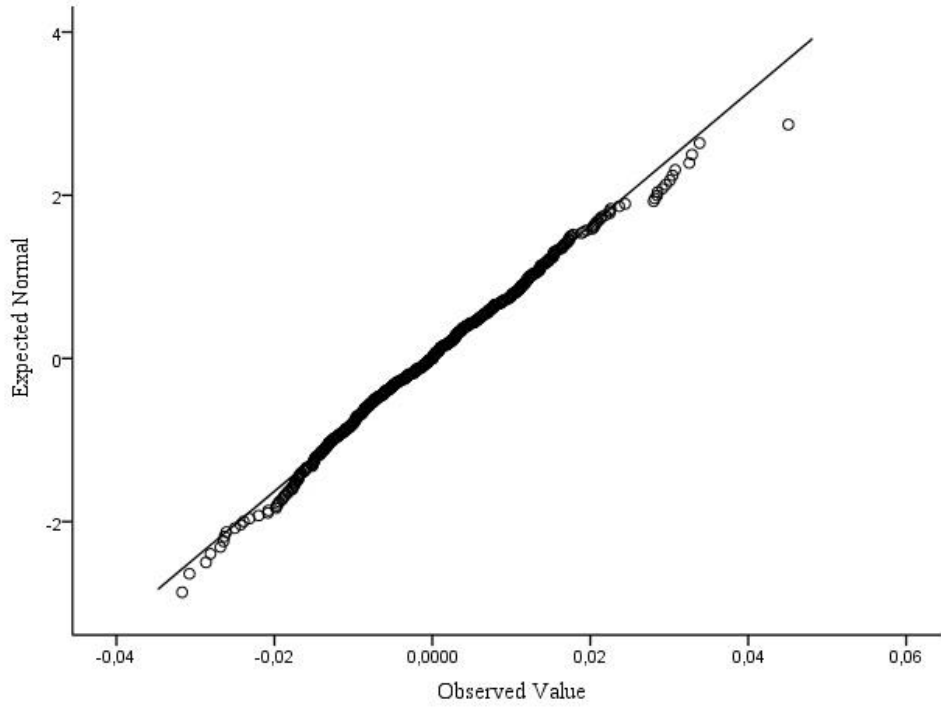


Figure A 2. 3 - Normal Q-Q plot of unstandardized residual for single linear regression model.

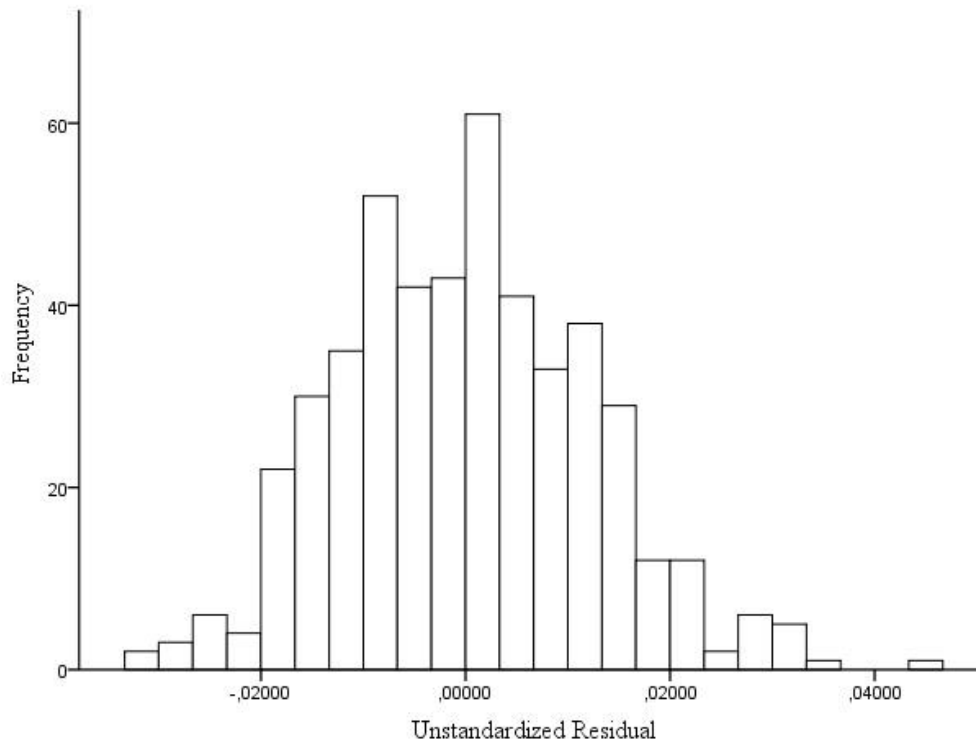


Figure A 2. 4 - Histogram of unstandardized residual for single linear regression model.

Appendix B

Multiple Linear Regression Assumptions Check

Appendix B 1 Multiple Linear Regression Assumptions Check for Centre of Gravity Determination

A random scatterplot of the regression standardized residual against regression standardized predicted value provided evidence of linearity, Figure B 1. 1 . The assumption of normality was tested via examination of unstandardized residuals and plots. The boxplot suggested a relatively normal distributional shape (with no outliers) of the residuals, Figure B 1. 2 . Q-Q plot showed some deviation from normal at the tails, but the histogram of unstandardized residuals suggested normality was reasonable, Figure B 1. 3 and Figure B 1. 4 . However, Kolmogorov-Smirnov test with Lilliefors Significance Correction for normality ($K-S = .020$; $df = 3987$; $p < .05$) and skewness ($-.008$) and kurtosis ($-.556$) statistics suggested that residuals were not normal. Based on reference [73], normality of error distribution is the least important assumption in regression since, for estimating the regression line, the assumption of normality is barely important at all. As such, the result of the Kolmogorov-Smirnov test was not considered a problem. Independence of errors was assessed using the Durbin-Watson statistic ($d = 1.755$), which was considered acceptable. A relatively random display of points of regression standardized residual against regression standardized predicted value provided evidence of homogeneity of variance. Collinearity statistics revealed no collinearity, tolerance equal to 0.988 and VIF equal to 1.012.

Outlier observations were removed (i.e, observations with a studentized residual, in absolute value, above 1.96). Analyses were performed using the software SPSS Statistics (v. 20; IBM SPSS, Chicago, IL). Outputs from the software are presented below. The considered probability for the occurrence of type I error (α) was 0.05 for all the analyses.

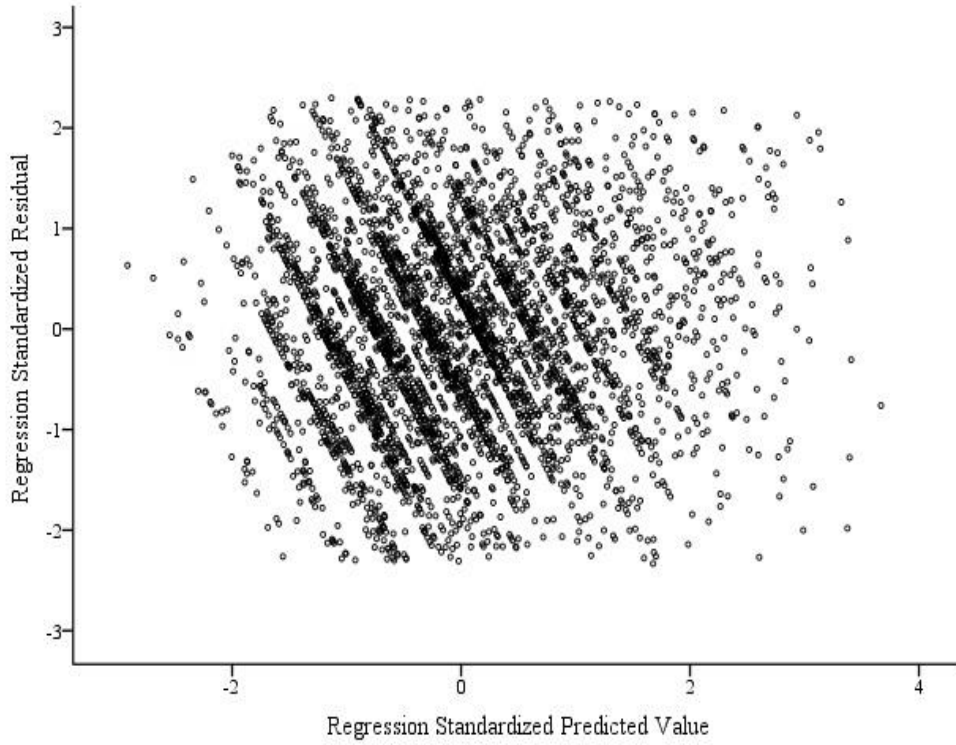


Figure B 1. 1 - Scatter plot for regression standardized predicted value vs regression standardized residual.

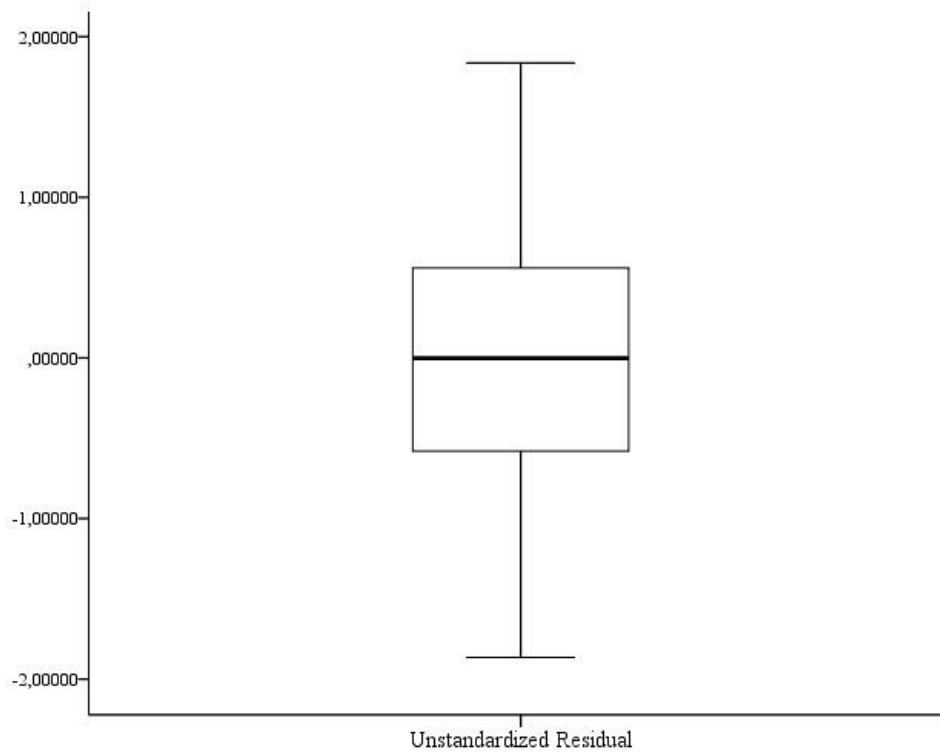


Figure B 1. 2 - Boxplot of unstandardized residual for multiple linear regression model.

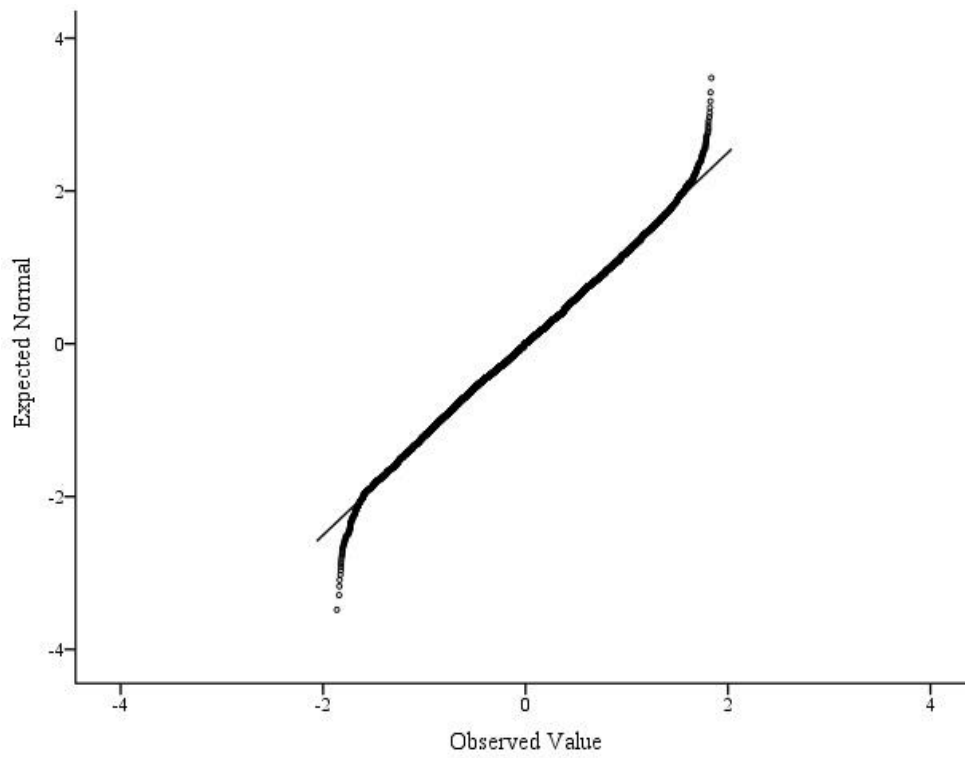


Figure B 1. 3 - Normal Q-Q plot of unstandardized residual for multiple linear regression model.

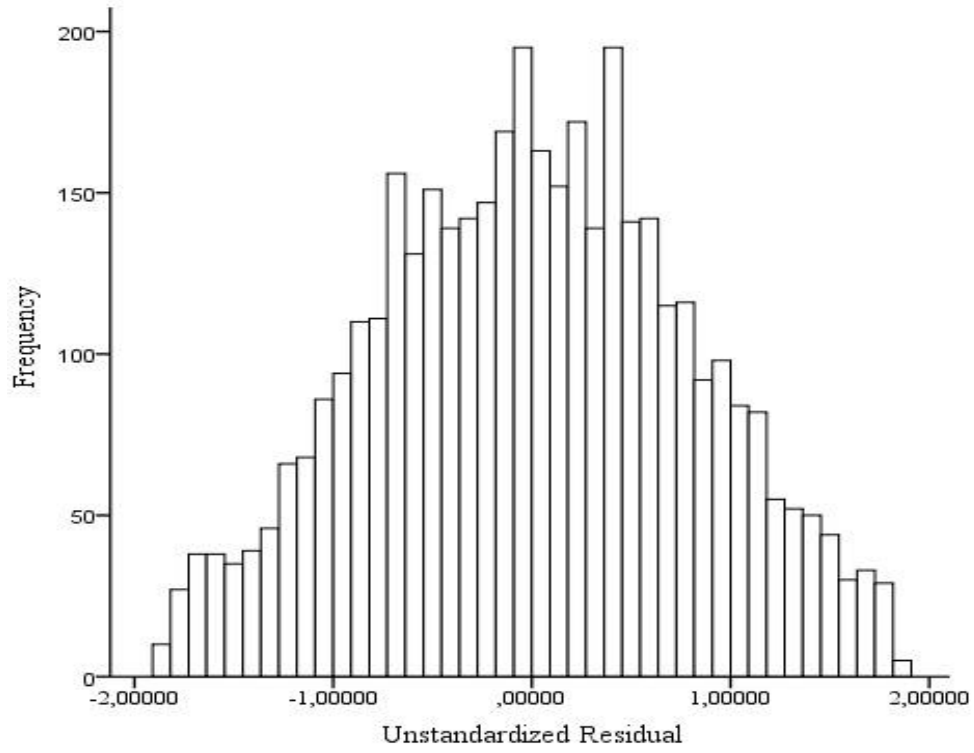


Figure B 1. 4 - Histogram of unstandardized residual for multiple linear regression model.

Appendix C

Publications

List of Publications

Peer Reviewed Journal Articles

- I. F.A.V. Chaves, M.A.R. Silvestre, P.V. Gamboa, Preliminary development of an onboard weight and balance estimator for commercial aircraft, *Aerosp. Sci. Technol.* 72 (2018) 316-326. doi: 10.1016/j.ast.2017.11.018.



Preliminary development of an onboard weight and balance estimator for commercial aircraft



F.A.V. Chaves*, M.A.R. Silvestre, P.V. Gamboa

University of Beira Interior, Aerospace Sciences Department, Edifício II das Engenharias, Calçada Fonte do Lameiro, n.º 1, 6201-001 Covilhã, Portugal

ARTICLE INFO

Article history:

Received 5 December 2016
Received in revised form 9 November 2017
Accepted 9 November 2017
Available online 14 November 2017

Keywords:

Weight and balance
Estimators
Onboard
In-flight
Airliners

ABSTRACT

A novel approach to onboard in-flight weight and balance estimation systems is presented. Data from an Airbus A320 fleet from an airline were used to assess the feasibility of the approach. Simple flight mechanics in combination with statistics allowed for the identification of weight and center of gravity position using cruise angle of attack, Mach number and elevator deflection values. The good agreement between the theoretical model and the obtained values for the lift curve slope as a function of Mach as well as the standard error of the estimate for center of gravity position and cruise flying weight indicate that the method is sound. The major implication of this work is that the development of onboard and in-flight weight and balance systems can be significantly simpler than previous literature suggested. The impact of this paper could be immediate for airlines since all the tools required to implement the system as described are readily available. This could have an effect in operating costs, safety and environment.

© 2017 Elsevier Masson SAS. All rights reserved.

1. Introduction

For a given aircraft, weight and center of gravity position have a significant impact on performance and handling, specifically stall speed, take-off and landing distance, climb performance and cruise performance [1–5]. Incorrect Weight and Balance (W&B) management may also result in severe safety issues, e.g. tail strikes, runway overrun, degraded handling qualities, among others [6–8]. Documentation on accidents and incidents involving inaccurate W&B calculations is plenty and although such occurrences have decreased over the years [9] the potential for disaster exists.

The current dispatching methodology revolves around the use of standardized weights for passengers and their baggage, both cabin and sometimes checked baggage, to calculate aircraft weight [5]. Center of gravity (CG) position is also determined based on baggage count and passenger location. These calculations provide for an estimate at best and any error will result as a penalty in an aircraft flying optimized for a non-optimal condition, incurring in unnecessary fuel burn which costs money to airlines and harms the environment. IATA reports that the share of fuel cost on the total operating costs of the typical airline can be as much as over 30% [10–12]. Thus, fuel costs play a significant role in total operating costs and hence profitability of an airline. Consider the study

by Gabriel et al. [13] where for the A330 the difference in fuel consumption, from the least favorable to the most favorable CG position, was 211 kg. This small difference, over a typical life cycle of 40,000 flights, represents 8,440,000 kg (about 1%) of fuel saved. At the time of writing, with the jet fuel price at 0.97\$ per gallon, this is as much as 2,689,955\$ (about 1%) saved per aircraft over the course of its operational lifetime and a cut in total emissions of about 26,539,039 kg of CO₂ (about 1%) per aircraft over the course of its life cycle. In short, accurate W&B is not just a matter of safety, but also one of saving costs and reducing aviation's environmental impact. So, an onboard weight and balance system could provide a solution to minimize such problems [9]. Generally, there are two different approaches to such a system, on-ground or in-flight. Table 1 presents both advantages and disadvantages of each method.

On-ground methods were the first to appear with the earliest recorded system dating from 1932 [14]. The Society of Allied Weight Engineers has an extensive backlog of papers related to onboard weight and balance systems. Some of the most relevant are [15–17]. In-flight W&B systems appear in two kinds, those that detect center of gravity only and those which detect both weight and CG position.

- Center of gravity and weight estimation: The authors identified at least two different methods, one dating from 2004 based on artificial neural networks [18] and another based on Kalman filters and applied to helicopters [19].

* Corresponding author.

E-mail address: ichavesaero@gmail.com (F.A.V. Chaves).

<https://doi.org/10.1016/j.ast.2017.11.018>

1270-9638/© 2017 Elsevier Masson SAS. All rights reserved.

Nomenclature			
a	Lift slope	$IATA$	International Air Transport Association
a_0	Incompressible flow lift slope	ISA	International Standard Atmosphere
$ACMS$	Aircraft Condition Monitoring System	k_c	Compressibility coefficient
$AIDS$	Aircraft Integrated Data System	L	Lift
AMM	Aircraft Maintenance Manual	M	Mach Number
c	Wing chord	MAC	Mean aerodynamic chord
CAS	Calibrated Airspeed	M_y	Pitching moment
CI	Confidence Interval	p	P-value
CFD	Computational Fluid Dynamics	q	Relative wind dynamic pressure coefficient
CG	Center of Gravity	QA	Aircraft Quality Number
C_L	Lift Coefficient	R^2	Coefficient of determination
C_M	Pitching moment coefficient	S	Planform Wing Area
$C_{M,0}$	Pitching moment about reference point O	t	t-test statistic
$C_{M,0}^a$	Aerodynamic pitching moment about reference point O	T	Thrust
C_T	Thrust coefficient	$TOL(N)$	Individual Variation of N value
C_W	Weight coefficient	$VAR(N)$	Individual Variance of N value
C_x	Force coefficient along the x axis	W	Weight
C_z	Force coefficient along the Z axis	$W\&B$	Weight and Balance
D	Drag	α	Angle of attack
df	Degrees of freedom	α_T	Thrust line angle
DMU	Data Management Unit	γ	Flight path angle
EAS	Equivalent Airspeed	δ_{Elev}	Elevator deflection
F	F-test statistic	δ_{HT}	Equivalent horizontal tail deflection
$FDIMU$	Flight Data Interface Management Unit	θ	Pitch angle
FMS	Flight Management System	Λ	Wing Sweep
		ρ_0	ISA mean sea level air density

Table 1
Advantages and disadvantages of on-ground and in-flight approaches to onboard weight and balance systems.

On-ground	In-flight
✓ Prevents mistakes that can happen before flight.	✓ Allows for detection of anomalous situations after take-off such as weight shifts.
✓ May provide for faster dispatching if used as primary W&B method.	✓ May allow for icing detection.
✗ Susceptible to terrain inclination.	✗ Does not prevent W&B problems before flight.
✗ Does not detect problems in-flight such as weight shift.	

- Center of gravity estimation: two works were found in the literature, one from 2012 [20] where common sensors and rigid body equations are used and a second from 2014 [21] where accelerometers were used.

These systems and methods, both in-flight and on-ground, have in common their complexity. They usually require either specific sensors and extensive calibration and maintenance or when common sensors can be used the theoretical background might be extensive and not so easy to implement in an online system identification fashion (i.e. for real time W&B identification). The fact remains; so far, no single onboard weight and balance system has made its way and become common practice on everyday airline/cargo operations.

In this paper, a new approach to such systems is presented, one that is based on basic flight mechanics equations. The objective is to allow for the in-flight correction of the current estimation of weight and longitudinal CG position information during cruise. In aircraft equipped with trim fuel tanks this should allow for a safer and more efficient cruise by optimization of the center of gravity position through redistribution of fuel to the trim tanks. In every case, an update of the weight information will allow for a more accurate setting of optimum cruise Mach number and altitude as well as actual landing weight and detection of overweight and possibly in-flight ice formation.

2. Methodology

2.1. Onboard weight measurement and correction

The current passenger and cargo dispatching methodology is based on standardized weights for passengers and hand luggage to calculate aircraft weight data that is introduced into the Flight Management System. From this, a potential source of error for passenger's weight and respective carry-on luggage arises. However, since during cruise lift is equal to weight, it is possible to determine and correct weight information through the lift coefficient and atmospheric air properties in an existing permanent cruise flight setting, Equation (1). The weight can be calculated from:

$$W = q_\infty S C_L \tag{1}$$

where C_L is the lift coefficient; S the wing planform area; q_∞ is the relative wind dynamic pressure:

$$q_\infty = \frac{1}{2} \rho_0 EAS^2 \tag{2}$$

where EAS is the Equivalent Air Speed; ρ_0 is the International Standard Atmosphere (ISA) mean sea level air density, 1.225 kg/m³.

One problem with Equation (2) is that the cruise airspeed is available from the current onboard data acquisition system only in the form of Calibrated Air Speed (CAS). Per reference [22] the EAS can be calculated from CAS using:

$$EAS = k_c CAS \tag{3}$$

In Equation (3), k_c is the compressibility coefficient whose value is 1 if $CAS < 200$ knots and is otherwise calculated by:

$$k_c = \frac{1}{100} \left(102.5 - \frac{Z \cdot CAS}{12} 10^{-5} \right) \quad (4)$$

where Z is the altitude in feet and CAS is in knots.

The lift coefficient is a function of angle of attack (α) and Mach number (M). This function is known by the manufacturer and thus determination of weight should be possible from the use of the simple flight mechanics relation of Equation (1). To test the validity of such simple approach to onboard aircraft weight measurement, the logged flight data of an airline Airbus's A320-200 fleet was used. However, the C_L function is not known to us. The following section shall describe the method used to attain the relationship between α , M and the lift coefficient to estimate the weight of the aircraft. The primary uncertainty for the measured altitude is ± 0.5 feet and ± 0.5 m/s for CAS based on a datasheet provided by the airline. The uncertainty in the measured weight data is 2%.

2.2. Estimating the lift coefficient function

The weight estimate comes from the values introduced by the crew. Since these values are based on standard values derived from statistical averages, an assumption is made that over the course of several flights the data points will become statistically distributed around a position which over time should approach the actual weight of the aircraft.

Thus, the lift coefficient should too become distributed around the actual lift coefficient. Its value can thus be estimated using Equation (5) from the weight estimate introduced by the crew and the logged flight data. Combining Equations (1) through (3):

$$C_L = \frac{2W}{\rho_0 k_c^2 CAS^2 S} \quad (5)$$

where k_c is estimated from Equation (4).

To derive the C_L function, the α and Mach number of each CAS data point must be registered. This produces a dispersion of data points on a C_L vs α plot for each Mach number that expresses the true function of C_L which can be found using linear regression. To create a uniform function for all Mach numbers, non-linear and linear regressions were used to create a single function that estimates lift coefficient based on Mach number and angle of attack. Since the Mach number influences the lift versus α curve slope, then, the slope for each M is used as a measure of whether there is sound basis to the method by checking its obtained values against those estimated with a theoretical model [23]. Accordingly, the compressible branch of the lift curve slope can be calculated from:

$$\frac{\partial C_L}{\partial \alpha_{Compressible}} = \frac{a_0 \cos \Lambda}{\sqrt{1 - M_\infty^2 \cos^2 \Lambda + \left(\frac{a_0 \cos \Lambda}{\pi A}\right)^2 + \left(\frac{a_0 \cos \Lambda}{\pi A}\right)^2}} \quad (6)$$

While the incompressible branch is calculated by:

$$\frac{\partial C_L}{\partial \alpha_{Incompressible}} = \frac{a_0 \cos \Lambda}{\sqrt{1 + \left(\frac{a_0 \cos \Lambda}{\pi A}\right)^2 + \left(\frac{a_0 \cos \Lambda}{\pi A}\right)^2}} \quad (7)$$

where a_0 is the lift-curve slope given by thin airfoil theory (2π), Λ is the wing sweep and A is the aspect ratio.

2.3. Flight logged dataset

The data for this study was gathered from the A320's "Cruise Performance Reports < O2 >". This data was provided by an airline sponsoring the project. One of the functions of the Data Management Unit/Flight Data Interface Management Unit (DMU/FDIMU)

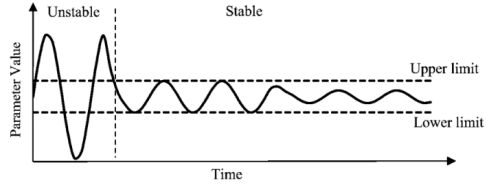


Fig. 1. Example of parameter variation. A stable frame report occurs whenever the parameter variation is within prescribed limits for a defined amount of time.

is the generation of aircraft and engine reports as result of triggering settings. These reports are part of the Airbus Standard Report which is a set of pre-programmed Aircraft Integrated Data System/Aircraft Condition Monitoring System (AIDS/ACMS) reports that are operative at delivery of the DMU/FDIMU [24]. The process by which these reports are produced and their contents have been defined and validated by Airbus and they depend on the aircraft and engine types [24].

A dataset was used to develop the current W&B estimator and was labeled the development dataset; this set had $n = 4225$ data points, however some of these were corrupted (missing data on some of the cells of the file received) and had to be filtered into non-usable data points and usable data points. Out of the initial $n = 4225$ points there were $n = 4184$ usable data points. The quality of the data points must be taken in consideration. For this, Airbus defined the Aircraft Quality Number (QA) which is defined as:

$$QA = \sum \overline{W(N)} \frac{VAR(N)}{TOL(N)^2} \quad (8)$$

where N is the parameter number (it can be the $N1$, fuel flow...), $\overline{W(N)}$ is a weighting factor defined by Airbus (between 0 and 1), $VAR(N)$ is the individual variance and $TOL(N)$ is the individual variation value. The lower the QA , the lower the variation of the parameters and the better the stable frame report. A stable frame report happens whenever the variation of the target parameter is within an upper and lower bound (defined by Airbus or the airline), see Fig. 1.

QA varies between 0 and 999. Common values seen in routine monitoring are around 40 [24]. For the development dataset, the average QA was 16.723, 95% CI [16.382, 17.064], which indicates better than average quality of the reports.

A second separate dataset was provided by the airline for validation of the method and was labeled evaluation dataset. The evaluation dataset had $n = 2392$ data points of which $n = 1795$ were usable; the average QA of the evaluation dataset was 21.348, 95% CI [20.782, 21.913], i.e. lower quality than that of the development dataset.

2.4. Center of gravity measurement and correction

In steady symmetric flight, there is equilibrium between lift L , drag D , thrust T and weight W and the pitching moment M_y on the airplane is zero. Per [18], transforming these forces and moments into standard dimensionless quantities (coefficients), where the product of dynamic pressure q_∞ and wing area S are used as a unit of force and the wing mean aerodynamic chord (c) is used as a unit of length, we get the dimensionless total pitching moment C_M and weight C_W defined by:

$$C_M = \frac{M_y}{q_\infty S c} \quad (9)$$

$$C_W = \frac{W}{q_\infty S} \quad (10)$$

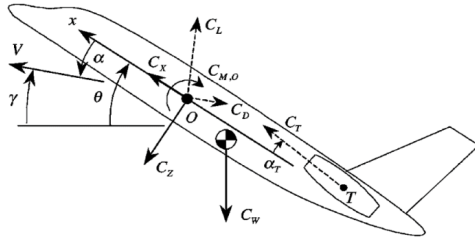


Fig. 2. Non-dimensional forces and moments [18].

The dimensionless lift, drag and propulsive forces are obtained in a similar fashion.

Equilibrium condition involves two equations of force balance and one of pitching-moment balance. From Fig. 2 [18] these are:

$$C_X - C_W \sin \theta = 0 \quad (11)$$

$$C_Z + C_W \cos \theta = 0 \quad (12)$$

where:

$$C_X = C_L \sin \alpha - C_D \cos \alpha + C_T \cos \alpha_T \quad (13)$$

$$C_Z = -(C_L \cos \alpha + C_D \sin \alpha + C_T \sin \alpha_T) \quad (14)$$

The conditions for vanishing pitching moment are:

$$C_{M,0} + C_Z x_{CG} - C_X z_{CG} = 0 \quad (15)$$

where x_{CG} is the center of gravity position and:

$$C_{M,0} = C_{M,0}^a + C_T x_T \sin \alpha_T + C_T z_T \cos \alpha_T \quad (16)$$

$C_{M,0}^a$ is the aerodynamic pitching moment which depends on the elevator deflection. The thrust line angle (α_T) is defined in the aircraft design stage as a function of x_T and z_T such that the aircraft thrust setting has minimal influence in $C_{M,0}$. So, it is reasonable to assume that $C_{M,0} = C_{M,0}^a$ which is a function of the elevator deflection alone.

Using Equations (11) and (12) in Equation (15):

$$C_{M,0} + C_Z (x_{CG} + z_{CG} \tan \theta) = 0 \quad (17)$$

which can be solved for the CG position x_{CG} .

$$x_{CG} = -\left(\frac{C_{M,0}}{C_Z} + z_{CG} \tan \theta\right) \quad (18)$$

The pitching moment, lift and drag coefficients are functions of M , α and elevator deflection δe only. From Equation (18) it is possible to determine the location of the aircraft CG, which has been done previously in [18] using neural networks but only for numerically simulated flight-test data.

However, such implementation might prove rather complex or impractical to perform for routine airline operations. An alternative may be the use of statistical methods in a similar way as described in Section 2.2 for determining the C_L function but, in this case, making use of the available flight data with known estimates of x_{CG} as presented hereafter.

Some assumptions are made. First, it is assumed that z_{CG} is nearly coincident with the origin of the reference frame and thus that the second term on the right-hand side of Equation (18) is negligible. The second and third terms of Equation (13) have the same order of magnitude and are opposite thus canceling each other out. As such, it is assumed that only lift coefficient and elevator deflection influence the prediction of x_{CG} position. Information

on elevator deflection and stabilizer trim position can come directly from sensing systems on the aircraft, while lift coefficient can also be measured as described in Section 2.1.

To validate this method of determining x_{CG} it was applied to the A320 dataset. In the A320 we have differential elevator and moving stabilizer trim data directly from the aircraft sensors and data collection system. So, different combinations of elevators deflection and stabilizer trim position may result in the same influence on the pitching moment, i.e. due to the same local lift coefficient being produced by the horizontal tail.

Since there is no information available about the airfoils used on the horizontal tail of the A320, it is not possible to use CFD or other similar methods to reliably obtain the lift coefficients produced for every elevator deflection and stabilizer trim position. As such an equivalent horizontal tail deflection, named δ_{HT} , was defined. This δ_{HT} is based on the ratio of chords between the horizontal stabilizer and the elevator of the A320. δ_{HT} is given by:

$$\delta_{HT} = 0.2 \left(\frac{\delta_{Elev1} + \delta_{Elev2}}{2} \right) + 0.8 (Stab) \quad (19)$$

where $Stab$ is the stabilizer deflection. The equivalent horizontal tail deflection was used to convert the elevator 1, elevator 2 and stabilizer deflection flight data points into a single δ_{HT} . Multiple linear regression was then used to relate the airplane's δ_{HT} and aircraft C_L with x_{CG} . The regression line produced can then be used in the W&B estimator as a tool to update the x_{CG} information that was originally introduced by the crew. The primary uncertainty in elevator 1 and 2 deflection is $\pm 0.5^\circ$ and $\pm 0.05^\circ$ for the stabilizer deflection based on a datasheet provided by the airline. The uncertainty in the measured x_{CG} data is 1%.

3. Results and discussion

3.1. Lift coefficient determination

A simple linear regression was calculated to predict lift coefficient based on angle of attack. This was done for different Mach numbers as discussed in Section 2.1. Regarding the Mach numbers that had adequate amount of data for analysis were Mach 0.76, $n = 28$ data points, Mach 0.77, $n = 42$ data points, Mach 0.78, $n = 260$ data points, Mach 0.79, $n = 97$ data points and Mach 0.80, $n = 53$ data points. Based on the methodology described in [25], model assumptions were analyzed for linearity, normality, homogeneity and statistical independence of the errors, see Appendix A. Table 2 summarizes the results for the regressions. Figs. 3 and 4 provide a visual representation of the same results.

All regressions are highly significant as demonstrated by the p -value of the F-test statistic and with a high coefficient of determination which indicates that the model fits the data well (also an indication that a high number of the variance on the lift coefficient is explained by the angle of attack, which is per theory). Looking at the unstandardized slope and the associated 95% CI we see that it does not include zero, an indication that angle of attack influences the lift coefficient, as predicted in theory. The unstandardized slope in the context of this work is simply the lift curve slope. On the other hand, the standardized slope, sometimes called standardized beta, provides information on how many standard deviations a dependent variable will change per standard deviation increase in the predictor variable. In the context of univariate regression, it also works similarly to the correlation coefficient and thus the closer to 1 or -1 the stronger the relationship between independent and dependent variable. The unstandardized and standardized slopes are highly significant (as shown by the t-test statistic) with the standardized slope approaching the value of 1. The previous results show that linear regression models adapt well to our data and are valid for the purposes of this work. Some of the data points

Table 2
Summary of the results for the linear regressions.

Mach number	F	R ²	B	β	t	95% CI for B	
	df		Intercept			Lower	Upper
0.76	1274***	0.98	0.131	0.990	35.36***	0.113	0.149
	1, 25		0.246				
0.77	760***	0.95	0.139	0.975	27.26***	0.121	0.157
	1, 39		0.241				
0.78	2402***	0.90	0.142	0.950	48.99***	0.120	0.158
	1, 257		0.245				
0.79	1323***	0.93	0.144	0.966	36.23***	0.126	0.162
	1, 94		0.247				
0.80	529***	0.91	0.139	0.955	22.73***	0.119	0.159
	1, 50		0.269				

Note. F, F-test statistic; df, degrees of freedom; R², coefficient of determination; B, unstandardized slope; β , standardized slope; t, t-test statistic; CI, confidence interval. * $p < 0.05$, ** $p < 0.01$ and *** $p < 0.001$.

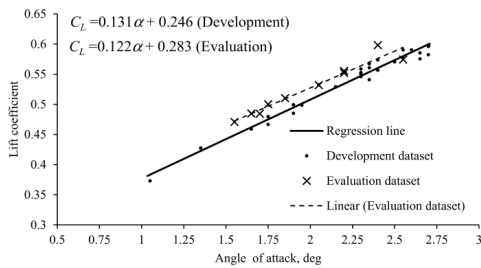


Fig. 3. Data points and linear regression line for Mach 0.76.

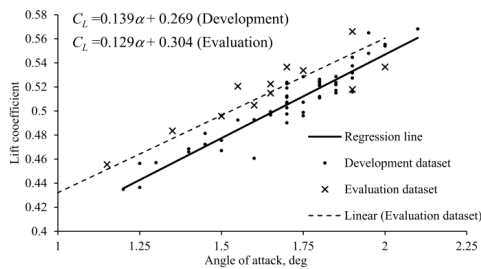


Fig. 4. Data points and linear regression line for Mach 0.80.

revealed a large deviation from the regression line. These points could be revealing of instances where current W&B methodologies have led to large discrepancies between the calculated and the actual weight. For the evaluation dataset, these large deviations can also be caused by discrepancies between the calculated and the actual weight, but the lower quality of the dataset also contributes to this effect (due to larger fluctuations when capturing the stable frame report). Fig. 5 shows the compilation of the linear regressions obtained for all cruise Mach numbers.

After obtaining the lift curve slopes for different Mach numbers, these were compared with the values of the Kuchemann theoretical model, see Fig. 6. There is a good agreement between the theoretical model and the values that were experimentally obtained. This provides further evidence that the model is sound.

The previous results were used to create a single function that estimates lift coefficient based on Mach number and angle of attack. The equation developed was:

$$C_L = (-16.490M^2 + 25.903M - 10.050)\alpha + 0.287 \quad (20)$$

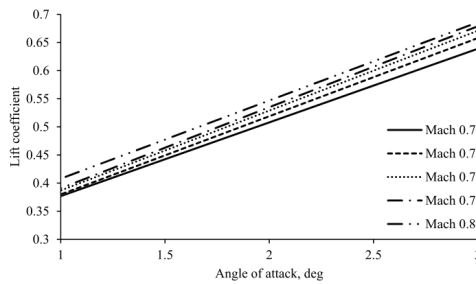


Fig. 5. Obtained lift curves for the different Mach numbers (Development dataset).

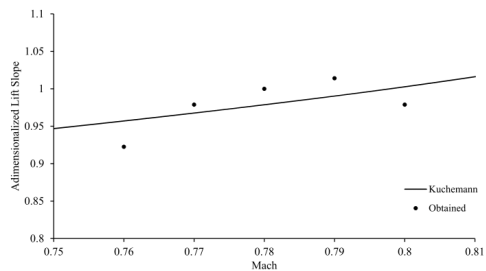


Fig. 6. Estimated Airbus A320 lift curve slope vs Mach number based on Kuchemann [23] and obtained from flight data. Non-dimensionalized by the Mach 0.78 lift slope value.

The non-linear term of Equation (20) was determined using a non-linear quadratic regression.

This constitutes a significant regression equation, with $F(1, 478) = 2854$, $p < 0.001$, with an $R^2 = 0.85$. The 95% CI was $[-30.28, -8.29]$ for the first parameter of the non-linear term, $[13.14, 47.45]$ for the second parameter and $[-18.44, -5.07]$ for the constant. The standard error of the estimate was 0.001165. Linear regression models are restricted equations where each term must be either a constant or the product of a parameter and a predictor variable and the equation is a sum of each of these terms. Because of this, it is possible to develop a hypothesis test where the parameters are either zero, having no effect, or different from zero, thus having an effect in the response value. The p -value tests this null hypothesis in linear regression. Non-linear models can have several different equations with few restrictions on how parameters are used, bringing flexibility to the curve fitting; however,

Table 3
Summary of the results for the multiple linear regression.

F	R ²	Variable	B	β	t	95% CI for B	
						Lower	Upper
df							
9885***	0.83	CG	-0.591	-0.908	-139.093***	-0.598	-0.583
2, 3984		C _L	14.749	0.232	35.586***	13.937	15.560

Note. F, F-test statistic; df, degrees of freedom; R², coefficient of determination; B, unstandardized slope; β, standardized slope; t, t-test statistic; CI, confidence interval. *p < 0.05, **p < 0.01 and ***p < 0.001.

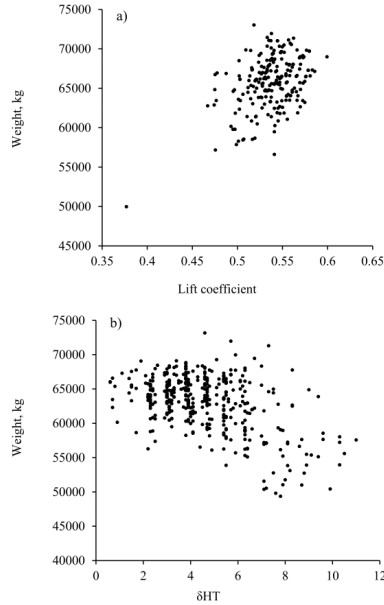


Fig. 7. a) Distribution of points with constant δ_{HT} ($\delta_{HT} = 5.4$) and b) Distribution of points with constant lift coefficient ($C_L = 0.5$).

the null hypothesis value for each parameter depends on the expectation function, the place of the parameter in the expectation function and field of study. For this reason, and since expectation functions can vary so much, it is impossible to have a hypothesis test that works for all non-linear models. This also invalidates the use of *p*-values and R² to determine the significance and goodness of fit of non-linear models and as such, *p*-values and R² are not presented for the non-linear regression [26]. Instead, the standard error of the regression and the confidence intervals around each parameter were provided to assess the model fit. The fitting was considered acceptable.

3.2. Cruise flying weight estimation

After obtaining the regression lines for the lift coefficient, it is finally possible to estimate and update the weight information based on lift coefficient, density, speed and wing surface area, as described in Section 2.1.

Fig. 7a) shows the results for the cruise flying weight versus the lift coefficient in a scatter plot. The data scatter is explained by the fact that the points in the graph are from different flights. The scatter also appears to be random meaning that the flying weight

and the lift coefficient are independent variables. Fig. 7b) shows the results for the cruise flying weight versus the equivalent horizontal tail deflection in a scatter plot. Here, the scatter seems not totally random and the motive can be that a horizontal tail deflection can, in fact, have an influence in the lift coefficient for a given angle of attack. Nevertheless, the data was not sufficient to obtain a reliable correlation function.

The cruise flying weight estimator was tested using the evaluation dataset to check how well the curves developed fit a different dataset.

The average mass standard error of the estimate for the regressions was 1236 kg. This value corresponds to about 1.9% of the development dataset mean cruise flying weight. Comparing the values introduced by the crew into the flight management computer with the expected or statistically predicted values it was verified that for the development dataset, in 99% of the tested points the error was no greater than 3408 kg, see Fig. 8. When applying the developed equation to the evaluation dataset, in 99% of the tested points the error was no greater than 6193 kg, see Fig. 8. The average error for the evaluation data set was 2574 kg, 95% CI [2227, 2921].

For the single function, Equation (20), the mass standard error of the estimate was 1501 kg. After obtaining the linear regression it is possible to compare the values introduced by the crew into the flight management computer with the expected or statistically predicted values. It was verified that for the development dataset, in 99% of the tested points the error was no greater than 5200 kg, see Fig. 9. When applying the developed equation to the evaluation dataset, in 97% of the tested points the error was no greater than 5000 kg, see Fig. 9. The average error for the evaluation data set was 1182 kg, 95% CI [1080, 1284]. This reveals that the estimator had a good adaptation and predictive power for the evaluation dataset even though the dataset included data points with Mach values between 0.70 through 0.75. There were however some extreme outliers such as one data point with a difference over 35000 kg. These data points are associated with low Mach numbers, well outside the range for which the estimator was developed and could be a result of that.

3.3. Center of gravity position estimation

As described in Section 2.2, multiple linear regression was used to obtain x_{CG} from the airplane's cruise trim horizontal tail equivalent deflection position and the lift coefficient obtained in Section 3.1. Model assumptions were analyzed namely linearity, normality, homogeneity and statistical independence of the errors, see Appendix A. Table 3 summarizes the results for the multiple linear regression.

Equation (21) presents the obtained regression solved for x_{CG} . The standard error was 1.35% of the MAC. Fig. 10 shows the corresponding data dispersion, which is a consequence of the load and trim sheet methods currently in use (which use standard passenger weights and moment arms and indices to calculate the x_{CG} position), causing a statistical distribution of points around a position which over time should approach the actual x_{CG} position.

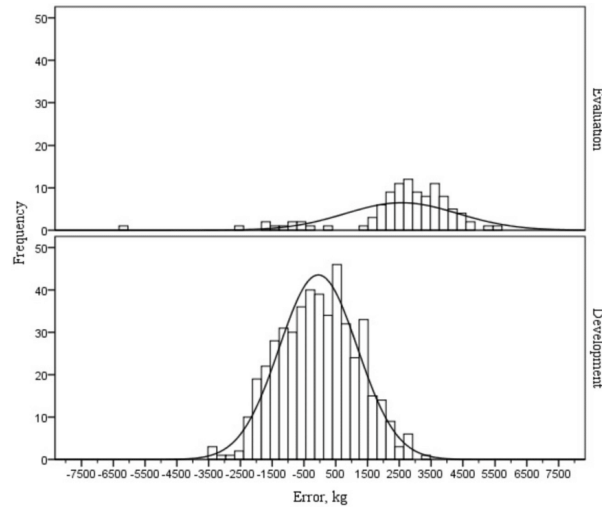


Fig. 8. Distribution of weight estimation error for the development dataset and for the evaluation dataset.

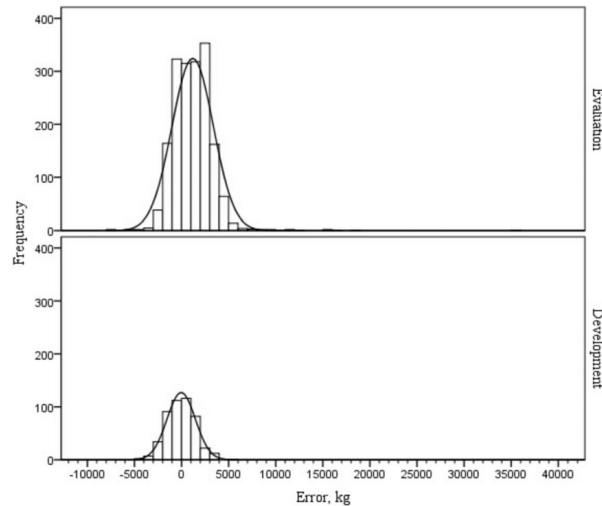


Fig. 9. Distribution of weight estimation error for the development dataset and for the evaluation dataset using a single function.

$$x_{CG} = 24.956C_L - 1.692\delta_{HT} + 25.928 \quad (21)$$

After obtaining the linear regression line it is possible to compare the values introduced by the crew into the flight management computer with the expected or statistically predicted values. It was verified that for the development dataset, in 99% of the tested points the error was no greater than 3.15% of the MAC, see Fig. 11. When applying the developed equation to the evaluation dataset, in 99% of the tested points the error was no greater than 9.62% of the MAC. The average error was 1.24% of the MAC, 95%

CI [1.155, 1.328]. Please refer to Fig. 11. The results suggest that the current weight and balance procedures do produce discrepancies between the CG position introduced by the crew and the true CG position although, for the most part of the data points, such discrepancies do not appear to be large enough to seriously jeopardize the safety of the flight.

The methods previously presented are subject to improvement over time. As flights are performed and more data points are produced better estimates can be attained, especially if the data points are of good quality. What this means to airlines is that conditions

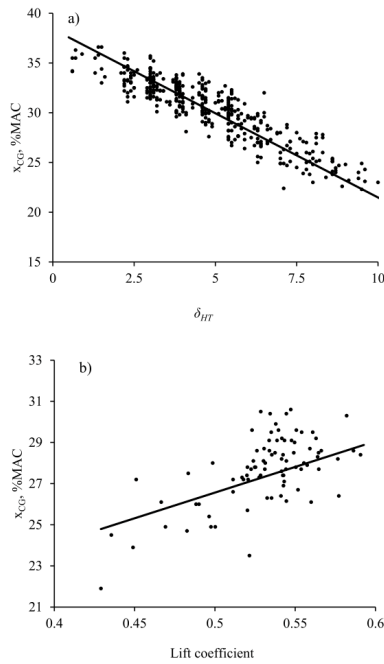


Fig. 10. a) Data points dispersion and prediction line with constant lift coefficient ($C_L = 0.5$) and 10 b) Data points dispersion and prediction line with constant δ_{HTR} ($\delta_{HTR} = 7$ deg).

that can lead to better quality of the data points should be pursued. This can be achieved through proper maintenance of sensors and associated systems. Another method to achieve better quality of the data points is by making the criteria that lead to the recording of a stable frame report stricter [27].

The system, as it was presented herein, is dependent on how accurate the development dataset is for the W&B data. This means that the estimator is also sensitive to the accuracy of the current standard passenger weights making it dependent on authorities, such as the FAA, since these are the entities responsible for the publishing and definition of these weights [28]. The deviations in weight in the evaluation dataset confirm that the system is susceptible to the quality of the data (the evaluation dataset had a higher QA, i.e., lower quality), but this problem should be easy to solve if accurate development datasets are used to improve the estimator, either by properly maintaining the aircraft systems, or by making the allowed parameter variation stricter [27]. These two faults can be resolved through a partnership with the manufacturer. Conceptually, using a combination of modern CFD, wind tunnel testing and flight testing, there is no reason why a modern airliner cannot be fully characterized in such a way, namely in the lift slope versus Mach number and CG position versus cruise elevator trim setting, as to allow the creation of a modern onboard in-flight weight and balance system that functions on the readings of angle of attack, Mach number, elevator deflection and thrust line effects. To this end and to better measure the accuracy of the proposed estimator, flight testing with well-defined center of gravity positions and weights can be conducted, preferably by the manufacturer. After such assessment is made, and based on the flight test results, it

should be determined if the methodology meets the criteria for onboard weight and balance systems [29].

Also, the results expose instances where there were large deviations between the weight predicted and the weight introduced by the crew, one can wonder if these were flights where the use of standard weights was inadequate and lead to significant error. Interestingly, the FAA is currently working on a draft for an update of the AC120-27E. The draft, named AC120-27F, will further increase standard weights revealing that the FAA acknowledges the need to consistently revise standard weights, another disadvantage of current methodologies [30].

To provide an idea of how the estimator may be used and the influence it can have in fuel consumption, we will offer a concise example. Suppose an A320 is cruising at 35000 feet; at this altitude, all else being equal, every additional ton represents an average increase in fuel consumption of 17.6 kg per engine per hour (values based on flight crew operating manual and considering cruise at optimum airspeed). The weight at the beginning of the cruise, because of the use of standard weights, is estimated at 64000 kg. At this weight, optimum speed would be around Mach 0.781. For the purposes of illustrating the use of the estimator, presume the pilot receives an indication from the system that points to actual weight being 60000 kg. At this stage, the pilot should first look for evidence that supports the indication: Was the aircraft accelerating faster than expected during the take-off run? Was the aircraft “light” during rotation? Does current fuel flow match the expected values for the present conditions? If the evidence supports the indication the pilot may then adjust the cruising speed accordingly. At 60000 kg and cruising at 35000 feet, optimum speed is Mach 0.771. Optimizing the Mach number would result in a reduction of fuel consumption of 19 kg per engine per hour, a seemingly small saving that can accumulate to several tons over the course of many flights. As for the influence of the center of gravity, Airbus claims that due to complex aerodynamic interactions, center of gravity position does not affect fuel consumption on the A320 [1]. Our data suggests there is a very small decrease in fuel consumption when the center of gravity is near the rear limit, however fuel consumption modeling and discussion is beyond the scope of this work. The estimator can also be implemented in flight data monitoring programs for the detection of abnormal weight or center of gravity deviations from expected values

4. Conclusion

Weight and center of gravity position information has been surveyed from data provided by a sponsoring airline with the objective of laying the foundation for further development of a new onboard W&B estimator tool.

The results, namely the good agreement between the lift slopes calculated and those of the theoretical model, suggest that there is a sound basis to the approach that was used. This may have significant implications since, so far, all efforts to develop onboard W&B systems relied on the addition of complex sensors, usually to the landing gear in the case of on-ground systems, or accelerometers combined with comparatively more complex theoretical formulations for in-flight estimator systems. Such approaches result in higher maintenance requirements to ensure calibration is maintained, higher maintenance costs as well as an increase in acquisition costs for the airlines since the aircraft comes equipped with more sensors. The use of sensors which are already available on the aircraft in combination with a simple theoretical formulation solves all these problems and provides an attractive alternative for airlines and manufacturers alike since development and implementation costs of the system, as presented, should be low. Through a simple software update this W&B estimator could be implemented.

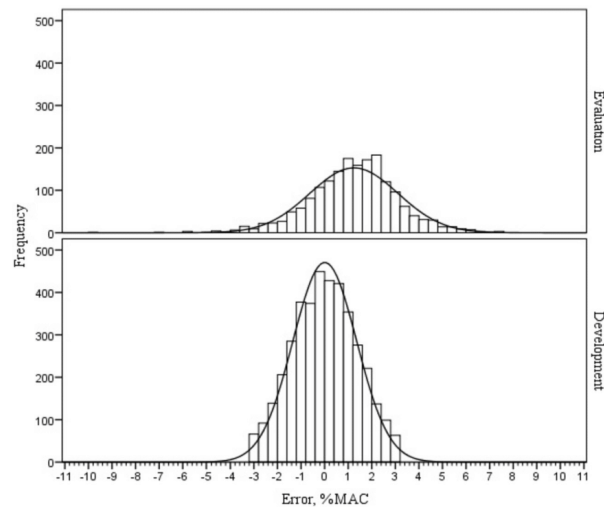


Fig. 11. Distribution of center of gravity estimation error for the development dataset and for the evaluation dataset.

W&B information could be displayed to the pilot in-flight on one of the screens of the aircraft; a simple look-up table can also suffice.

However, the method does have its flaws. There is a trade-off between simplicity of the formulation and precision. This results in the simplest estimator to date but also the least precise. Since the system is not on-ground, it cannot be used as a faster dispatching tool and neither can it identify a serious W&B problem before flight which may lead to accident. On aircraft without trim tanks the pilot does not have the means to make use of the information to rebalance the aircraft, but it does have the chance to update weight information for the cruise phase and for the landing.

A replication of this study but with data from other airlines, particularly airlines with large fleets and many flights per year, would quickly allow for the validation of the method presented herein and for its further development. The simplicity of the methodology means this could be done rather quickly.

A suggestion for a future work is that the presence of onboard and in-flight W&B systems may provide different means for the detection of ice accumulation during flight. This could be done by detecting abnormal changes in weight during flight or detection of abnormal changes on the aerodynamic characteristics of the aircraft due to the formation of ice on the aerodynamic surfaces. In flight ice detection, has been addressed by researchers by more complex means [31,32].

Conflicts of interest

The authors declare no conflicts of interest with the publication of this work.

This research did not receive any specific grant from funding agencies in the public, commercial, or not-for-profit sectors.

Acknowledgements

The authors would like to show their appreciation for all the support provided by Azores Airlines and Grupo SATA, to Miguel Amaral, Otilio Machado, Paulo Ornelas, Nuno Campos, Pedro Lopes,

Ângelo Oliveira and especially to Isabel Barata, who welcomed the project from the beginning with open arms, providing all the data that was required as well as responding to our enquiries.

Appendix A

A.1. Multiple linear regression assumptions check for center of gravity determination

A random scatterplot of the regression standardized residual against regression standardized predicted value provided evidence of linearity, Fig. A.1. The assumption of normality was tested via examination of unstandardized residuals and plots. The boxplot suggested a relatively normal distributional shape (with no outliers) of the residuals, Fig. A.2. Q-Q plot showed some deviation from normal at the tails, but the histogram of unstandardized residuals suggested normality was reasonable, Figs. A.3 and A.4. However, Kolmogorov–Smirnov test with Lilliefors Significance Correction for normality ($K-S = .020$; $df = 3987$; $p < .05$) and skewness ($-.008$) and kurtosis ($-.556$) statistics suggested that residuals were not normal. Based on reference [34], normality of error distribution is the least important assumption in regression since, for estimating the regression line, the assumption of normality is barely important at all. As such, the result of the Kolmogorov–Smirnov test was not considered a problem. Independence of errors was assessed using the Durbin–Watson statistic ($d = 1.755$), which was considered acceptable. A relatively random display of points of regression standardized residual against regression standardized predicted value provided evidence of homogeneity of variance. Collinearity statistics revealed no collinearity, tolerance equal to 0.988 and VIF equal to 1.012.

Outlier observations were removed (i.e., observations with a studentized residual, in absolute value, above 1.96). Analyses were performed using the software SPSS Statistics (v. 20; IBM SPSS, Chicago, IL) [33]. Outputs from the software are presented below. The considered probability for the occurrence of type I error (α) was 0.05 for all the analyses. Similar methods were used for angle of attack and CG position.

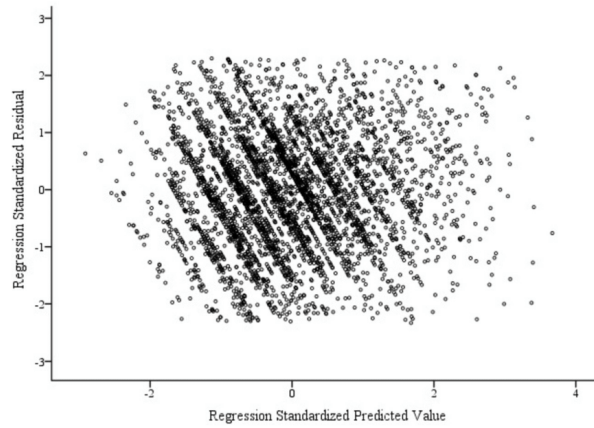


Fig. A.1. Scatter plot for regression standardized predicted value vs regression standardized residual.

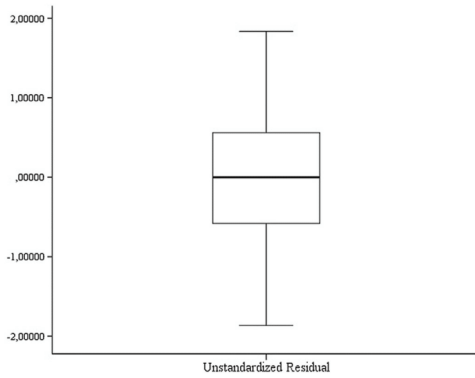


Fig. A.2. Boxplot of unstandardized residual for multiple linear regression model.

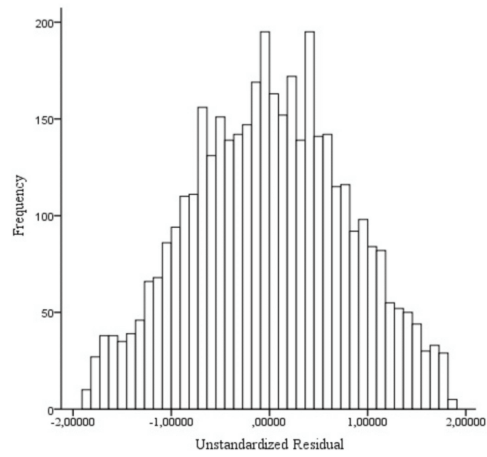


Fig. A.4. Histogram of unstandardized residual for multiple linear regression model.

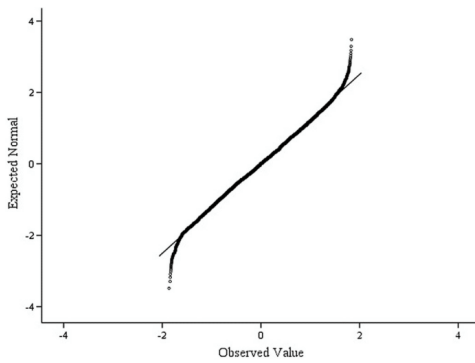


Fig. A.3. Normal Q-Q plot of unstandardized residual for multiple linear regression model.

References

- [1] Airbus, Getting to Grips with Weight and Balance, Flight Operations Support & Line Assistance, 2004.
- [2] Airbus, Optimum CG position, in: 16th Perform. Oper. Conf., 2009.
- [3] J. Roskam, C.-T. Lan, Airplane Aerodynamics and Performance, Roskam Aviation and Engineering Corporation, 2000.
- [4] J.D. Anderson, Aircraft Performance and Design, McGraw Hill Co., 1999.
- [5] A. Filippone, Advanced Aircraft Flight Performance, Cambridge University Press, New York, 2012.
- [6] A.T.S.B. Take-off, Performance Calculation and Entry Errors: A Global Perspective, 2011.
- [7] ATSB, Aircraft Loading Occurrences, 2011.
- [8] NASA, Callback Number 291, 2003.
- [9] G.W.H. van Es, Analysis of Aircraft Weight and Balance Related Safety Occurrences, 2007.
- [10] IATA, US DOT 41 Airline Operational Cost Analysis Report, 2011.
- [11] IATA, IATA Economic Briefing: Airline Fuel and Labour Cost Share, 2010.
- [12] IATA, Economic Performance of the Airline Industry, 2015.

- [13] T. Gabriel, J.M. Silva, P. Gamboa, J. Silva, J. Viegas, N. Leal, An optimized approach to reduced fuel costs in the operational procedures of an airline, in: 8th World Congr. Struct. Multidiscip. Optim., Lisbon, 2009.
- [14] E. Westrum, Load indication gauge for vehicles, 1864876, 1932.
- [15] U. Kehlenbeck, Airbus A340 weight and balance system, in: 58th Annu. Conf. Allied Weight Eng., 1999.
- [16] P. Schneider, K. Thrane, J. Wenzl, S. Matthiesen, Investigation into the feasibility of an onboard weight and balance system for rotary wing aircraft with wheeled landing gear, in: 71th Annu. Conf. Allied Weight Eng., 2012.
- [17] H.K. Nelson, Primary system certification considerations for on-board weight and balance systems, in: 40th Annu. Conf. Allied Weight Eng., 1981.
- [18] M. Idan, G. Iosilevskii, S. Nazarov, In-flight weight and balance identification using neural networks, *J. Aircr.* 41 (2004) 137–143, <https://doi.org/10.2514/1.592>.
- [19] M. Abraham, M. Costello, In-flight estimation of helicopter gross weight and mass center location, *J. Aircr.* 46 (2009) 1042–1049, <https://doi.org/10.2514/1.41018>.
- [20] A.J. Komendat, Center-of-Gravity Estimation of an Aircraft Solely Using Traditional Aircraft Measurement Sensors, Rochester Institute of Technology, 2012.
- [21] Y. Al-Rawashdeh, M. Elshafei, M. Al-Malki, In-flight estimation of center of gravity position using all-accelerometers, *Sensors* 14 (2014) 17567–17585, <https://doi.org/10.3390/s140917567>.
- [22] J.M. Lescuré, Navigation aérienne, E.N.A.C, 1981.
- [23] D. Kuchemann, A simple method for calculating the span and chordwise loading on straight and swept wings of any given aspect ratio at subsonic speeds, *Aeronaut. Res. Coun. Rep. Memo.* (1952).
- [24] Airbus, Getting to Grips with Aircraft Performance Monitoring, Airbus Flight Operations Support & Line Assistance, 2002.
- [25] M. João, Análise Estatística com o SPSS Statistics, ReportNumber, Lda, 2011.
- [26] A.-N. Spiess, N. Neumeyer, An evaluation of R2 as an inadequate measure for nonlinear models in pharmacological and biochemical research: a Monte Carlo approach, *BMC Pharmacol.* 10 (2010) 6, <https://doi.org/10.1186/1471-2210-10-6>.
- [27] C.J.L. Palmeiro, Estudo e desenvolvimento de um algoritmo de detecção de pontos de estabilidade, Instituto Superior Técnico, 2009.
- [28] FAA, Advisory Circular AC 120-27E: Aircraft Weight and Balance Control, 2005.
- [29] F.A.A. Advisory, Circular AC 20-161: Aircraft Onboard Weight and Balance Systems, 2008.
- [30] FAA, Advisory Circular AC 120-27F: Aircraft Weight and Balance Control, n.d.
- [31] Y. Dong, J. Ai, Research on inflight parameter identification and icing location detection of the aircraft, *Aerosp. Sci. Technol.* 29 (2013) 305–312, <https://doi.org/10.1016/j.ast.2013.03.012>.
- [32] J.W. Melody, T. Başar, W.R. Perkins, P.G. Voulgaris, Parameter identification for inflight detection and characterization of aircraft icing, *Control Eng. Pract.* 8 (2000) 985–1001, [https://doi.org/10.1016/S0967-0661\(00\)00046-0](https://doi.org/10.1016/S0967-0661(00)00046-0).
- [33] IBM, IBM SPSS Statistics 20 Command Syntax Reference, International Business Machines, 2011.
- [34] A. Gelman, J. Hill, *Data Analysis Using Regression and Multilevel/Hierarchical Models*, Cambridge University Press, New York, 2006.